

Abundance Analysis of Barium Stars

G. Q. Liu^{1,2*}, Y. C. Liang^{1**} and L. Deng¹

¹ National Astronomical Observatories, Chinese Academy of Sciences, Beijing 100012, P. R. China

² Graduate University of Chinese Academy of Sciences, Beijing 100049, P. R. China

Abstract We obtain the chemical abundances of six barium stars and two CH subgiant stars based on the high signal-to-noise ratio and high resolution Echelle spectra. The neutron capture process elements Y, Zr, Ba, La, Eu show obvious overabundance relative to the Sun, for example, their [Ba/Fe] values are from 0.45 to 1.27. Other elements, including Na, Mg, Al, Si, Ca, Sc, Ti, V, Cr, Mn, Ni, show comparable abundances to the Solar ones, and their [Fe/H] cover a range from -0.40 to 0.21 , which means they belong to Galactic disk. The predicts of the theoretical model of wind accretion for binary systems can explain the observed abundance patterns of the neutron capture process elements in these stars, which means that their overabundant heavy-elements could be caused by accreting the ejecta of AGB stars, the progenitors of the present white dwarf companions in the binary systems.

Key words: Stars: abundances — Stars: atmospheres — Stars: chemically peculiar — Stars: evolution — binaries: spectroscopic

1 INTRODUCTION

As first identified by Bidelman & Keeman (1951), barium stars appear as a distinct group of chemically peculiar red giants. These G and K giants show enhanced features of Ba II, Sr II, CH, CN and sometimes C₂ lines. The following studies also found enhanced abundances of some other heavy elements, e.g. Y, Zr, La, Ce, Pr, Nd and Sm.

Since Burbidge et al. (1957) suggested the elements heavier than iron are synthesized in the interior of asymptotic giant branch (AGB) stars through the slow neutron capture process (s-process) (the rapid neutron capture process, r-process, occurs in supernova explosion), one generally believe that the overabundant heavy elements of Ba stars could be caused by binary accretion because they should not be evolved to the thermal pulse (TP) AGB stage to synthesize these heavy elements due to their low luminosity and the absence of the unstable nucleus ⁹⁹Tc ($\tau_{1/2}=2\times 10^5$ yr) (see Liang et al. 2000, 2003 and references therein). The binarity and heavy-element abundances of Ba stars have been studied by

* E-mail: lgq@bao.ac.cn, ycliang@bao.ac.cn

Table 1 Basic data of the sample stars. The HD identifications, spectral types, $B - V$ color, trigonometric parallaxes and their errors.

| HD | Sp. | V_{mag} | $B - V$ | π (mas) | σ_{π} |
|--------|-------|------------------|---------|----------------|----------------|
| 4395 | G5 | 7.70 | 0.69 | 9.16 | 1.12 |
| 180622 | K2 | 7.63 | 1.25 | 3.37 | 1.04 |
| 201657 | K2 | 8.00 | 1.27 | 4.49 | 1.07 |
| 201824 | K0 | 8.90 | 1.09 | 0.56 | 1.56 |
| 210946 | K0 | 8.08 | 1.095 | 3.42 | 1.14 |
| 211594 | K0 | 8.05 | 1.143 | 4.59 | 1.18 |
| 216219 | G0IIp | 7.44 | 0.64 | 10.74 | 0.93 |
| 223617 | G5 | 6.91 | 1.155 | 4.61 | 0.95 |

many researchers (Griffin 1980; Jorissen & Mayor 1988; McClure et al. 1980; McClure 1983; McClure & Woodsworth 1990; Jorissen et al. 1998; Liang et al. 2000, 2003; Liu et al. 2000; Lü et al. 1991; Han et al. 1995; Začs 1994; Smiljanic et al. 2007). These Ba stars could have accreted the matter ejected by their companions (the former AGB stars, the present white dwarfs) about 1×10^6 years ago through wind accretion, disk accretion or common envelope ejection (Han et al. 1995; Jorissen et al. 1998; Liang et al. 2000).

At present, a large sample of Ba stars have been measured their binary orbital elements (Carquillat et al. 1998; Udry et al. 1998a, 1998b; Jorissen et al. 1998), absolute magnitudes and kinematics (Gómez et al. 1997; Mennessier et al. 1997). However, the corresponding heavy-element abundances have not been obtained from high resolution observations, which is very useful to understand the formation scenario of Ba stars, but need lots of telescope time and lots of efforts on data analysis. Therefore, we propose to observe the high resolution and high signal-to-noise (S/N) ratio spectra of a sample of Ba stars to obtain their chemical abundances, hence, to understand their formation scenario by combining with their binary orbital elements. Moreover, by taking advantage of the present high precision Hipparcos data, precise photometric parameters, improved methods to determine stellar atmospheric parameters and developed stellar evolutionary tracks etc., the reliable chemical abundances of stars could be obtained from the spectra. We could also understand the formation scenario of Ba stars from theoretical models by comparing the model predicts with the observed abundances, e.g. the angular momentum conservation model of wind accretion of Ba binaries (Liang et al. 2000; Liu et al. 2000; Boffin & Jorissen 1988).

This paper is organized as follows. Description of the spectral observations and data reduction for the sample stars are presented in Section 2. In Section 3 the derived stellar atmospheric parameters are presented. Stellar atmosphere model, spectral lines and their measured equivalent widths (EWs) are described in Section 4. The analysis on abundance results is given in Section 5. The predicted abundances from wind accretion model are presented and compared with the observed abundance patterns in Section 6. The discussions and conclusions are given in Section 7.

2 OBSERVATIONS AND DATA REDUCTION

The sample stars have been firstly identified as mild or strong Ba stars in Lü et al. (1991) and have been obtained their binary orbital elements (e.g. orbital period and eccentricity) in Jorissen et al. (1998) except HD 4395. HD 4395 and HD 216219 were classified as CH subgiants (Luck & Bond 1982; Sneden 1983;

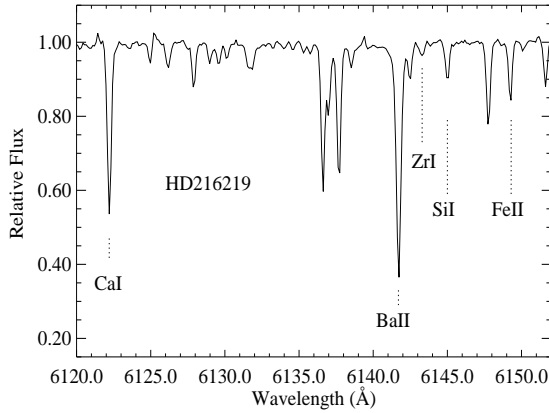


Fig. 1 A portion of spectrum of the sample star HD 216219 in the wavelength range 6120Å–6152Å. Major features include Ca I 6122.226 Å, Ba II 6141.727 Å, Zr I 6143.180 Å, Si I 6145.020 Å and Fe II 6149.249 Å.

Krishnaswamy & Sneden 1985; Lambert et al. 1993; Smith et al. 1993; Preston & Sneden 2001), but HD 216219 has also been classified as mild Ba star by Lü et al. (1991) and Jorissen et al. (1998). A common point of view is that CH subgiants also belong to binary systems and their overabundances of s-process elements are caused by accreting the ejected material of the companion AGB progenitors, which is the same scenario as the Ba stars. The CH subgiants could evolve to be the classical Ba stars (Luck & Bond 1982; Smith et al. 1993). In this work we take these two stars as the same with other samples to study their abundances and formation scenario. These two common stars with Smith et al. (1993) are good examples to compare our EW measurements, atmospheric parameters and abundances with theirs carefully.

Table 1 presents the basic parameters of the sample stars. The Column (1)-(6) consequently present their HD identifications, spectral type and luminosity class, visual magnitudes, $B - V$ color index, trigonometric parallaxes and the corresponding errors taken from SIMBAD database.

The spectroscopic observations were carried out with the Coudé Echelle Spectrograph of National Astronomical Observatories (NAOC) mounted on the 2.16 m telescope at Xinglong station (Xinglong, P. R. China). The detector was a Tektronix CCD with 1024×1024 pixels ($24 \times 24 \mu m^2$ each in size). The wavelength coverage of total spectra is roughly from 5500–8000 Å over 34 orders. The spectra were observed during September 12–14, 2000 and most of them had $S/N > 100$. Figure 1 presents the spectrum of HD 216219 showing main features of absorption in the region around Ba II $\lambda 6141.727$ line.

Data reductions of all the spectra were carried out through ECHELLE package in the MIDAS environment by standard routines proceeding with order identification, background subtraction, flat-field correction, order extraction, wavelength calibration with a thorium-argon lamp calibration frame. Bias, dark current and scattered light corrections were taken into account in the background subtraction. The pixel-to-pixel sensitivity variations were corrected by using the flat-field. The EWs of the spectral lines are measured from the normalized spectra corrected by radial velocity, which were measured from more than 20 absorption lines at least. The selected spectral lines for abundance analysis are unblended or slightly blended and have reliable atomic data.

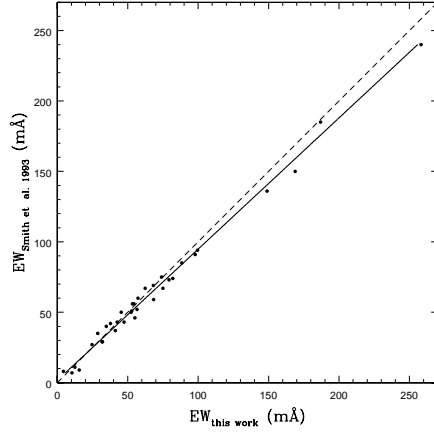


Fig. 2 Comparison of equivalent width measurements of 35 common absorption lines in HD 216219 and HD 4395 in this work and Smith et al. (1993). The solid line is the least square fit to the points (Eq.(1)), and the dashed line refers to the one-to-one relation.

The EWs of spectral line were measured by applying two different methods: direct integration of the line profile and Gaussian fitting. The latter is preferable in the case of faint lines ($EW < 20 \text{ m}\text{\AA}$), but unsuitable for the strong lines in which the damping wings contribute significantly to the equivalent width. The final EWs are weighted averages of these two measurements, depending on the line intensity (see Zhao et al. 2000 for details). The EW values of 110–180 lines in the wavelength range from 5500–8100 \AA were obtained for each of the sample stars. Table 2 presents the final EWs of the lines measured in the spectra of the sample stars as input data for the abundance analysis. Since the very weak lines would lead to an increase of random errors in the abundance determination and the too strong lines are not so sensitive to abundance, we use the lines with $EW_s=10 - 200 \text{ m}\text{\AA}$ for abundance analysis, and most of them within $20 - 150 \text{ m}\text{\AA}$ except some of the s-process elements. The reliability of our EW measurements have been confirmed by the consistence in the comparison between our data and those of Smith et al. (1993) for 35 common lines of HD 216219 and HD 4395. This comparison is shown in Figure 2. The systematic difference between the two sets of data is small and could be given by a linear least square fit as:

$$EW_{\text{Smith93}} = 0.92(\pm 0.02)EW_{\text{this work}} + 2.19(\pm 1.30)m\text{\AA}, \quad (1)$$

with the standard deviation of 0.061.

3 STELLAR ATMOSPHERIC PARAMETERS

The stellar atmospheric model is composed of four basic parameters, i.e., effective temperature, surface gravity, metallicity and microturbulent velocity. In this section, we describe the determinations of these four model-atmosphere parameters.

3.1 Effective temperature

Effective temperatures T_{eff} were determined from $[\text{Fe}/\text{H}]$ and $B-V$ color indices by using the empirical calibration of Alonso et al. (1999 & 2001), which is suit-

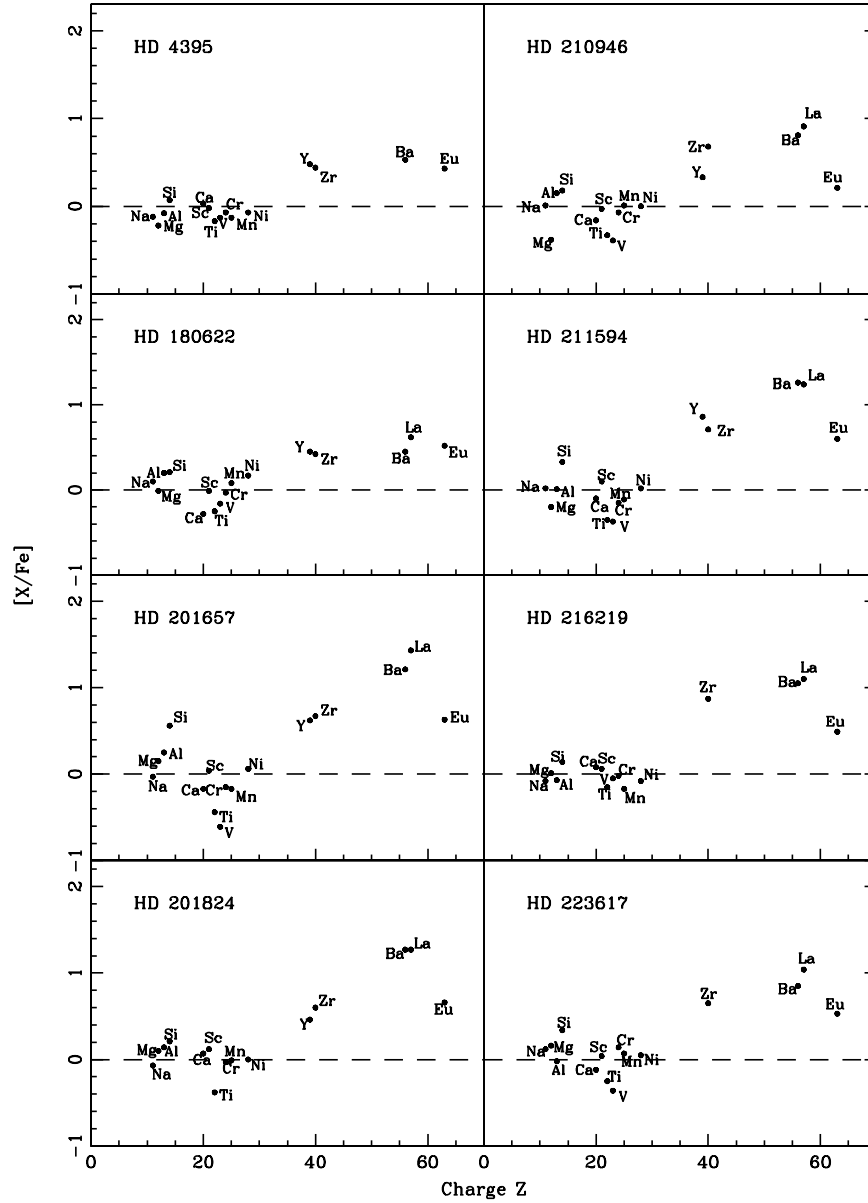


Fig. 3 The abundance patterns of sample stars.

able for giant stars. We use $B-V$ color here since the $B-V$ data are more complete than other color indices for the sample stars. Considering the uncertainties of photometric data, $[\text{Fe}/\text{H}]$, and the errors in the calibration relation, we estimate the uncertainty in T_{eff} is about 100 K for our sample stars.

Table 3 Atmospheric parameters of the sample stars: effective temperature (T_{eff}), surface gravity ($\log g$), mass (M/M_{\odot}) and their uncertainties, microturbulence velocity (ξ_t) and metallicity ([Fe/H]).

| HD | T_{eff} | $\log g$ | M/M_{\odot} | ξ_t | [Fe/H] |
|--------|------------------|----------|-------------------|---------|--------|
| 4395 | 5447 | 3.60 | 1.60(+0.13,−0.10) | 1.3 | −0.16 |
| 180622 | 4391 | 2.24 | 1.92(+1.07,−0.36) | 1.5 | 0.21 |
| 201657 | 4284 | 2.17 | 0.78(+0.08,−0.02) | 1.7 | −0.31 |
| 201824 | 4552 | 1.67 | 4.58(−,−3.32) | 1.5 | −0.40 |
| 210946 | 4577 | 2.42 | 1.40(+0.72,−0.28) | 1.6 | −0.22 |
| 211594 | 4490 | 2.44 | 0.90(+0.41,−0.09) | 1.6 | −0.23 |
| 216219 | 5553 | 3.64 | 1.48(+0.07,−0.08) | 1.4 | −0.34 |
| 223617 | 4501 | 2.27 | 1.78(+0.47,−0.33) | 1.5 | −0.10 |

3.2 Surface Gravity

Based on the *Hipparcos* parallaxes, precise value of the surface gravity of nearby stars can be obtained using the following relations:

$$\log \frac{g}{g_{\odot}} = \log \frac{\mathcal{M}}{\mathcal{M}_{\odot}} + 4 \log \frac{T_{\text{eff}}}{T_{\text{eff},\odot}} + 0.4 (M_{\text{bol}} - M_{\text{bol},\odot}) \quad (2)$$

and

$$M_{\text{bol}} = V + BC + 5 \log \pi + 5, \quad (3)$$

where \mathcal{M} is the stellar mass, M_{bol} the absolute bolometric magnitude, V the visual magnitude, BC the bolometric correction, and π the parallax. We adopt solar value $\log g_{\odot}=4.44$, $T_{\text{eff},\odot}=5770$ K, $M_{\text{bol},\odot}=4.77$ mag. The parallax π and its errors are taken from the *Hipparcos* Satellite observations (ESA 1997). Stellar mass was determined from the position of the star in $M_{\text{bol}}-\log T_{\text{eff}}$ diagram. We adopt the stellar evolutionary tracks of Yonsei-Yale (Yi et al. 2003), whose isochrones determined with high quality observational data cover the stage from pre-main-sequence birthline to the helium-core flash. The uncertainty of $\log g$ estimated by this method is about 0.2 dex generally for our sample stars.

3.3 Metal abundance

The initial metallicities of the sample stars in their model atmospheres were taken from literature if available. Otherwise, we adopt [Fe/H]=0 as the initial value and then the final model metallicity derived from the consistency with the other parameters in the abundance calculation. The estimated error in [Fe/H] is about 0.1 dex.

3.4 Microturbulence velocity

The value of microturbulence velocity ξ_t was determined from the abundance analysis by requiring a null correlation between [Fe/H] and the EWs. We applied this calculation with a large range of EWs (20 – 150 mÅ) for Fe I lines. With this selection, the uncertainty of the microturbulence velocity is about 0.2 km s^{−1}.

Table 3 presents the atmospheric parameters for the sample stars, where Column (1)-(6) list, consequently, the HD identifications, T_{eff} , $\log g$, mass, microturbulence velocity and [Fe/H]. The temperature coverage of the stars are from 4284 to 5553 K, the surface gravity coverage are from 1.67 to 3.64. The microturbulence velocity is from 1.3 to 1.7, and their [Fe/H] is from −0.40 to

Table 4 Element abundances of the sample stars.

| | HD 4395 | | | HD 180622 | | | HD 201657 | | | HD 201824 | | |
|--------|---------|-------------------|--------|-----------|-------------------|--------|-----------|-------------------|--------|-----------|-------------------|--------|
| [Fe/H] | -0.16 | | | 0.21 | | | -0.31 | | | -0.40 | | |
| Ion | N | log $\epsilon(X)$ | [X/Fe] | N | log $\epsilon(X)$ | [X/Fe] | N | log $\epsilon(X)$ | [X/Fe] | N | log $\epsilon(X)$ | [X/Fe] |
| Fe I | 51 | 7.34 | — | 35 | 7.71 | — | 45 | 7.18 | — | 28 | 7.10 | — |
| Fe II | 8 | 7.32 | — | 2 | 7.73 | — | 2 | 7.31 | — | 2 | 7.14 | — |
| Na I | 2 | 6.05 | -0.12 | 2 | 6.64 | 0.10 | 2 | 5.99 | -0.03 | 2 | 5.86 | -0.07 |
| Mg I | 2 | 7.20 | -0.22 | 1 | 7.78 | -0.01 | 1 | 7.42 | 0.15 | 2 | 7.28 | 0.10 |
| Al I | 4 | 6.23 | -0.08 | 3 | 6.88 | 0.20 | 3 | 6.41 | 0.25 | 3 | 6.21 | 0.14 |
| Si I | 13 | 7.46 | 0.07 | 6 | 7.97 | 0.21 | 4 | 7.80 | 0.56 | 6 | 7.36 | 0.21 |
| Ca I | 12 | 6.23 | 0.03 | 2 | 6.29 | -0.28 | 9 | 5.88 | -0.17 | 17 | 6.03 | 0.07 |
| Sc II | 2 | 2.99 | -0.02 | 3 | 3.37 | -0.01 | 3 | 2.90 | 0.04 | 3 | 2.89 | 0.12 |
| Ti I | 6 | 4.69 | -0.17 | 6 | 4.98 | -0.25 | 6 | 4.27 | -0.44 | 9 | 4.24 | -0.38 |
| V I | 1 | 3.71 | -0.13 | 3 | 4.05 | -0.16 | 1 | 3.08 | -0.61 | 0 | — | — |
| Cr I | 7 | 5.44 | -0.07 | 5 | 5.85 | -0.03 | 4 | 5.21 | -0.15 | 4 | 5.24 | -0.03 |
| Mn I | 2 | 5.10 | -0.13 | 2 | 5.68 | 0.08 | 2 | 4.91 | -0.17 | 2 | 4.98 | -0.01 |
| Ni I | 25 | 6.02 | -0.07 | 21 | 6.63 | 0.17 | 21 | 5.97 | 0.06 | 25 | 5.85 | 0.00 |
| Y I | 1 | 2.56 | 0.48 | 1 | 2.90 | 0.45 | 1 | 2.55 | 0.62 | 1 | 2.30 | 0.46 |
| Zr I | 3 | 2.88 | 0.44 | 4 | 3.23 | 0.42 | 3 | 2.84 | 0.67 | 2 | 2.80 | 0.60 |
| Ba II | 3 | 2.50 | 0.53 | 3 | 2.79 | 0.45 | 3 | 3.03 | 1.21 | 3 | 3.00 | 1.27 |
| La II | 0 | — | — | 1 | 2.00 | 0.62 | 1 | 2.29 | 1.43 | 1 | 2.04 | 1.27 |
| Eu II | 1 | 0.78 | 0.43 | 1 | 1.24 | 0.52 | 1 | 0.83 | 0.63 | 1 | 0.77 | 0.66 |

| | HD 210946 | | | HD 211594 | | | HD 216219 | | | HD 223617 | | |
|--------|-----------|-------------------|--------|-----------|-------------------|--------|-----------|-------------------|--------|-----------|-------------------|--------|
| [Fe/H] | -0.22 | | | -0.23 | | | -0.34 | | | -0.10 | | |
| Ion | N | log $\epsilon(X)$ | [X/Fe] | N | log $\epsilon(X)$ | [X/Fe] | N | log $\epsilon(X)$ | [X/Fe] | N | log $\epsilon(X)$ | [X/Fe] |
| Fe I | 51 | 7.28 | — | 49 | 7.27 | — | 51 | 7.15 | — | 34 | 7.39 | — |
| Fe II | 3 | 7.38 | — | 0 | — | — | 3 | 7.30 | — | 4 | 7.46 | — |
| Na I | 1 | 6.12 | 0.01 | 2 | 6.12 | 0.02 | 2 | 5.91 | -0.08 | 2 | 6.35 | 0.12 |
| Mg I | 2 | 6.98 | -0.38 | 1 | 7.15 | -0.2 | 3 | 7.25 | 0.01 | 2 | 7.64 | 0.16 |
| Al I | 2 | 6.40 | 0.15 | 2 | 6.25 | 0.01 | 3 | 6.06 | -0.07 | 1 | 6.35 | -0.02 |
| Si I | 4 | 7.51 | 0.18 | 8 | 7.65 | 0.33 | 13 | 7.35 | 0.14 | 8 | 7.79 | 0.34 |
| Ca I | 16 | 5.98 | -0.16 | 18 | 6.03 | -0.10 | 15 | 6.10 | 0.08 | 9 | 6.14 | -0.12 |
| Sc II | 3 | 2.92 | -0.03 | 5 | 3.04 | 0.10 | 4 | 2.89 | 0.06 | 3 | 3.11 | 0.04 |
| Ti I | 6 | 4.47 | -0.33 | 2 | 4.44 | -0.35 | 3 | 4.53 | -0.15 | 6 | 4.67 | -0.25 |
| V I | 3 | 3.39 | -0.39 | 1 | 3.40 | -0.37 | 2 | 3.61 | -0.05 | 2 | 3.54 | -0.36 |
| Cr I | 5 | 5.38 | -0.07 | 5 | 5.29 | -0.15 | 5 | 5.31 | -0.02 | 5 | 5.71 | 0.14 |
| Mn I | 2 | 5.18 | 0.01 | 2 | 5.05 | -0.11 | 2 | 4.88 | -0.17 | 2 | 5.36 | 0.07 |
| Ni I | 21 | 6.03 | 0.00 | 20 | 6.04 | 0.02 | 30 | 5.83 | -0.08 | 17 | 6.20 | 0.05 |
| Y I | 1 | 2.35 | 0.33 | 1 | 2.87 | 0.86 | 0 | — | — | 1 | 2.64 | 0.50 |
| Zr I | 3 | 3.06 | 0.68 | 2 | 3.08 | 0.71 | 3 | 3.13 | 0.87 | 3 | 3.15 | 0.65 |
| Ba II | 3 | 2.72 | 0.81 | 3 | 3.16 | 1.26 | 3 | 2.84 | 1.05 | 3 | 2.88 | 0.85 |
| La II | 1 | 1.86 | 0.91 | 1 | 2.18 | 1.24 | 1 | 1.93 | 1.10 | 1 | 2.11 | 1.04 |
| Eu II | 1 | 0.50 | 0.21 | 1 | 0.88 | 0.60 | 1 | 0.66 | 0.49 | 1 | 0.94 | 0.53 |

0.21. The uncertainties of the parameters are: $\sigma(T_{\text{eff}}) = 100$ K, $\sigma(\log g) = 0.2$, $\sigma([\text{Fe}/\text{H}]) = 0.1$, and $\sigma(\xi_t) = 0.2$ km s⁻¹.

The reliability of the derived atmospheric parameters $T_{\text{eff}}/\log g/\xi_t$ are confirmed by the further checks. Taking HD 216219 as a representative, Figure 4a give the Fe abundances from different Fe I lines as a function of their excitation potential, which fulfills the excitation equilibrium; Figure 4b shows that the Fe abundances from Fe I lines and Fe II lines are consistent within 0.2 dex, which illustrates the ionization equilibrium, and also shows that there is no trend between Fe abundances and EWs of the lines.

Comparing our results with those of Smith et al. (1993), the derived atmospheric parameters for HD 4395 are $T_{\text{eff}}=5447/5450$ K, $\log g=3.60/3.3$, $\xi_t=1.3/1.3$, $[\text{Fe}/\text{H}]=-0.16/-0.33$; for HD 216219 are $T_{\text{eff}}=5553/5600$ K, $\log g=3.64/3.2$, $\xi_t=1.4/1.6$, $[\text{Fe}/\text{H}]=-0.34/-0.32$. They are well consistent.

Table 5 The detailed uncertainties of the abundance analysis for one representative star HD 216219, and the total uncertainties on the abundances for all other sample stars.

| HD 216219 $T_{\text{eff}} = 5197$ $\log g = 3.39$ $[\text{Fe}/\text{H}] = -0.63$ $\xi_t = 1.4$ | | | | | | | |
|--|---------------|----------------------------------|-------------------------|--------------------------------------|------------------------|----------------|--------|
| | σ_{EW} | ΔT_{eff} +100K | $\Delta \log g$ +0.2 | $\Delta[\text{Fe}/\text{H}]$ +0.1 | $\Delta \xi_t$ +0.2 | σ_{tot} | |
| $\Delta[\text{Fe}/\text{H}]_I$ | 0.07 | 0.08 | -0.01 | 0.00 | -0.04 | 0.11 | |
| $\Delta[\text{Fe}/\text{H}]_{II}$ | 0.06 | -0.03 | 0.08 | 0.03 | -0.04 | 0.12 | |
| $\Delta[\text{Na}/\text{Fe}]$ | 0.04 | 0.06 | 0.00 | 0.00 | 0.00 | 0.07 | |
| $\Delta[\text{Mg}/\text{Fe}]$ | 0.07 | 0.07 | -0.06 | 0.01 | -0.03 | 0.12 | |
| $\Delta[\text{Al}/\text{Fe}]$ | 0.03 | 0.04 | -0.02 | -0.01 | -0.01 | 0.06 | |
| $\Delta[\text{Si}/\text{Fe}]$ | 0.05 | 0.03 | 0.00 | 0.00 | -0.02 | 0.06 | |
| $\Delta[\text{Ca}/\text{Fe}]$ | 0.08 | 0.08 | -0.04 | 0.00 | -0.06 | 0.13 | |
| $\Delta[\text{Sc}/\text{Fe}]$ | 0.09 | 0.01 | 0.06 | 0.02 | -0.07 | 0.13 | |
| $\Delta[\text{Ti}/\text{Fe}]$ | 0.04 | 0.10 | -0.01 | -0.01 | -0.02 | 0.11 | |
| $\Delta[\text{V}/\text{Fe}]$ | 0.04 | 0.11 | -0.01 | -0.01 | -0.02 | 0.12 | |
| $\Delta[\text{Cr}/\text{Fe}]$ | 0.04 | 0.07 | -0.01 | -0.01 | -0.02 | 0.08 | |
| $\Delta[\text{Mn}/\text{Fe}]$ | 0.07 | 0.09 | -0.02 | 0.00 | -0.05 | 0.13 | |
| $\Delta[\text{Ni}/\text{Fe}]$ | 0.06 | 0.08 | -0.01 | 0.00 | -0.04 | 0.11 | |
| $\Delta[\text{Zr}/\text{Fe}]$ | 0.04 | 0.13 | 0.00 | 0.00 | 0.00 | 0.14 | |
| $\Delta[\text{Ba}/\text{Fe}]$ | 0.06 | 0.04 | -0.02 | 0.04 | -0.05 | 0.10 | |
| $\Delta[\text{La}/\text{Fe}]$ | 0.04 | 0.03 | 0.08 | 0.04 | -0.03 | 0.11 | |
| $\Delta[\text{Eu}/\text{Fe}]$ | 0.03 | 0.00 | 0.08 | 0.02 | -0.02 | 0.09 | |
| σ_{tot} | 4395 | 180622 | 201657 | 201824 | 210946 | 211594 | 223617 |
| $\Delta[\text{Fe}/\text{H}]_I$ | 0.11 | 0.14 | 0.10 | 0.12 | 0.10 | 0.11 | 0.13 |
| $\Delta[\text{Fe}/\text{H}]_{II}$ | 0.13 | 0.24 | 0.22 | 0.19 | 0.20 | — | 0.20 |
| $\Delta[\text{Na}/\text{Fe}]$ | 0.08 | 0.16 | 0.14 | 0.10 | 0.13 | 0.13 | 0.14 |
| $\Delta[\text{Mg}/\text{Fe}]$ | 0.09 | 0.16 | 0.14 | 0.16 | 0.12 | 0.10 | 0.13 |
| $\Delta[\text{Al}/\text{Fe}]$ | 0.07 | 0.13 | 0.10 | 0.09 | 0.10 | 0.09 | 0.10 |
| $\Delta[\text{Si}/\text{Fe}]$ | 0.07 | 0.14 | 0.12 | 0.10 | 0.10 | 0.11 | 0.11 |
| $\Delta[\text{Ca}/\text{Fe}]$ | 0.15 | 0.18 | 0.20 | 0.21 | 0.18 | 0.19 | 0.20 |
| $\Delta[\text{Sc}/\text{Fe}]$ | 0.14 | 0.22 | 0.17 | 0.19 | 0.17 | 0.18 | 0.18 |
| $\Delta[\text{Ti}/\text{Fe}]$ | 0.12 | 0.24 | 0.21 | 0.20 | 0.19 | 0.22 | 0.21 |
| $\Delta[\text{V}/\text{Fe}]$ | 0.12 | 0.30 | 0.23 | — | 0.22 | 0.20 | 0.25 |
| $\Delta[\text{Cr}/\text{Fe}]$ | 0.10 | 0.21 | 0.15 | 0.15 | 0.14 | 0.14 | 0.19 |
| $\Delta[\text{Mn}/\text{Fe}]$ | 0.14 | 0.20 | 0.19 | 0.24 | 0.21 | 0.19 | 0.20 |
| $\Delta[\text{Ni}/\text{Fe}]$ | 0.11 | 0.17 | 0.14 | 0.19 | 0.13 | 0.15 | 0.15 |
| $\Delta[\text{Y}/\text{Fe}]$ | 0.12 | 0.26 | 0.24 | 0.22 | 0.17 | 0.23 | — |
| $\Delta[\text{Zr}/\text{Fe}]$ | 0.13 | 0.25 | 0.25 | 0.26 | 0.19 | 0.22 | 0.24 |
| $\Delta[\text{Ba}/\text{Fe}]$ | 0.16 | 0.17 | 0.09 | 0.09 | 0.13 | 0.13 | 0.11 |
| $\Delta[\text{La}/\text{Fe}]$ | — | 0.17 | 0.20 | 0.21 | 0.13 | 0.18 | 0.17 |
| $\Delta[\text{Eu}/\text{Fe}]$ | 0.11 | 0.15 | 0.10 | 0.14 | 0.11 | 0.12 | 0.11 |

4 STELLAR ATMOSPHERE MODEL AND SPECTRAL LINES

The stellar atmospheric model is implemented by ATLAS9 code (Kurucz 1993) to do the abundance analysis. This is LTE, plane-parallel, line-blanketed models. Abundances of chemical elements were determined by using the input atmospheric parameters given in Table 3 and the measured EWs of the absorption lines. All the lines adopted in determining element abundances are presented in Table 2, which shows the spectral lines and wavelengths, excitation potential χ , oscillator strengths $\log gf$, EWs and $\log \epsilon$ of each line. The selections of the lines have been described in Sect.2. The oscillator strengths $\log gf$ of spectral lines

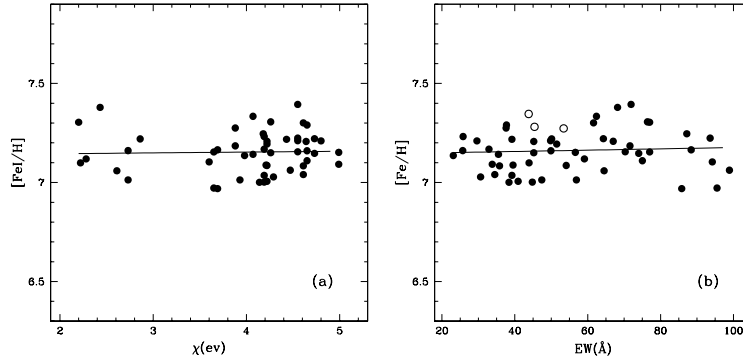


Fig.4 To check the reliability of the determined atmospheric parameters $T_{\text{eff}}/\log g/\xi_t$ of the stars by taking HD216219 as an example: (a). Fe abundances from Fe I lines as a function of excitation potential. There is no significant trend of $[\text{Fe}/\text{H}]$ with χ , indicating a correct temperature distribution in the model atmosphere. (b). The consistence of the Fe I and Fe,II abundances (the filled and open circles refer to the Fe I and Fe II abundances respectively), which mean that the determined $\log g$ are reliable; and an illustration of the determination of the microturbulence velocity since there is no significant trend between $[\text{Fe}/\text{H}]$ and EWs.

are taken from the NIST database (<http://physics.nist.gov>), Lambert & Warner (1968), Weise & Martin (1980), Biémont et al. (1981, 1982), Hannaford et al. (1982), Fuhr et al. (1988), Luck & Bond (1991), O’Brian et al. (1991), Bard & Kock (1994), Lambert et al. (1996), Nissen & Schuster (1997), Chen et al. (2000), Liang et al. (2003) and the references therein. Col. (5) of Table 2 gives these reference sources for the spectral lines.

5 CHEMICAL ABUNDANCES AND ANALYSIS

In this section, we present the determined abundances of the sample stars for about 20 elements based on the spectral observations and atmospheric model.

5.1 Abundance of barium stars

The derived element abundances of all the sample stars are given in Table 4, including $\log \epsilon$ and the corresponding $[X/\text{Fe}]$ values for all ions. The solar abundances are adopted from Grevesse & Sauval (1998).

Figure 3 directly presents the abundance results of our sample stars, including the chemical elements, Na, Mg, Al, Si, Ca, Sc, Ti, V, Cr, Mn, Ni, Y, Zr, Ba, La and Eu. It is obvious to show that the neutron capture process elements, Y, Zr, Ba, La, Eu, are overabundant than the solar abundances. Especially, Y and Zr exhibit as the first peak while Ba and La exhibit as the second peak, and the second peak is higher than the first one. Other elements from Na to Ni, such as α elements and iron elements, show similar abundances to the solar, which means that these Ba stars belong to disk stars. The behaviors of Sc and Mn are compatible to the results of Nissen et al. (2000) and Chen et al. (2000a), who demonstrated that decreasing $[\text{Sc}/\text{Fe}]$ with increasing metallicity in disk stars, whereas $[\text{Mn}/\text{Fe}]$ increases with increasing $[\text{Fe}/\text{H}]$.

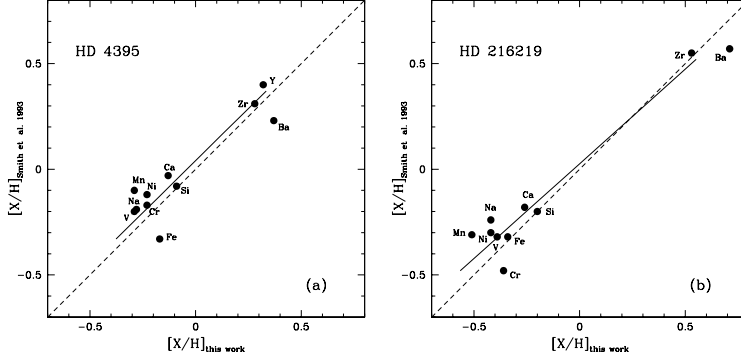


Fig. 5 The comparisons between our abundances determinations and those of Smith et al. (1993) for the two common stars: (a). for HD 4395; (b). for HD 216219. The solid lines are the least square fits for the data and the dashed lines are the one-to-one relations. Our results are consistent with theirs.

5.2 Uncertainties in the abundances

There are two kinds of uncertainties in the abundance determination: the systematic errors introduced by the atmospheric parameters, and the random errors in determining EWs, oscillator strengths, and damping constants. We ignore the uncertainties in atomic data since they could be small (Chen et al. 2000b) and consider the uncertainties in atmospheric parameter determinations and EW measurements. Assuming that the effects of the uncertainties of the parameters are independent, we can estimate the total uncertainty with Eq. (4):

$$\sigma_{total} = \sqrt{(\sigma_{EW})^2 + (\Delta T_{eff})^2 + (\Delta \log g)^2 + (\Delta [Fe/H])^2 + (\Delta \xi_t)^2}, \quad (4)$$

where σ_{EW} , ΔT_{eff} , $\Delta \log g$, $\Delta [Fe/H]$ and $\Delta \xi_t$ are the corresponding variations in the ion abundances due to the variations on equivalent widths, T_{eff} , $\log g$, metal abundance and microturbulent velocity, respectively.

For our spectra, the typical uncertainty of the EW is about 6.1%. Table 5 shows the effects on the derived abundances changed by 6.1% in EW, 100 K in effective temperature, 0.2 dex in surface gravity, 0.1 dex in metallicity, and 0.2 km s^{-1} in microturbulence velocity for one representative star, HD 216219. The total uncertainties on the output abundances have also be given in Table 5 for all other sample stars by considering the same errors as above in the individual atmospheric parameter.

5.3 Comparisons with Smith et al. (1993)

As for the two common stars with Smith et al. (1993), we compare our abundance determinations with theirs for HD 4395 and HD 216219. Figure 5 shows the consistences between our abundance estimations with theirs are within 0.2 dex, but most are in 0.1 dex.

6 COMPARING WITH WIND ACCRETION MODEL RESULTS

We try to use the wind accretion model to predict the theoretical heavy element abundances of Ba stars in binary systems, and then compare these theoretical predicts with the observed abundance patterns of our sample stars. Following Liang et al. (2000, 2003), the calculations of theoretical abundances are made in

Table 6 Orbital elements of the sample stars derived from literatures.

| HD | P (days) | e | Classes | Reference |
|--------|---------------|------|---------|-----------------------|
| 4395 | 6200 | 0.65 | — | Preston & Sneden 2001 |
| 180622 | 4049.2 | 0.06 | mild | Jorissen et al. 1998 |
| 201657 | 1710.4 | 0.17 | strong | Jorissen et al. 1998 |
| 201824 | 2837 | 0.34 | strong | Jorissen et al. 1998 |
| 210946 | 1529.5 | 0.13 | mild | Jorissen et al. 1998 |
| 211594 | 1018.9 | 0.06 | strong | Jorissen et al. 1998 |
| 216219 | 4098.0 | 0.10 | mild | Jorissen et al. 1998 |
| 223617 | 1293.7 | 0.06 | mild | Jorissen et al. 1998 |

two steps: the AGB nucleosynthesis based on the latest TP-AGB model and the branch path of the s -process nucleosynthesis, and the binary accretion based on the angular momentum conservation model of wind accretion.

The standard case of our wind accretion model is: $M_{1,0}=3.0M_{\odot}$, $M_{2,0}=1.3M_{\odot}$, $v_{ej}=15 \text{ km s}^{-1}$ ($M_{1,0}$ is the main sequence mass of the intrinsic AGB star, the present white dwarf, in the binary system; $M_{2,0}$ is the corresponding mass of the present Ba star; v_{ej} is the wind velocity). We assumed the standard accretion rate is 0.15 times of the Bondi-Hoyle's accretion rate (Liang et al. 2000; Boffin & Zacs 1994). The observed orbital elements of the sample stars are listed in Table 6, which are taken from Jorissen et al. (1998) and Preston & Sneden (2001). The observed orbital periods of our sample stars cover from 1018.9 to 6200 days and the eccentricities range from 0.06 to 0.65.

Figure 6 shows the comparisons between the theoretical abundances from the wind accretion model and the observed abundances of the sample stars, and the uncertainties of the observed abundances are marked as well. In the figure, the variable “ a ” represents the times of the corresponding standard neutron exposure in the ^{13}C profile in the AGB progenitor companion suggested by Gallino et al. (1998) and the higher a value reflects the higher neutron exposure occurred in interiors of the AGB progenitor. P refers to the orbital period of the sample star.

There is good agreement between our observed abundances and the theoretical ones for the sample stars. These mean that wind accretion can be the formation scenario of these Ba stars in binary systems. These are consistent with the suggestions of Jorissen et al. (1998), Zhang et al. (1999) and Liang et al. (2000), who mentioned that Ba stars with periods longer than 1500 or 1600 days could be formed through wind accretion. We should notice that the heavy element abundance patterns of two sample stars with $P > 1000$ days, HD 211594 and HD 223617, can also be explained by wind accretion. Figure 6 also shows that the strong Ba stars generally require the higher “ a ” values in the model than the mild Ba stars, i.e., the stronger neutron exposure occurred in the AGB progenitors in their s -process nucleosynthesis.

7 DISCUSSIONS AND CONCLUSIONS

The chemical compositions of six Ba stars and two CH subgiant stars were obtained on the basis of the high S/N ratio and high resolution spectra observed by using the 2.16m telescope at NAOC/Xinglong station. Their stellar atmospheric parameters were determined from the reliable methods, and show the ranges of $4284 < T_{\text{eff}} < 5553$, $1.67 < \log g < 3.64$, $-0.40 < [\text{Fe}/\text{H}] < 0.21$, and $1.3 < \xi_t < 1.7$. The model atmospheres were generated by using ATLAS9 code and the updated atomic data of the selected spectral lines for measuring EWs.

Then we obtain the abundances of chemical elements, Na, Mg, Al, Si, Ca, Sc, Ti, V, Cr, Mn, Ni, Y, Zr, Ba, La, Eu for our eight sample stars. The elements from

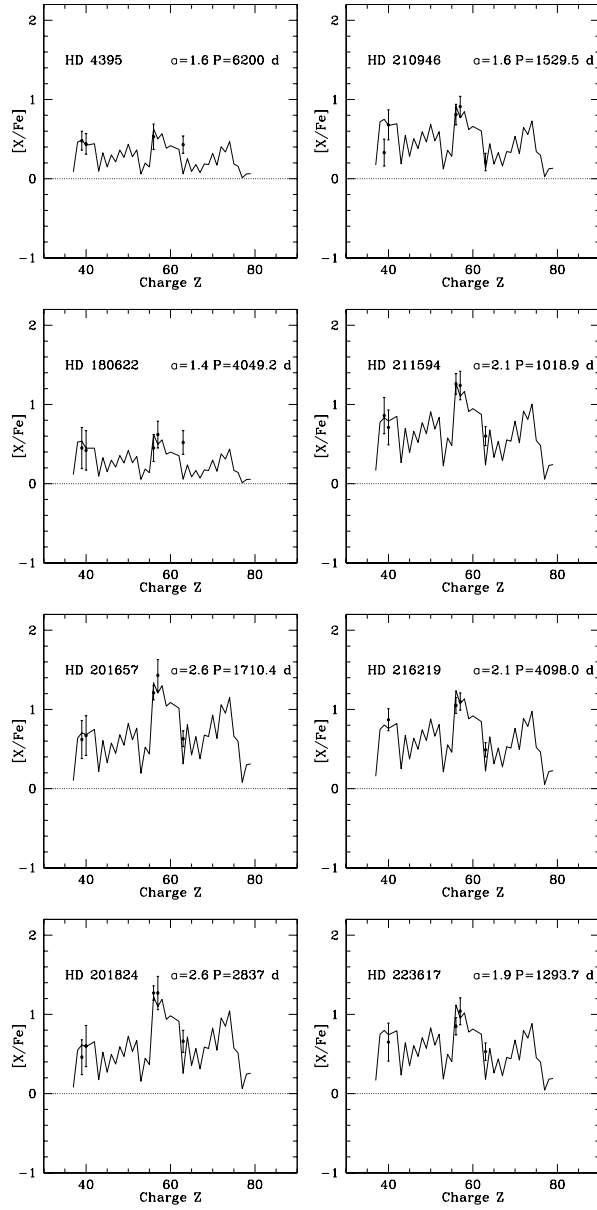


Fig. 6 The fitting of the theoretical to observed heavy-element abundances of sample stars with standard case of wind accretion. Label “ α ” represents the times of the corresponding standard neutron exposures in the ^{13}C profile in the AGB progenitor suggested by Gallino et al. (1998). P refers to the orbital period of the sample star.

Na to Ni, such as α and iron peak elements, show comparable abundances to the Sun, associated with the $[\text{Fe}/\text{H}]$ in a range of -0.40 to 0.21 , which mean these Ba stars belong to the Galactic disk. The neutron capture process elements Y, Zr, Ba, La, Eu show obvious overabundances than the solar abundances, for example, their $[\text{Ba}/\text{Fe}]$ values are from 0.45 to 1.27 . The abundance patterns of our sample stars are consistent with those obtained for other Ba stars in Začs (1994), Liang

et al. (2003), Smiljanic et al. (2007). Our study enlarge the sample of Ba stars with known chemical abundances. And we further check the formation scenario of these sample stars through theoretical wind accretion model.

We adopt the angular momentum conservation model of wind accretion to calculate the chemical abundances of Ba stars in the binary systems. The predicted results by the model can explain well the observed abundance patterns of the *s*-process elements. The abundance patterns of two sample stars, HD 211594 and HD 223617, can also be explained by the wind accretion model although their orbital periods are 1018.9 and 1293.7 days respectively, which are lower than the low limit of wind accretion formation of Ba stars suggested by Jorissen et al. (1998), 1500 days, and Zhang et al. (1999), Liang et al. (2000), 1600 days. This result could further decrease such low limit to be about 1000 days.

The masses of the sample stars are also determined and given in Table 3, as well as their errors. For most of them, their masses ($0.78\text{-}1.92M_{\odot}$) are close to the average masses of typical mild and strong Ba stars given in Jorissen et al. (1998) (their Table 9), who suggested that the average mass of typical mild Ba stars is 1.9 or $2.3M_{\odot}$ with the 0.60 or $0.67M_{\odot}$ companion white dwarfs, and the average mass of typical strong Ba stars is 1.5 or $1.9M_{\odot}$ with the 0.60 or $0.67M_{\odot}$ companion white dwarfs. However, the very high mass ($4.58M_{\odot}$) of HD 201824 should not be real and the reason could be the big error of its parallax, up to 3 times ($1.56/0.56$) uncertainty, which will cause the uncertainties of ~ 0.4 dex in $\log g$ and $3.2M_{\odot}$ in mass. This 0.4 dex uncertainty in $\log g$ is larger than the general case (0.2 dex) of the sample stars, but will not affect much the abundances. In Table 5 and Figure 6, we adopt the general uncertainties of $\log g$, 0.2 dex, to estimate the uncertainties on abundances for HD 201824.

The derived abundances of our sample stars confirm well their “strong” or “mild” Ba star properties. As shown in Table 4, Figure 3 and Figure 6, for the four mild Ba stars, namely, HD 180622, HD 210946, HD 216219 and HD 223617, their average abundances of *s*-process elements are $[\text{Ba}/\text{Fe}]=0.79$, $[\text{La}/\text{Fe}]=0.92$, $[\text{Y}/\text{Fe}]=0.43$, $[\text{Zr}/\text{Fe}]=0.66$, $[\text{Eu}/\text{Fe}]=0.44$; and for the three strong Ba stars, HD 201657, HD 201824 and HD 211594, their average abundances of *s*-process elements are $[\text{Ba}/\text{Fe}]=1.25$, $[\text{La}/\text{Fe}]=1.31$, $[\text{Y}/\text{Fe}]=0.65$, $[\text{Zr}/\text{Fe}]=0.66$, $[\text{Eu}/\text{Fe}]=0.63$. These show that the *s*-process element abundances of strong Ba stars are about 0.4 dex (or 0.2 dex) higher than those of the mild Ba stars. However, there are no obvious trend to show that the strong and mild Ba stars have different ranges in metallicity (also see Smiljanic et al. 2007). Also, there are no obvious indication to show that the orbital periods of mild Ba stars are longer than those of the strong Ba stars.

HD 4395 is a CH subgiant star. HD 216219 has also been classified as a CH subgiant (Smith et al. 1993 and the reference therein) or a mild Ba stars (Jorissen et al. 1998; Lü et al. 1991). CH subgiant was firstly discovered by Bond (1974). As Luck & Bond (1982) discussed, some of their CH subgiants might more properly be called subgiant barium stars or even main-sequence barium stars. We did not find obvious difference in the abundance patterns of our CH subgiant sample stars and the Ba sample stars except HD 4395 shows a bit relatively lower overabundances in its *s*-process elements. Moreover, the wind accretion models for binary system can explain well the observed overabundances of *s*-process elements in the CH subgiant stars as for other Ba stars. However, our results are not enough to check the suggested evolutionary relation between CH subgiants and classical Ba stars, which will need C/O and Li abundances (Smith et al. 1993; Lambert et al. 1993).

Acknowledgements We thank our referee for very valuable comments which help us a lot to improve this work. We would like to thank Prof. Gang Zhao, Yuqin Chen, Jianrong Shi, Yujuan Liu, Shu Liu, Kefeng Tan and the *Stellar Abundance and Galactic Evolution Group* at NAOC for sharing their programs for abundance analysis and the helpful discussions about data reduction and abundance analysis. This work was supported by the Natural Science Foundation of China (NSFC) Foundation under No.10403006, 10433010, 10673002, 10573022, 10333060, and 10521001; and the National Basic Research Program of China (973 Program) No.2007CB815404, 2007CB815406, 2009CB824800.

References

- Alonso S., Arribas S., Martínez-Roger C., 1999, *A&AS*, 140, 261
 Alonso S., Arribas S., Martínez-Roger C., 2001, *A&A*, 376, 1039
 Bard A., Kock M., 1994, *A&A*, 282, 1014
 Bidelman W. K., Keenan P. C., 1951, *ApJ*, 114, 473
 Biémont E., Grevesse N., Hannaford P., Lowe R. M., 1981, *ApJ*, 248, 867
 Biémont E., Karner C., Meyer G., Traeger F., Zu Putlitz G., 1982, *A&A*, 107, 166
 Boffin H. M. J., Jorissen A., 1988, *A&A*, 205, 155
 Boffin H. M. J., Začs L., 1994, *A&A*, 291, 811
 Bond H. E., 1974, *ApJ*, 194, 95
 Burbidge E. M., Burbidge G. R., Fowler W. A., Hoyle F., 1957, *RvMP*, 29, 547
 Carquillat J. M., Jorissen A., Udry S., Ginestet N., 1998, *AAS*, 131, 49
 Chen Y. Q., Nissen P. E., Zhao G., Schuster W. J., Zhang H. W., Benoni, T., 2000a, *LIACo*, 35, 219
 Chen Y. Q., Nissen P. E., Zhao G., Zhang H. W., Benoni T., 2000b, *A&AS*, 141, 491
 ESA 1997, the Hipparcos and Tycho Catalogues, ESA SP-1200
 Fuhr J. R., Martin G. A., Wiese W. L., 1988, *JPCRD*, 17, Suppl.4
 Gallino R., Arlandini C., Busso M. et al., 1998, *ApJ*, 497, 388
 Gómez A. E., Luri X., Grenier S. et al., 1997, *A&A*, 319, 881
 Grevesse N., Sauval A. J., 1998, *Space Sci. Rev.*, 85, 161
 Griffin R. F., 1980, *MNRAS*, 193, 957
 Han Z. W., Eggleton P. P., Podsiadlowski P., Tout, C. A., 1995, *MNRAS*, 277, 1443
 Hannaford P., Lowe R. M., Grevesse N., Biémont E., Whaling W., 1982, *ApJ*, 261, 736
 Jorissen A., Mayor, M., 1988, *A&A*, 198, 187
 Jorissen A., Van Eck S., Mayor M., Udry, S., 1998, *A&A*, 332, 877
 Krishnaswamy K., Sneden C., 1985, *PASP*, 97, 407
 Kurucz R. L., 1993, CD-ROM, Vol. 13, Smithsonian Astrophysics Observatory, Cambridge
 Lambert D. L., Warner B., 1968, *MNRAS*, 139, 115
 Lambert D. L., Smith V. V., Heath J., 1993, *PASP*, 105, 568
 Lambert D. L., Heath J. H., Lemke M. et al., 1996, *ApJS*, 103, 183
 Liang Y. C., Zhao G., Zhang B., 2000, *A&A*, 363, 555
 Liang Y. C., Zhao G., Chen Y. Q., Qiu H. M., Zhang B., 2003, *A&A*, 397, 257
 Liu J. H., Zhang B., Liang Y. C., Peng, Q. H., 2000, *A&A*, 363, 660
 Luck R. E., Bond H. E., 1982, *ApJ*, 259, 792
 Luck R. E., Bond H. E., 1991, *ApJS*, 77, 515
 Lü Phillip K., 1991, *AJ*, 101, 2229

- McClure R. D., Fletcher J. M., Nemeč, J. M., 1980, ApJ, 238, L35
McClure R. D., 1983, ApJ, 268, 264
McClure R. D., Woodsworth A. W., 1990, ApJ, 352, 709
Mennessier M. O., Luri X., Figueras F. et al., 1997, A&A, 326, 722
Nissen P. E., Chen Y. Q., Schuster W. J., Zhao G., 2000, A&A, 353, 722
O'Brian T. R., Wickliffe M. E., Lawler J. E. et al., 1991, JOSAB, 8, 1185
Preston G. W., Sneden C., 2001, AJ, 122, 1545
Smith V. V., Coleman H., Lambert D., 1993, MNRAS, 417, 287
Smiljanic R., Porto de Mello G. F., da Silva L., 2007, A&A, 468, 679
Sneden C., 1983, PASP, 95, 745
Udry S., Jorissen A., Mayor M., Van Eck, S., 1998a, A&AS, 131, 25
Udry S., Mayor M., Van Eck S., Jorissen A., Prévot L., Grenier, S., Lindgren H., 1998b, A&AS, 131, 43
Weise W. L., Martin, G. A., 1980, NSDRS-NBS, 68
Yi S. K., Kim Y. C., Demarque P., 2003, ApJS, 144, 259
Začs L., 1994, A&A, 283, 937
Zhang B., Liu J. H., Liang Y. C., Peng Q. H., 1999, ChA&A, 23, 189
Zhao G., Qiu H. M., Chen Y. Q., Li Z. W., 2000, ApJ, 126, 461

Table 2 (continued)

| λ (Å) | Ion | χ | $\log gf$ | Ref. | HD 4395 | | HD 180622 | | HD 201657 | | HD 201824 | | HD 210946 | | HD 211594 | | HD 216219 | | HD 223617 | |
|---------------|------|--------|-----------|------|---------|-----------------|-----------|-----------------|-----------|-----------------|-----------|-----------------|-----------|-----------------|-----------|-----------------|-----------|-----------------|-----------|-----------------|
| | | | | | EW | $\log \epsilon$ | EW | $\log \epsilon$ | EW | $\log \epsilon$ | EW | $\log \epsilon$ | EW | $\log \epsilon$ | EW | $\log \epsilon$ | EW | $\log \epsilon$ | EW | $\log \epsilon$ |
| 5859.596 | Fe I | 4.55 | -0.66 | lz | — | — | — | — | — | — | — | — | — | — | — | — | 71.9 | 7.394 | — | — |
| 5862.368 | Fe I | 4.55 | -0.45 | lz | — | — | — | — | 94.1 | 6.912 | — | — | — | — | 87.6 | 6.871 | 70.3 | 7.155 | — | — |
| 5905.680 | Fe I | 4.65 | -0.73 | lz | — | — | — | — | 71.2 | 6.914 | — | — | — | — | 66.7 | 6.897 | 49.9 | 7.160 | 75.6 | 7.096 |
| 5927.797 | Fe I | 4.65 | -1.09 | lz | — | — | 81.3 | 7.617 | 50.0 | 6.906 | — | — | — | — | 45.6 | 6.884 | 37.7 | 7.290 | — | — |
| 5929.682 | Fe I | 4.55 | -1.41 | lz | — | — | — | — | 59.8 | 7.269 | 57.3 | 7.206 | 56.4 | 7.283 | 60.7 | 7.349 | — | — | 63.5 | 7.426 |
| 5930.191 | Fe I | 4.65 | -0.23 | lz | — | — | — | — | — | — | — | — | — | — | — | — | 75.0 | 7.110 | — | — |
| 5934.665 | Fe I | 3.93 | -1.17 | lz | 77.2 | 7.352 | — | — | — | — | — | — | — | — | — | — | 56.9 | 7.013 | — | — |
| 5952.726 | Fe I | 3.98 | -1.44 | nd | — | — | — | — | — | — | — | — | — | — | 81.0 | 7.033 | — | — | — | — |
| 6003.022 | Fe I | 3.88 | -1.12 | lz | 90.4 | 7.497 | — | — | — | — | — | — | — | — | — | — | 71.6 | 7.185 | — | — |
| 6024.068 | Fe I | 4.55 | -0.12 | nd | — | — | — | — | — | — | — | — | — | — | — | — | 93.6 | 7.224 | — | — |
| 6027.059 | Fe I | 4.07 | -1.09 | cn | 67.0 | 7.208 | — | — | — | — | — | — | 94.8 | 7.062 | 91.9 | 6.991 | — | — | 98.0 | 7.165 |
| 6034.033 | Fe I | 4.31 | -2.42 | nd | — | — | 45.2 | 7.847 | — | — | — | — | — | — | — | — | — | — | — | — |
| 6056.013 | Fe I | 4.73 | -0.46 | lz | 71.6 | 7.316 | — | — | 88.8 | 7.044 | 89.7 | 7.088 | 90.0 | 7.141 | 80.8 | 6.969 | 64.3 | 7.221 | 94.5 | 7.275 |
| 6079.016 | Fe I | 4.65 | -1.12 | lz | — | — | 86.8 | 7.746 | 68.6 | 7.251 | — | — | 73.3 | 7.404 | 66.5 | 7.278 | — | — | 77.2 | 7.507 |
| 6093.649 | Fe I | 4.61 | -1.50 | lz | 26.2 | 7.355 | 71.6 | 7.787 | 49.4 | 7.248 | 38.6 | 7.022 | 50.9 | 7.344 | 45.9 | 7.247 | — | — | 58.9 | 7.500 |
| 6094.370 | Fe I | 4.65 | -1.94 | nd | — | — | — | — | — | — | — | — | — | — | 32.1 | 7.472 | — | — | — | — |
| 6096.671 | Fe I | 3.98 | -1.93 | lz | 41.9 | 7.471 | 83.1 | 7.638 | 62.4 | 7.091 | — | — | 65.7 | 7.263 | 54.4 | 7.051 | 23.1 | 7.136 | 69.9 | 7.350 |
| 6105.150 | Fe I | 4.55 | -2.07 | nd | — | — | — | — | — | — | — | — | 32.2 | 7.492 | — | — | — | — | — | — |
| 6137.002 | Fe I | 2.20 | -2.87 | cn | — | — | — | — | — | — | — | — | — | — | — | — | 77.0 | 7.304 | — | — |
| 6151.623 | Fe I | 2.18 | -3.28 | cn | 56.6 | 7.213 | — | — | — | — | — | — | — | — | — | — | — | — | — | — |
| 6157.733 | Fe I | 4.07 | -1.26 | nd | — | — | — | — | — | — | — | — | — | — | — | — | 62.4 | 7.334 | — | — |
| 6159.370 | Fe I | 4.61 | -1.97 | nd | — | — | — | — | 37.2 | 7.494 | 28.7 | 7.288 | — | — | 42.0 | 7.643 | — | — | — | — |
| 6165.363 | Fe I | 4.14 | -1.47 | cn | 42.5 | 7.187 | 98.5 | 7.682 | 82.3 | 7.180 | — | — | 80.5 | 7.259 | 71.6 | 7.086 | — | — | 82.9 | 7.331 |
| 6173.341 | Fe I | 2.22 | -2.88 | cn | 79.3 | 7.301 | — | — | — | — | — | — | — | — | — | — | — | — | — | — |
| 6180.209 | Fe I | 2.73 | -2.58 | cn | 68.4 | 7.327 | — | — | — | — | — | — | — | — | — | — | 47.4 | 7.013 | — | — |
| 6187.995 | Fe I | 3.94 | -1.72 | cn | 55.8 | 7.482 | 97.8 | 7.657 | 84.8 | 7.208 | 75.1 | 7.066 | 70.1 | 7.074 | 83.5 | 7.294 | — | — | 86.8 | 7.401 |
| 6200.321 | Fe I | 2.61 | -2.44 | cn | 74.4 | 7.172 | — | — | — | — | — | — | — | — | — | — | 64.5 | 7.059 | — | — |

Table 2 (continued)

| λ (Å) | Ion | χ | $\log gf$ | Ref. | HD 4395 | | HD 180622 | | HD 201657 | | HD 201824 | | HD 210946 | | HD 211594 | | HD 216219 | | HD 223617 | |
|---------------|------|--------|-----------|------|---------|-----------------|-----------|-----------------|-----------|-----------------|-----------|-----------------|-----------|-----------------|-----------|-----------------|-----------|-----------------|-----------|-----------------|
| | | | | | EW | $\log \epsilon$ | EW | $\log \epsilon$ | EW | $\log \epsilon$ | EW | $\log \epsilon$ | EW | $\log \epsilon$ | EW | $\log \epsilon$ | EW | $\log \epsilon$ | EW | $\log \epsilon$ |
| 6213.437 | Fe I | 2.22 | -2.58 | nd | 89.2 | 7.197 | — | — | — | — | — | — | — | — | — | — | — | — | — | — |
| 6215.149 | Fe I | 4.19 | -1.13 | lz | 76.9 | 7.551 | — | — | — | — | 91.9 | 7.117 | — | — | — | — | 44.8 | 7.002 | — | — |
| 6229.232 | Fe I | 2.84 | -2.81 | cn | 42.7 | 7.168 | — | — | — | — | — | — | 86.5 | 7.065 | — | — | — | — | 99.2 | 7.313 |
| 6232.648 | Fe I | 3.65 | -1.22 | cn | 91.0 | 7.365 | — | — | — | — | — | — | — | — | — | — | 77.0 | 7.154 | — | — |
| 6240.653 | Fe I | 2.22 | -3.27 | cn | 70.9 | 7.514 | — | — | — | — | — | — | — | — | — | — | 43.9 | 7.099 | — | — |
| 6246.327 | Fe I | 3.60 | -0.88 | cn | — | — | — | — | — | — | — | — | — | — | — | — | 94.2 | 7.104 | — | — |
| 6270.231 | Fe I | 2.86 | -2.61 | cn | 63.1 | 7.377 | — | — | — | — | — | — | — | — | — | — | 50.1 | 7.220 | — | — |
| 6301.508 | Fe I | 3.65 | -0.72 | cn | — | — | — | — | — | — | — | — | — | — | — | — | 95.5 | 6.972 | — | — |
| 6330.852 | Fe I | 4.73 | -1.74 | nd | — | — | — | — | — | — | — | — | — | — | 49.1 | 7.683 | — | — | — | — |
| 6336.830 | Fe I | 3.69 | -0.86 | cn | — | — | — | — | — | — | — | — | — | — | — | — | 85.8 | 6.969 | — | — |
| 6344.155 | Fe I | 2.43 | -2.90 | cn | — | — | — | — | — | — | — | — | — | — | — | — | 68.2 | 7.379 | — | — |
| 6358.687 | Fe I | 0.86 | -4.17 | cn | 90.6 | 7.299 | — | — | — | — | — | — | — | — | — | — | — | — | — | — |
| 6380.750 | Fe I | 4.19 | -1.29 | cn | 59.8 | 7.375 | — | — | — | — | — | — | 97.5 | 7.431 | 85.2 | 7.195 | 39.2 | 7.036 | — | — |
| 6408.026 | Fe I | 3.69 | -1.01 | cn | — | — | — | — | — | — | — | — | — | — | — | — | 88.4 | 7.165 | — | — |
| 6419.956 | Fe I | 4.73 | -0.24 | nd | — | — | — | — | — | — | — | — | — | — | — | — | 74.0 | 7.147 | — | — |
| 6481.878 | Fe I | 2.28 | -2.97 | cn | 78.4 | 7.401 | — | — | — | — | — | — | — | — | — | — | 59.1 | 7.119 | — | — |
| 6551.676 | Fe I | 0.99 | -5.79 | nd | — | — | — | — | — | — | — | — | 58.2 | 7.187 | — | — | — | — | — | — |
| 6593.884 | Fe I | 2.43 | -2.42 | cn | 97.7 | 7.381 | — | — | — | — | — | — | — | — | — | — | — | — | — | — |
| 6597.561 | Fe I | 4.80 | -1.06 | lz | 40.4 | 7.379 | — | — | 57.0 | 7.171 | 58.7 | 7.155 | 60.3 | 7.276 | 51.2 | 7.118 | 29.6 | 7.210 | 66.1 | 7.401 |
| 6608.024 | Fe I | 2.28 | -4.04 | nd | 20.6 | 7.306 | 92.2 | 7.638 | — | — | — | — | — | — | — | — | — | — | — | — |
| 6609.118 | Fe I | 2.56 | -2.66 | cn | 71.3 | 7.233 | — | — | — | — | — | — | — | — | — | — | — | — | — | — |
| 6646.932 | Fe I | 2.61 | -3.99 | nd | 14.0 | 7.397 | — | — | — | — | — | — | 48.4 | 7.302 | 50.3 | 7.288 | — | — | — | — |
| 6703.576 | Fe I | 2.76 | -3.16 | lz | 42.5 | 7.400 | — | — | — | — | 74.5 | 6.942 | 95.8 | 7.433 | 92.6 | 7.340 | — | — | — | — |
| 6716.220 | Fe I | 4.58 | -1.93 | nd | 16.9 | 7.467 | — | — | — | — | — | — | — | — | — | — | — | — | — | — |
| 6725.353 | Fe I | 4.19 | -2.30 | nd | 15.0 | 7.378 | 55.9 | 7.741 | 42.2 | 7.367 | 26.8 | 7.039 | 37.0 | 7.362 | — | — | — | — | — | — |
| 6726.673 | Fe I | 4.61 | -1.00 | cn | 43.8 | 7.186 | 81.7 | 7.441 | 62.6 | 6.958 | — | — | 70.5 | 7.155 | 59.0 | 6.954 | 35.8 | 7.084 | 69.9 | 7.170 |
| 6733.151 | Fe I | 4.64 | -1.58 | lz | 18.4 | 7.222 | 64.8 | 7.745 | 52.1 | 7.395 | 32.7 | 6.991 | — | — | 52.5 | 7.455 | — | — | 52.7 | 7.473 |

Table 2 (continued)

| λ (Å) | Ion | χ | $\log gf$ | Ref. | HD 4395 | | HD 180622 | | HD 201657 | | HD 201824 | | HD 210946 | | HD 211594 | | HD 216219 | | HD 223617 | |
|---------------|------|--------|-----------|------|---------|-----------------|-----------|-----------------|-----------|-----------------|-----------|-----------------|-----------|-----------------|-----------|-----------------|-----------|-----------------|-----------|-----------------|
| | | | | | EW | $\log \epsilon$ | EW | $\log \epsilon$ | EW | $\log \epsilon$ | EW | $\log \epsilon$ | EW | $\log \epsilon$ | EW | $\log \epsilon$ | EW | $\log \epsilon$ | EW | $\log \epsilon$ |
| 6745.090 | Fe I | 4.58 | -2.17 | nd | — | — | 40.4 | 7.812 | — | — | 19.9 | 7.211 | 22.8 | 7.398 | — | — | — | — | — | — |
| 6746.932 | Fe I | 2.61 | -4.25 | nd | — | — | — | — | — | — | — | — | 23.0 | 7.079 | — | — | — | — | — | — |
| 6752.716 | Fe I | 4.64 | -1.20 | bk | 29.1 | 7.121 | — | — | — | — | — | — | — | — | 84.0 | 7.625 | — | — | — | — |
| 6786.856 | Fe I | 4.19 | -2.06 | nd | 26.6 | 7.459 | 71.6 | 7.779 | 47.6 | 7.221 | — | — | 55.3 | 7.438 | 46.7 | 7.281 | — | — | — | — |
| 6806.856 | Fe I | 2.73 | -3.21 | lz | 43.0 | 7.421 | — | — | — | — | 80.9 | 7.054 | 92.6 | 7.379 | 89.8 | 7.294 | 25.7 | 7.161 | 99.7 | 7.515 |
| 6810.267 | Fe I | 4.61 | -0.99 | cn | 51.5 | 7.311 | 91.6 | 7.605 | 76.5 | 7.177 | — | — | 77.0 | 7.249 | 67.1 | 7.077 | 34.5 | 7.040 | 79.2 | 7.320 |
| 6828.596 | Fe I | 4.64 | -0.92 | lz | 59.0 | 7.412 | — | — | 97.6 | 7.503 | 73.2 | 7.065 | 91.4 | 7.468 | 93.8 | 7.510 | 45.2 | 7.207 | — | — |
| 6839.835 | Fe I | 2.56 | -3.45 | lz | 42.9 | 7.477 | — | — | — | — | 76.6 | 6.997 | 97.6 | 7.483 | — | — | — | — | — | — |
| 6841.341 | Fe I | 4.61 | -0.75 | nd | — | — | — | — | — | — | — | — | — | — | — | 61.6 | 7.301 | — | — | |
| 6842.689 | Fe I | 4.64 | -1.32 | lz | — | — | 85.0 | 7.853 | 70.0 | 7.438 | 55.7 | 7.151 | 67.4 | 7.453 | 67.6 | 7.455 | — | — | 69.1 | 7.507 |
| 6843.655 | Fe I | 4.55 | -0.93 | lz | 62.3 | 7.390 | — | — | 97.5 | 7.394 | — | — | — | — | 88.0 | 7.305 | 49.8 | 7.211 | — | — |
| 6858.155 | Fe I | 4.61 | -0.93 | cn | 59.7 | 7.403 | 97.6 | 7.656 | 83.6 | 7.238 | — | — | 81.5 | 7.268 | 85.5 | 7.336 | — | — | 86.1 | 7.387 |
| 6999.885 | Fe I | 4.10 | -1.56 | nd | — | — | — | — | 91.9 | 7.331 | — | — | 90.7 | 7.418 | — | — | — | — | 96.1 | 7.549 |
| 7022.957 | Fe I | 4.19 | -1.25 | nd | — | — | — | — | 87.6 | 7.066 | 92.7 | 7.171 | — | — | 98.7 | 7.344 | — | — | — | — |
| 7071.866 | Fe I | 4.61 | -1.70 | lz | — | — | 68.8 | 7.891 | 51.7 | 7.463 | 42.2 | 7.246 | — | — | — | — | — | — | 55.9 | 7.605 |
| 7112.170 | Fe I | 2.99 | -2.99 | cn | — | — | — | — | — | — | — | — | 88.5 | 7.400 | 98.3 | 7.532 | — | — | — | — |
| 7132.985 | Fe I | 4.07 | -1.63 | cn | 47.5 | 7.308 | 93.8 | 7.573 | 75.3 | 7.077 | — | — | 69.6 | 7.079 | 77.6 | 7.199 | 35.5 | 7.142 | 77.6 | 7.234 |
| 7219.680 | Fe I | 4.07 | -1.35 | ow | — | — | — | — | — | — | 93.6 | 7.119 | — | — | — | — | — | — | — | — |
| 7284.842 | Fe I | 4.14 | -1.75 | nd | — | — | 80.1 | 7.528 | — | — | 70.8 | 7.193 | — | — | — | — | — | — | — | — |
| 7306.570 | Fe I | 4.18 | -1.74 | lz | — | — | 99.5 | 7.909 | 65.8 | 7.168 | — | — | 77.9 | 7.454 | 68.5 | 7.285 | — | — | 72.9 | 7.388 |
| 7401.691 | Fe I | 4.19 | -1.60 | cn | 46.4 | 7.366 | 91.9 | 7.638 | 75.3 | 7.189 | 64.9 | 6.994 | 76.1 | 7.289 | 73.2 | 7.229 | 32.9 | 7.168 | 92.7 | 7.604 |
| 7418.672 | Fe I | 4.14 | -1.38 | ow | — | — | — | — | 80.7 | 6.987 | — | — | 83.4 | 7.126 | 80.3 | 7.061 | 38.4 | 7.001 | 87.6 | 7.226 |
| 7443.026 | Fe I | 4.19 | -1.82 | nd | — | — | 85.5 | 7.742 | — | — | — | — | — | — | — | — | 25.8 | 7.232 | — | — |
| 7583.796 | Fe I | 3.02 | -1.88 | cn | 89.2 | 7.197 | — | — | — | — | — | — | — | — | — | — | — | — | — | — |
| 7710.367 | Fe I | 4.22 | -1.11 | cn | — | — | — | — | 99.0 | 7.107 | 93.1 | 7.023 | — | — | — | — | 54.1 | 7.086 | — | — |
| 7723.210 | Fe I | 2.28 | -3.62 | fm | 39.9 | 7.234 | — | — | — | — | — | — | 98.3 | 7.206 | — | — | — | — | — | — |
| 7746.605 | Fe I | 5.06 | -1.34 | nd | — | — | 58.1 | 7.874 | — | — | — | — | 34.0 | 7.355 | 42.8 | 7.519 | — | — | — | — |

Table 2 (continued)

| λ (Å) | Ion | χ | $\log gf$ | Ref. | HD 4395 | | HD 180622 | | HD 201657 | | HD 201824 | | HD 210946 | | HD 211594 | | HD 216219 | | HD 223617 | |
|---------------|-------|--------|-----------|------|---------|-----------------|-----------|-----------------|-----------|-----------------|-----------|-----------------|-----------|-----------------|-----------|-----------------|-----------|-----------------|-----------|-----------------|
| | | | | | EW | $\log \epsilon$ | EW | $\log \epsilon$ | EW | $\log \epsilon$ | EW | $\log \epsilon$ | EW | $\log \epsilon$ | EW | $\log \epsilon$ | EW | $\log \epsilon$ | EW | $\log \epsilon$ |
| 7751.116 | Fe I | 4.99 | -0.72 | cn | 40.4 | 7.175 | — | — | — | — | — | — | 79.7 | 7.440 | — | — | 33.8 | 7.092 | — | — |
| 7780.568 | Fe I | 4.47 | -0.09 | cn | — | — | — | — | — | — | — | — | — | — | — | — | 98.9 | 7.062 | — | — |
| 7941.096 | Fe I | 3.27 | -2.58 | nd | 51.6 | 7.445 | — | — | — | — | — | — | 72.8 | 7.036 | 73.6 | 7.005 | — | — | — | — |
| 5991.378 | Fe II | 3.15 | -3.56 | cn | 37.6 | 7.279 | 46.8 | 7.732 | — | — | — | — | — | — | — | — | 43.8 | 7.346 | — | — |
| 6084.110 | Fe II | 3.20 | -3.97 | nd | 20.3 | 7.318 | — | — | — | — | — | — | — | — | — | — | — | — | — | — |
| 6149.249 | Fe II | 3.89 | -2.72 | cn | 37.8 | 7.189 | — | — | — | — | — | — | — | — | — | — | 45.4 | 7.281 | 47.4 | 7.536 |
| 6247.562 | Fe II | 3.89 | -2.26 | lh | 68.5 | 7.371 | — | — | 51.7 | 7.319 | — | — | 64.5 | 7.351 | — | — | — | — | 62.1 | 7.412 |
| 6369.462 | Fe II | 2.89 | -4.36 | nd | 29.5 | 7.628 | — | — | — | — | — | — | — | — | — | — | — | — | — | — |
| 6416.928 | Fe II | 3.89 | -2.74 | cn | — | — | — | — | — | — | 50.6 | 7.109 | — | — | — | — | — | — | — | — |
| 6432.683 | Fe II | 2.89 | -3.58 | cn | 52.4 | 7.344 | 58.9 | 7.738 | 46.1 | 7.308 | — | — | 57.4 | 7.354 | — | — | 53.4 | 7.273 | 51.2 | 7.316 |
| 6456.391 | Fe II | 3.90 | -2.07 | cn | 76.1 | 7.335 | — | — | — | — | — | — | 77.1 | 7.435 | — | — | — | — | — | — |
| 7711.731 | Fe II | 3.90 | -2.47 | cn | 47.6 | 7.087 | — | — | — | — | 66.4 | 7.161 | — | — | — | — | — | — | 59.5 | 7.570 |
| 6154.230 | Na I | 2.10 | -1.57 | cn | 28.7 | 6.007 | 125.2 | 6.688 | 86.4 | 5.993 | 53.0 | 5.829 | — | — | 83.3 | 6.145 | 24.7 | 5.987 | 96.6 | 6.369 |
| 6160.753 | Na I | 2.10 | -1.23 | cn | 55.1 | 6.102 | 141.6 | 6.583 | 112.1 | 5.993 | 81.3 | 5.890 | 101.7 | 6.123 | 104.5 | 6.090 | 34.8 | 5.843 | 117.1 | 6.323 |
| 5528.418 | Mg I | 4.34 | -0.78 | nd | — | — | — | — | — | — | — | — | — | — | — | — | 193.0 | 7.286 | — | — |
| 5711.095 | Mg I | 4.34 | -1.82 | nd | 80.3 | 7.126 | 162.8 | 7.780 | 151.0 | 7.416 | 136.7 | 7.463 | 82.6 | 6.606 | — | — | 88.4 | 7.288 | 146.3 | 7.555 |
| 7657.606 | Mg I | 5.11 | -1.19 | nd | 91.3 | 7.265 | — | — | — | — | 104.6 | 7.103 | — | — | 111.5 | 7.148 | 80.8 | 7.176 | 153.1 | 7.722 |
| 6696.020 | Al I | 3.14 | -1.33 | lw | 43.3 | 6.211 | — | — | — | — | — | — | — | — | — | — | — | — | — | — |
| 6698.670 | Al I | 3.14 | -1.87 | cn | 19.7 | 6.275 | 105.9 | 6.987 | 71.4 | 6.374 | 43.0 | 6.207 | 50.8 | 6.321 | 64.4 | 6.452 | 13.3 | 6.134 | 56.0 | 6.352 |
| 7835.317 | Al I | 4.02 | -0.58 | cn | 42.5 | 6.258 | 129.3 | 7.032 | 110.5 | 6.653 | 67.6 | 6.304 | — | — | — | — | 23.3 | 5.944 | — | — |
| 7836.130 | Al I | 4.02 | -0.40 | cn | 48.7 | 6.169 | 111.8 | 6.625 | 88.4 | 6.201 | 67.9 | 6.128 | 96.5 | 6.488 | 68.5 | 6.055 | 40.9 | 6.092 | — | — |
| 5665.563 | Si I | 4.92 | -2.04 | cn | 37.0 | 7.382 | 103.6 | — | — | — | — | — | — | — | — | — | 32.8 | 7.330 | 78.9 | 7.918 |
| 5690.433 | Si I | 4.93 | -1.87 | cn | — | — | 79.3 | 7.882 | — | — | — | — | — | — | — | — | — | — | — | — |
| 5701.108 | Si I | 4.93 | -2.05 | cn | 51.6 | 7.655 | — | — | 67.1 | 7.749 | — | — | 57.0 | 7.524 | 43.9 | 7.329 | 31.7 | 7.328 | 66.7 | 7.729 |
| 5772.149 | Si I | 5.08 | -1.67 | cn | 47.9 | 7.349 | — | — | — | — | — | — | — | — | — | — | 46.0 | 7.338 | 88.1 | 7.882 |
| 5793.079 | Si I | 4.93 | -1.95 | cn | 53.7 | 7.582 | 88.1 | 8.112 | 76.9 | 7.810 | — | — | 62.1 | 7.505 | 71.7 | 7.701 | 43.7 | 7.438 | 71.4 | 7.706 |
| 5948.548 | Si I | 5.08 | -1.19 | cn | 84.7 | 7.447 | — | — | — | — | 84.6 | 7.127 | — | — | 120.5 | 7.866 | 74.7 | 7.304 | — | — |

Table 2 (continued)

| λ (Å) | Ion | χ | $\log gf$ | Ref. | HD 4395 | | HD 180622 | | HD 201657 | | HD 201824 | | HD 210946 | | HD 211594 | | HD 216219 | | HD 223617 | |
|---------------|------|--------|-----------|------|---------|-----------------|-----------|-----------------|-----------|-----------------|-----------|-----------------|-----------|-----------------|-----------|-----------------|-----------|-----------------|-----------|-----------------|
| | | | | | EW | $\log \epsilon$ | EW | $\log \epsilon$ | EW | $\log \epsilon$ | EW | $\log \epsilon$ | EW | $\log \epsilon$ | EW | $\log \epsilon$ | EW | $\log \epsilon$ | EW | $\log \epsilon$ |
| 6125.026 | Si I | 5.61 | -1.54 | lz | 42.5 | 7.642 | — | — | — | — | — | — | — | — | 77.7 | 8.177 | — | — | — | — |
| 6142.494 | Si I | 5.62 | -1.48 | ns | — | — | 58.0 | 7.940 | — | — | — | — | — | — | — | — | 31.8 | 7.415 | 50.8 | 7.686 |
| 6145.020 | Si I | 5.62 | -1.43 | ns | 41.2 | 7.519 | — | — | 55.3 | 7.771 | 41.3 | 7.253 | — | — | 29.7 | 7.229 | 32.1 | 7.370 | 53.5 | 7.685 |
| 7034.910 | Si I | 5.87 | -0.81 | cn | 51.7 | 7.279 | 83.7 | 8.001 | — | — | 53.7 | 7.135 | — | — | 60.1 | 7.463 | 51.9 | 7.287 | — | — |
| 7226.208 | Si I | 5.61 | -1.30 | nd | 35.1 | 7.226 | — | — | — | — | 49.5 | 7.235 | 61.4 | 7.617 | — | — | 32.4 | 7.189 | 68.9 | 7.801 |
| 7405.790 | Si I | 5.61 | -0.68 | cn | 84.2 | 7.360 | 118.4 | 8.070 | 110.9 | 7.855 | 97.6 | 7.404 | — | — | 119.4 | 7.884 | 82.5 | 7.334 | 115.6 | 7.889 |
| 7415.958 | Si I | 5.61 | -0.71 | cn | 94.9 | 7.549 | — | — | — | — | — | — | — | — | — | — | 93.4 | 7.524 | — | — |
| 7918.383 | Si I | 5.95 | -0.54 | cn | 79.9 | 7.433 | — | — | — | — | — | — | — | — | — | — | 65.8 | 7.245 | — | — |
| 7932.351 | Si I | 5.96 | -0.35 | cn | 106.1 | 7.576 | 98.0 | 7.823 | — | — | 134.4 | 7.982 | 83.7 | 7.411 | 93.4 | 7.574 | 94.9 | 7.435 | — | — |
| 5512.989 | Ca I | 2.93 | -0.53 | cn | — | — | — | — | 132.5 | 5.968 | 135.4 | 6.507 | 107.3 | 5.885 | 136.1 | 6.242 | 80.8 | 6.172 | — | — |
| 5581.979 | Ca I | 2.52 | -0.67 | cn | 111.3 | 6.364 | — | — | 192.2 | 6.336 | 153.5 | 6.440 | 147.9 | 6.179 | 184.3 | 6.481 | 98.7 | 6.222 | 159.5 | 6.358 |
| 5588.764 | Ca I | 2.52 | 0.06 | cn | — | — | — | — | 191.1 | 5.592 | 197.6 | 6.219 | 183.7 | 5.855 | 186.5 | 5.769 | — | — | 190.1 | 5.953 |
| 5590.126 | Ca I | 2.52 | -0.70 | cn | 102.6 | 6.267 | — | — | — | — | 118.7 | 5.864 | 128.0 | 5.908 | 133.2 | 5.890 | 93.1 | 6.164 | 149.8 | 6.255 |
| 5601.286 | Ca I | 2.52 | -0.52 | cn | 125.8 | 6.411 | — | — | 162.9 | 5.867 | 120.8 | 5.724 | — | — | 161.5 | 6.095 | 106.7 | 6.191 | — | — |
| 5867.572 | Ca I | 2.93 | -1.61 | cn | — | — | 81.9 | 6.367 | — | — | — | — | 45.4 | 5.942 | 43.3 | 5.830 | 18.5 | 6.101 | — | — |
| 6102.727 | Ca I | 1.88 | -0.79 | nd | 138.6 | 6.156 | — | — | — | — | 189.2 | 6.077 | 191.3 | 5.886 | — | — | — | — | — | — |
| 6122.226 | Ca I | 1.89 | -0.32 | nd | 185.2 | 6.107 | — | — | — | — | 199.5 | 5.727 | — | — | — | — | — | — | — | — |
| 6161.295 | Ca I | 2.52 | -1.19 | cn | 75.0 | 6.264 | — | — | — | — | 129.5 | 6.452 | 112.4 | 6.060 | 128.6 | 6.221 | 54.4 | 5.981 | — | — |
| 6163.754 | Ca I | 2.52 | -1.07 | nd | — | — | — | — | — | — | 136.0 | 6.429 | — | — | — | — | — | — | — | — |
| 6166.440 | Ca I | 2.52 | -1.19 | cn | 68.2 | 6.144 | 130.4 | 6.214 | 133.1 | 6.009 | 103.8 | 5.987 | 110.8 | 6.030 | 121.9 | 6.112 | 57.3 | 6.030 | 117.3 | 6.116 |
| 6169.044 | Ca I | 2.52 | -0.80 | lz | 97.9 | 6.251 | — | — | — | — | 125.2 | 5.980 | 145.3 | 6.168 | 125.2 | 5.773 | 82.0 | 6.048 | 153.7 | 6.293 |
| 6169.564 | Ca I | 2.52 | -0.51 | cn | — | — | — | — | — | — | 128.4 | 5.750 | 163.3 | 6.115 | 150.8 | 5.853 | 99.5 | 6.048 | 158.5 | 6.071 |
| 6439.083 | Ca I | 2.52 | 0.16 | cn | 168.9 | 6.201 | — | — | 185.7 | 5.328 | 166.5 | 5.625 | 193.5 | 5.763 | 188.4 | 5.604 | 148.9 | 5.998 | — | — |
| 6449.820 | Ca I | 2.52 | -0.50 | cn | 122.2 | 6.316 | — | — | — | — | — | — | — | — | 157.7 | 5.915 | — | — | — | — |
| 6455.605 | Ca I | 2.52 | -1.29 | cn | — | — | — | — | 110.9 | 5.736 | — | — | 93.3 | 5.821 | 100.7 | 5.847 | — | — | 105.4 | 5.981 |
| 6471.668 | Ca I | 2.52 | -0.69 | cn | 94.9 | 6.159 | — | — | — | — | 123.5 | 5.822 | 139.9 | 6.006 | — | — | 83.7 | 6.009 | — | — |
| 6493.788 | Ca I | 2.52 | -0.09 | cn | — | — | — | — | — | — | 168.1 | 5.952 | 178.6 | 5.954 | 185.6 | 5.942 | 116.9 | 5.981 | — | — |

Table 2 (continued)

| λ (Å) | Ion | χ | $\log gf$ | Ref. | HD 4395 | | HD 180622 | | HD 201657 | | HD 201824 | | HD 210946 | | HD 211594 | | HD 216219 | | HD 223617 | |
|---------------|-------|--------|-----------|------|---------|-----------------|-----------|-----------------|-----------|-----------------|-----------|-----------------|-----------|-----------------|-----------|-----------------|-----------|-----------------|-----------|-----------------|
| | | | | | EW | $\log \epsilon$ | EW | $\log \epsilon$ | EW | $\log \epsilon$ | EW | $\log \epsilon$ | EW | $\log \epsilon$ | EW | $\log \epsilon$ | EW | $\log \epsilon$ | EW | $\log \epsilon$ |
| 6499.654 | Ca I | 2.52 | -0.81 | cn | 88.6 | 6.156 | — | — | 141.4 | 5.750 | 106.0 | 5.620 | 127.5 | 5.921 | 129.3 | 5.856 | 71.0 | 5.893 | 139.2 | 6.096 |
| 6717.687 | Ca I | 2.71 | -0.52 | cn | — | — | — | — | 196.9 | 6.333 | 156.8 | 6.364 | — | — | 179.2 | 6.393 | 107.0 | 6.322 | — | — |
| 7148.150 | Ca I | 2.71 | -0.14 | cn | — | — | — | — | — | — | — | — | 191.7 | 6.180 | 190.5 | 6.058 | 137.2 | 6.292 | 189.5 | 6.179 |
| 5526.821 | Sc II | 1.77 | 0.13 | nd | — | — | 122.6 | 3.138 | 124.5 | 2.867 | 146.1 | 3.158 | 124.8 | 3.011 | 142.4 | 3.307 | 96.5 | 2.936 | 124.3 | 3.072 |
| 5657.880 | Sc II | 1.51 | -0.50 | nd | 81.5 | 3.056 | 121.3 | 3.384 | 102.2 | 2.734 | 104.2 | 2.617 | 96.0 | 2.766 | 102.4 | 2.887 | 85.1 | 3.069 | 110.2 | 3.080 |
| 5684.198 | Sc II | 1.51 | -0.20 | nd | — | — | — | — | — | — | — | — | — | — | 110.0 | 2.725 | 79.8 | 2.668 | — | — |
| 6245.620 | Sc II | 1.51 | -0.98 | lz | — | — | — | — | — | — | 97.2 | 2.894 | — | — | 98.0 | 3.233 | — | — | — | — |
| 6604.600 | Sc II | 1.36 | -1.16 | lz | 51.3 | 2.926 | 114.9 | 3.585 | 102.3 | 3.101 | — | — | 86.2 | 2.990 | 90.8 | 3.068 | 51.1 | 2.887 | — | — |
| 5866.461 | Ti I | 1.07 | -0.84 | cn | 42.2 | 4.519 | 178.3 | 5.360 | 141.3 | 4.315 | 86.0 | 3.949 | 117.1 | 4.444 | 110.6 | 4.196 | 36.0 | 4.522 | — | — |
| 5953.170 | Ti I | 1.89 | -0.21 | cn | 50.6 | 4.899 | 140.0 | 5.158 | 100.3 | 4.140 | 83.5 | 4.353 | — | — | — | — | 25.8 | 4.515 | 104.1 | 4.623 |
| 6126.224 | Ti I | 1.07 | -1.32 | cn | 29.3 | 4.731 | 129.7 | 4.875 | 131.7 | 4.556 | 108.9 | 4.760 | 93.7 | 4.494 | 114.3 | 4.689 | — | — | 112.8 | 4.736 |
| 6258.110 | Ti I | 1.44 | -0.43 | cn | 57.8 | 4.757 | — | — | — | — | 109.7 | 4.381 | — | — | — | — | 40.2 | 4.557 | 135.0 | 4.743 |
| 6261.106 | Ti I | 1.43 | -0.48 | cn | 65.1 | 4.925 | — | — | 137.8 | 4.313 | 109.2 | 4.406 | 121.3 | 4.577 | — | — | — | — | — | — |
| 6312.241 | Ti I | 1.46 | -1.55 | lz | — | — | 75.4 | 4.693 | 52.0 | 4.147 | 32.2 | 4.280 | 40.0 | 4.432 | — | — | — | — | 57.5 | 4.597 |
| 6599.110 | Ti I | 0.90 | -2.08 | lz | — | — | — | — | 73.4 | 4.146 | 39.6 | 4.178 | 62.5 | 4.529 | — | — | — | — | 84.9 | 4.736 |
| 6743.120 | Ti I | 0.90 | -1.63 | lz | 12.1 | 4.332 | 133.9 | 4.857 | — | — | 55.9 | 3.952 | 84.1 | 4.349 | — | — | — | — | 107.6 | 4.603 |
| 5727.057 | V I | 1.08 | -0.01 | cn | — | — | 164.1 | 4.431 | — | — | — | — | 128.3 | 3.907 | 194.5 | 4.807 | 41.1 | 3.806 | — | — |
| 6090.216 | V I | 1.08 | -0.14 | cn | 36.7 | 3.710 | 138.6 | 3.948 | 109.7 | 3.081 | — | — | 91.6 | 3.326 | 81.6 | 3.036 | 18.3 | 3.410 | 113.8 | 3.631 |
| 6216.358 | V I | 0.28 | -0.75 | lz | — | — | 162.5 | 3.772 | — | — | — | — | 103.2 | 2.940 | 70.3 | 2.349 | — | — | 137.5 | 3.440 |
| 5783.866 | Cr I | 3.32 | -0.20 | cn | 45.4 | 5.478 | 116.7 | 5.902 | 111.7 | 5.570 | — | — | 86.9 | 5.451 | 106.3 | 5.713 | 32.6 | 5.299 | 108.1 | 5.826 |
| 5787.926 | Cr I | 3.32 | -0.18 | cn | 38.5 | 5.333 | 109.6 | 5.749 | 86.3 | 5.118 | 75.2 | 5.263 | 70.7 | 5.158 | 62.1 | 4.939 | 31.7 | 5.266 | 87.8 | 5.430 |
| 6925.280 | Cr I | 3.45 | -0.33 | nd | 40.2 | 5.587 | — | — | 61.7 | 4.979 | 60.9 | 5.246 | 62.9 | 5.269 | 45.9 | 4.930 | 24.3 | 5.322 | — | — |
| 6978.383 | Cr I | 3.46 | 0.14 | cn | 63.1 | 5.536 | — | — | — | — | — | — | — | — | — | — | — | — | — | — |
| 6979.806 | Cr I | 3.46 | -0.41 | lz | 30.6 | 5.484 | 106.3 | 5.952 | — | — | 73.1 | 5.538 | 80.5 | 5.637 | 85.4 | 5.655 | 22.7 | 5.371 | 97.1 | 5.886 |
| 7355.891 | Cr I | 2.89 | -0.29 | cn | 63.0 | 5.351 | 155.6 | 5.806 | — | — | 89.9 | 4.927 | — | — | — | — | 54.4 | 5.272 | 152.4 | 5.860 |
| 7400.188 | Cr I | 2.90 | -0.17 | cn | 67.2 | 5.315 | 164.7 | 5.825 | 137.9 | 5.168 | — | — | 126.4 | 5.369 | 120.9 | 5.191 | — | — | 140.6 | 5.571 |
| 6013.497 | Mn I | 3.07 | -0.15 | lz | 94.8 | 5.413 | 177.0 | 5.800 | 140.0 | 5.004 | 124.5 | 5.102 | 138.4 | 5.270 | 136.7 | 5.164 | 67.2 | 4.989 | 147.9 | 5.449 |

Table 2 (continued)

| λ (Å) | Ion | χ | $\log gf$ | Ref. | HD 4395 | | HD 180622 | | HD 201657 | | HD 201824 | | HD 210946 | | HD 211594 | | HD 216219 | | HD 223617 | |
|---------------|------|--------|-----------|------|---------|-----------------|-----------|-----------------|-----------|-----------------|-----------|-----------------|-----------|-----------------|-----------|-----------------|-----------|-----------------|-----------|-----------------|
| | | | | | EW | $\log \epsilon$ | EW | $\log \epsilon$ | EW | $\log \epsilon$ | EW | $\log \epsilon$ | EW | $\log \epsilon$ | EW | $\log \epsilon$ | EW | $\log \epsilon$ | EW | $\log \epsilon$ |
| 6021.803 | Mn I | 3.07 | 0.02 | lz | 68.5 | 4.778 | 170.2 | 5.555 | 138.4 | 4.810 | 121.0 | 4.864 | 137.7 | 5.090 | 132.5 | 4.933 | 64.5 | 4.773 | 147.3 | 5.271 |
| 5578.729 | Ni I | 1.68 | -2.80 | cn | — | — | — | — | — | — | 135.5 | 6.412 | — | — | 146.8 | 6.608 | — | — | 124.7 | 6.324 |
| 5587.868 | Ni I | 1.93 | -2.14 | fm | — | — | — | — | — | — | 128.4 | 5.930 | 137.3 | 6.167 | — | — | 62.5 | 5.750 | — | — |
| 5593.746 | Ni I | 3.90 | -0.84 | cn | 51.9 | 6.202 | 93.2 | 6.575 | 77.1 | 6.079 | 66.4 | 5.835 | 67.7 | 5.988 | 82.9 | 6.254 | 38.0 | 5.990 | — | — |
| 5625.328 | Ni I | 4.09 | -0.70 | fm | — | — | — | — | — | — | — | — | — | — | 86.5 | 6.400 | 39.1 | 6.056 | — | — |
| 5694.991 | Ni I | 4.09 | -0.61 | cn | 48.4 | 6.091 | — | — | 85.1 | 6.222 | 64.9 | 5.802 | 73.7 | 6.085 | 71.5 | 6.046 | 40.6 | 5.991 | — | — |
| 5754.666 | Ni I | 1.93 | -2.33 | fm | — | — | — | — | — | — | 138.3 | 6.278 | — | — | 130.0 | 6.142 | 69.5 | 6.056 | — | — |
| 5805.226 | Ni I | 4.17 | -0.64 | cn | — | — | 72.2 | 6.297 | 49.7 | 5.742 | — | — | 63.9 | 6.033 | — | — | — | — | — | — |
| 6086.288 | Ni I | 4.26 | -0.53 | cn | 44.3 | 6.088 | — | — | 62.5 | 5.961 | 73.0 | 6.060 | 60.6 | 5.963 | — | — | 29.8 | 5.850 | 67.2 | 6.116 |
| 6108.125 | Ni I | 1.68 | -2.63 | lz | 72.1 | 6.033 | 149.6 | 6.512 | 147.3 | 6.103 | — | — | 132.2 | 6.138 | — | — | 53.9 | 5.776 | 134.2 | 6.222 |
| 6111.078 | Ni I | 4.09 | -0.81 | fm | 30.6 | 5.927 | 76.5 | 6.436 | — | — | — | — | 62.9 | 6.076 | — | — | — | — | 74.3 | 6.316 |
| 6128.984 | Ni I | 1.68 | -3.33 | fm | 36.7 | 6.074 | 117.8 | 6.636 | 89.0 | 5.812 | 80.1 | 5.718 | 80.2 | 5.903 | 71.9 | 5.725 | 16.8 | 5.699 | 92.7 | 6.129 |
| 6130.141 | Ni I | 4.26 | -0.96 | cn | 25.6 | 6.139 | 63.3 | 6.555 | — | — | 43.9 | 5.951 | 38.8 | 6.004 | — | — | 14.4 | 5.872 | 40.3 | 6.047 |
| 6176.816 | Ni I | 4.09 | -0.26 | cn | — | — | — | — | — | — | — | — | 97.0 | 6.117 | — | — | 52.9 | 5.842 | 99.6 | 6.228 |
| 6327.604 | Ni I | 1.68 | -3.11 | cn | 40.5 | 5.911 | 132.5 | 6.654 | 120.0 | 6.098 | 94.6 | 5.737 | 94.9 | 5.915 | 84.6 | 5.699 | 25.2 | 5.686 | 108.7 | 6.184 |
| 6482.809 | Ni I | 1.93 | -2.63 | fm | 46.0 | 5.785 | 132.6 | 6.477 | 110.8 | 5.785 | — | — | — | — | — | — | — | — | — | — |
| 6586.319 | Ni I | 1.95 | -2.73 | cn | 55.4 | 6.071 | 120.0 | 6.359 | 90.3 | 5.560 | — | — | 105.3 | 6.039 | — | — | 27.4 | 5.624 | 106.4 | 6.082 |
| 6635.150 | Ni I | 4.42 | -0.83 | lz | 25.7 | 6.143 | 86.2 | 7.014 | — | — | 52.0 | 6.140 | — | — | — | — | 20.9 | 6.067 | — | — |
| 6643.638 | Ni I | 1.68 | -2.30 | fm | 107.5 | 6.300 | — | — | 168.1 | 5.964 | 133.0 | 5.601 | 160.3 | 6.131 | — | — | 87.4 | 6.007 | 177.0 | 6.410 |
| 6767.784 | Ni I | 1.83 | -2.17 | cn | 82.3 | 5.859 | 171.6 | 6.421 | 141.4 | 5.638 | — | — | — | — | — | — | 71.4 | 5.732 | 148.8 | 6.061 |
| 6772.321 | Ni I | 3.66 | -0.95 | lz | 48.2 | 5.938 | — | — | 87.6 | 6.009 | 63.9 | 5.528 | 83.2 | 6.014 | 78.6 | 5.937 | 35.5 | 5.753 | 89.7 | 6.171 |
| 7001.600 | Ni I | 1.94 | -3.66 | nd | 13.4 | 6.031 | 85.6 | 6.611 | — | — | 38.7 | 5.619 | 48.0 | 5.981 | 43.5 | 5.872 | — | — | — | — |
| 7030.010 | Ni I | 3.54 | -1.73 | nd | 20.2 | 5.995 | — | — | — | — | 30.4 | 5.542 | 39.4 | 5.893 | — | — | 14.9 | 5.891 | — | — |
| 7110.905 | Ni I | 1.93 | -2.92 | nd | 46.5 | 6.036 | 147.6 | 6.889 | 142.2 | 6.480 | — | — | — | — | 125.7 | 6.428 | 20.6 | 5.589 | — | — |
| 7122.206 | Ni I | 3.54 | 0.04 | cn | — | — | — | — | — | — | 162.5 | 6.031 | — | — | — | — | 98.6 | 5.691 | 194.5 | 6.417 |
| 7385.244 | Ni I | 2.74 | -1.97 | cn | 57.7 | 6.128 | 145.6 | 6.934 | 108.7 | 6.095 | 74.0 | 5.509 | 83.5 | 5.840 | 99.2 | 6.078 | 28.1 | 5.646 | 97.5 | 6.100 |
| 7414.514 | Ni I | 1.99 | -2.57 | cn | — | — | — | — | — | — | 120.3 | 5.923 | — | — | — | — | 61.4 | 6.073 | — | — |

Table 2 (continued)

| λ (Å) | Ion | χ | $\log gf$ | Ref. | HD 4395 | | HD 180622 | | HD 201657 | | HD 201824 | | HD 210946 | | HD 211594 | | HD 216219 | | HD 223617 | |
|---------------|-------|--------|-----------|------|---------|-----------------|-----------|-----------------|-----------|-----------------|-----------|-----------------|-----------|-----------------|-----------|-----------------|-----------|-----------------|-----------|-----------------|
| | | | | | EW | $\log \epsilon$ | EW | $\log \epsilon$ | EW | $\log \epsilon$ | EW | $\log \epsilon$ | EW | $\log \epsilon$ | EW | $\log \epsilon$ | EW | $\log \epsilon$ | EW | $\log \epsilon$ |
| 7422.286 | Ni I | 3.63 | -0.33 | cn | 88.9 | 5.939 | 180.4 | 6.816 | 154.5 | 6.266 | 135.2 | 6.066 | — | — | 151.4 | 6.301 | 82.4 | 5.865 | — | — |
| 7525.118 | Ni I | 3.63 | -0.65 | cn | 78.8 | 6.092 | 152.3 | 6.823 | 131.4 | 6.284 | 120.8 | 6.143 | — | — | 128.6 | 6.323 | 59.0 | 5.796 | — | — |
| 7574.048 | Ni I | 3.83 | -0.61 | cn | 63.5 | 5.986 | 116.3 | 6.499 | 93.9 | 5.937 | 84.6 | 5.709 | 101.9 | 6.128 | 93.0 | 5.983 | 51.2 | 5.818 | 106.2 | 6.257 |
| 7714.310 | Ni I | 1.93 | -1.91 | cn | 110.0 | 6.085 | — | — | — | — | 178.1 | 6.094 | — | — | 195.7 | 6.251 | 87.6 | 5.779 | — | — |
| 7715.591 | Ni I | 3.70 | -0.95 | cn | 43.0 | 5.832 | 123.8 | 6.792 | 68.3 | 5.701 | 66.0 | 5.567 | 93.1 | 6.164 | 68.9 | 5.770 | 33.5 | 5.704 | 92.1 | 6.208 |
| 7727.616 | Ni I | 3.68 | -0.17 | cn | — | — | 154.5 | 6.421 | — | — | — | — | 130.3 | 5.930 | 113.4 | 5.664 | 77.9 | 5.663 | — | — |
| 7748.894 | Ni I | 3.70 | -0.33 | cn | 82.6 | 5.883 | 141.1 | 6.445 | 121.5 | 5.891 | 108.4 | 5.683 | 128.6 | 6.086 | 101.2 | 5.657 | 74.7 | 5.788 | 124.7 | 6.121 |
| 7788.933 | Ni I | 1.95 | -2.42 | fm | — | — | 196.8 | 7.008 | 155.9 | 6.114 | 125.4 | 5.762 | — | — | 137.1 | 6.038 | 75.3 | 6.089 | — | — |
| 7797.588 | Ni I | 3.90 | -0.30 | lz | 78.0 | 5.975 | — | — | 90.8 | 5.656 | 92.3 | 5.599 | — | — | 91.5 | 5.722 | 60.6 | 5.724 | — | — |
| 6435.000 | Y I | 0.07 | -0.82 | hl | 10.4 | 2.560 | 126.9 | 2.896 | 132.1 | 2.552 | 96.0 | 2.300 | 83.3 | 2.354 | 126.0 | 2.871 | — | — | 108.2 | 2.642 |
| 6127.460 | Zr I | 0.15 | -1.06 | bg | 6.5 | 2.833 | 119.6 | 3.231 | 110.8 | 2.677 | — | — | — | — | 87.1 | 2.769 | 7.5 | 3.042 | 80.0 | 3.181 |
| 6134.570 | Zr I | 0.00 | -1.28 | bg | 4.4 | 2.711 | 111.7 | 3.031 | 106.9 | 2.568 | 76.6 | 2.480 | 82.3 | 2.776 | — | — | 5.9 | 2.997 | 71.6 | 2.976 |
| 6140.460 | Zr I | 0.52 | -1.41 | bg | — | — | 76.8 | 3.444 | 88.4 | 3.307 | — | — | 58.3 | 3.435 | — | — | — | — | — | — |
| 6143.180 | Zr I | 0.07 | -1.10 | bg | 12.5 | 3.097 | 125.3 | 3.231 | 151.5 | 3.279 | 117.6 | 3.127 | 100.9 | 2.980 | 132.5 | 3.396 | 15.6 | 3.360 | 92.2 | 3.292 |
| 5853.688 | Ba II | 0.60 | -1.01 | wm | 112.5 | 2.559 | 171.7 | 2.888 | 257.0 | 3.110 | 268.5 | 3.215 | 182.6 | 2.790 | 252.5 | 3.214 | 160.0 | 3.039 | 197.1 | 3.010 |
| 6141.727 | Ba II | 0.70 | -0.08 | wm | 186.9 | 2.423 | 249.9 | 2.619 | 477.9 | 2.972 | 416.2 | 2.863 | 303.2 | 2.639 | 485.0 | 3.094 | 258.2 | 2.745 | 311.0 | 2.755 |
| 6496.908 | Ba II | 0.60 | -0.38 | wm | 178.7 | 2.517 | 270.8 | 2.854 | 431.1 | 3.013 | 378.4 | 2.921 | 288.9 | 2.725 | 445.7 | 3.164 | 222.3 | 2.735 | 302.8 | 2.871 |
| 6390.480 | La II | 0.32 | -1.45 | lb | — | — | 73.5 | 1.999 | 108.6 | 2.292 | 95.0 | 2.040 | 68.2 | 1.859 | 88.1 | 2.185 | 32.9 | 1.933 | 81.4 | 2.109 |
| 6645.110 | Eu II | 1.37 | 0.20 | bc | 19.1 | 0.776 | 59.6 | 1.236 | 50.3 | 0.829 | 58.8 | 0.774 | 27.2 | 0.500 | 45.6 | 0.880 | 16.1 | 0.656 | 48.2 | 0.938 |

^{bc} Biémont et al. 1982^{bg} Biémont et al. 1981^{bk} Bard & Kock 1994^{cn} Chen et al. 2000b^{fm} Fuhr et al. 1988^{hl} Hannaford et al. 1982^{lb} Luck & Bond 1991^{lh} Lambert et al. 1996^{lw} Lambert & Warner 1968^{lz} Liang et al. 2003nd NIST database (<http://physics.nist.gov>)^{ns} Nissen & Schuster 1997^{ow} O'Brian et al. 1991^{wm} Weise & Martin 1980

Abundance Analysis of Barium Stars

G. Q. Liu^{1,2*}, Y. C. Liang^{1**} and L. Deng¹

¹ National Astronomical Observatories, Chinese Academy of Sciences, Beijing 100012, P. R. China

² Graduate University of Chinese Academy of Sciences, Beijing 100049, P. R. China

Abstract We obtain the chemical abundances of six barium stars and two CH subgiant stars based on the high signal-to-noise ratio and high resolution Echelle spectra. The neutron capture process elements Y, Zr, Ba, La, Eu show obvious overabundance relative to the Sun, for example, their [Ba/Fe] values are from 0.45 to 1.27. Other elements, including Na, Mg, Al, Si, Ca, Sc, Ti, V, Cr, Mn, Ni, show comparable abundances to the Solar ones, and their [Fe/H] cover a range from -0.40 to 0.21 , which means they belong to Galactic disk. The predicts of the theoretical model of wind accretion for binary systems can explain the observed abundance patterns of the neutron capture process elements in these stars, which means that their overabundant heavy-elements could be caused by accreting the ejecta of AGB stars, the progenitors of the present white dwarf companions in the binary systems.

Key words: Stars: abundances — Stars: atmospheres — Stars: chemically peculiar — Stars: evolution — binaries: spectroscopic

1 INTRODUCTION

As first identified by Bidelman & Keeman (1951), barium stars appear as a distinct group of chemically peculiar red giants. These G and K giants show enhanced features of Ba II, Sr II, CH, CN and sometimes C₂ lines. The following studies also found enhanced abundances of some other heavy elements, e.g. Y, Zr, La, Ce, Pr, Nd and Sm.

Since Burbidge et al. (1957) suggested the elements heavier than iron are synthesized in the interior of asymptotic giant branch (AGB) stars through the slow neutron capture process (s-process) (the rapid neutron capture process, r-process, occurs in supernova explosion), one generally believe that the overabundant heavy elements of Ba stars could be caused by binary accretion because they should not be evolved to the thermal pulse (TP) AGB stage to synthesize these heavy elements due to their low luminosity and the absence of the unstable nucleus ⁹⁹Tc ($\tau_{1/2}=2\times 10^5$ yr) (see Liang et al. 2000, 2003 and references therein). The binarity and heavy-element abundances of Ba stars have been studied by

* E-mail: lgq@bao.ac.cn, ycliang@bao.ac.cn

Table 1 Basic data of the sample stars. The HD identifications, spectral types, $B - V$ color, trigonometric parallaxes and their errors.

| HD | Sp. | V_{mag} | $B - V$ | π (mas) | σ_{π} |
|--------|-------|------------------|---------|----------------|----------------|
| 4395 | G5 | 7.70 | 0.69 | 9.16 | 1.12 |
| 180622 | K2 | 7.63 | 1.25 | 3.37 | 1.04 |
| 201657 | K2 | 8.00 | 1.27 | 4.49 | 1.07 |
| 201824 | K0 | 8.90 | 1.09 | 0.56 | 1.56 |
| 210946 | K0 | 8.08 | 1.095 | 3.42 | 1.14 |
| 211594 | K0 | 8.05 | 1.143 | 4.59 | 1.18 |
| 216219 | G0IIp | 7.44 | 0.64 | 10.74 | 0.93 |
| 223617 | G5 | 6.91 | 1.155 | 4.61 | 0.95 |

many researchers (Griffin 1980; Jorissen & Mayor 1988; McClure et al. 1980; McClure 1983; McClure & Woodsworth 1990; Jorissen et al. 1998; Liang et al. 2000, 2003; Liu et al. 2000; Lü et al. 1991; Han et al. 1995; Začs 1994; Smiljanic et al. 2007). These Ba stars could have accreted the matter ejected by their companions (the former AGB stars, the present white dwarfs) about 1×10^6 years ago through wind accretion, disk accretion or common envelope ejection (Han et al. 1995; Jorissen et al. 1998; Liang et al. 2000).

At present, a large sample of Ba stars have been measured their binary orbital elements (Carquillat et al. 1998; Udry et al. 1998a, 1998b; Jorissen et al. 1998), absolute magnitudes and kinematics (Gómez et al. 1997; Mennessier et al. 1997). However, the corresponding heavy-element abundances have not been obtained from high resolution observations, which is very useful to understand the formation scenario of Ba stars, but need lots of telescope time and lots of efforts on data analysis. Therefore, we propose to observe the high resolution and high signal-to-noise (S/N) ratio spectra of a sample of Ba stars to obtain their chemical abundances, hence, to understand their formation scenario by combining with their binary orbital elements. Moreover, by taking advantage of the present high precision Hipparcos data, precise photometric parameters, improved methods to determine stellar atmospheric parameters and developed stellar evolutionary tracks etc., the reliable chemical abundances of stars could be obtained from the spectra. We could also understand the formation scenario of Ba stars from theoretical models by comparing the model predicts with the observed abundances, e.g. the angular momentum conservation model of wind accretion of Ba binaries (Liang et al. 2000; Liu et al. 2000; Boffin & Jorissen 1988).

This paper is organized as follows. Description of the spectral observations and data reduction for the sample stars are presented in Section 2. In Section 3 the derived stellar atmospheric parameters are presented. Stellar atmosphere model, spectral lines and their measured equivalent widths (EWs) are described in Section 4. The analysis on abundance results is given in Section 5. The predicted abundances from wind accretion model are presented and compared with the observed abundance patterns in Section 6. The discussions and conclusions are given in Section 7.

2 OBSERVATIONS AND DATA REDUCTION

The sample stars have been firstly identified as mild or strong Ba stars in Lü et al. (1991) and have been obtained their binary orbital elements (e.g. orbital period and eccentricity) in Jorissen et al. (1998) except HD 4395. HD 4395 and HD 216219 were classified as CH subgiants (Luck & Bond 1982; Sneden 1983;

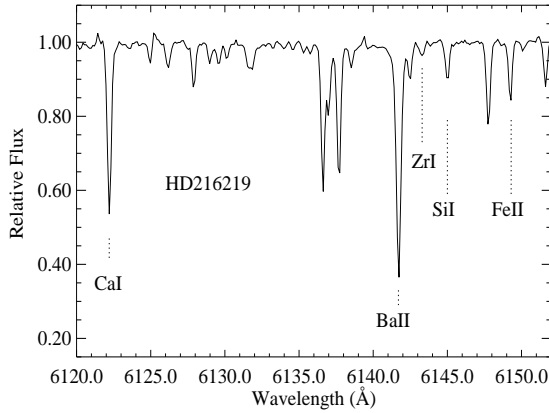


Fig. 1 A portion of spectrum of the sample star HD 216219 in the wavelength range 6120Å–6152Å. Major features include Ca I 6122.226 Å, Ba II 6141.727 Å, Zr I 6143.180 Å, Si I 6145.020 Å and Fe II 6149.249 Å.

Krishnaswamy & Sneden 1985; Lambert et al. 1993; Smith et al. 1993; Preston & Sneden 2001), but HD 216219 has also been classified as mild Ba star by Lü et al. (1991) and Jorissen et al. (1998). A common point of view is that CH subgiants also belong to binary systems and their overabundances of s-process elements are caused by accreting the ejected material of the companion AGB progenitors, which is the same scenario as the Ba stars. The CH subgiants could evolve to be the classical Ba stars (Luck & Bond 1982; Smith et al. 1993). In this work we take these two stars as the same with other samples to study their abundances and formation scenario. These two common stars with Smith et al. (1993) are good examples to compare our EW measurements, atmospheric parameters and abundances with theirs carefully.

Table 1 presents the basic parameters of the sample stars. The Column (1)-(6) consequently present their HD identifications, spectral type and luminosity class, visual magnitudes, $B - V$ color index, trigonometric parallaxes and the corresponding errors taken from SIMBAD database.

The spectroscopic observations were carried out with the Coudé Echelle Spectrograph of National Astronomical Observatories (NAOC) mounted on the 2.16 m telescope at Xinglong station (Xinglong, P. R. China). The detector was a Tektronix CCD with 1024×1024 pixels ($24 \times 24 \mu m^2$ each in size). The wavelength coverage of total spectra is roughly from 5500–8000 Å over 34 orders. The spectra were observed during September 12–14, 2000 and most of them had $S/N > 100$. Figure 1 presents the spectrum of HD 216219 showing main features of absorption in the region around Ba II $\lambda 6141.727$ line.

Data reductions of all the spectra were carried out through ECHELLE package in the MIDAS environment by standard routines proceeding with order identification, background subtraction, flat-field correction, order extraction, wavelength calibration with a thorium-argon lamp calibration frame. Bias, dark current and scattered light corrections were taken into account in the background subtraction. The pixel-to-pixel sensitivity variations were corrected by using the flat-field. The EWs of the spectral lines are measured from the normalized spectra corrected by radial velocity, which were measured from more than 20 absorption lines at least. The selected spectral lines for abundance analysis are unblended or slightly blended and have reliable atomic data.

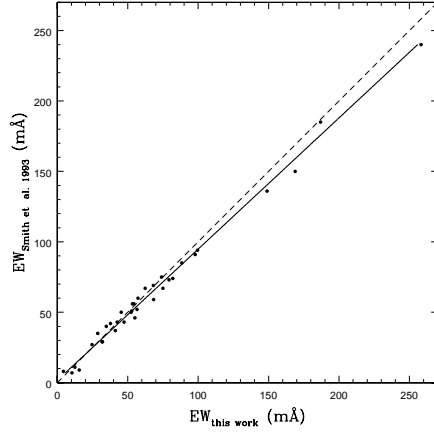


Fig. 2 Comparison of equivalent width measurements of 35 common absorption lines in HD 216219 and HD 4395 in this work and Smith et al. (1993). The solid line is the least square fit to the points (Eq.(1)), and the dashed line refers to the one-to-one relation.

The EWs of spectral line were measured by applying two different methods: direct integration of the line profile and Gaussian fitting. The latter is preferable in the case of faint lines ($EW < 20 \text{ m}\text{\AA}$), but unsuitable for the strong lines in which the damping wings contribute significantly to the equivalent width. The final EWs are weighted averages of these two measurements, depending on the line intensity (see Zhao et al. 2000 for details). The EW values of 110–180 lines in the wavelength range from 5500–8100 \AA were obtained for each of the sample stars. Table 2 presents the final EWs of the lines measured in the spectra of the sample stars as input data for the abundance analysis. Since the very weak lines would lead to an increase of random errors in the abundance determination and the too strong lines are not so sensitive to abundance, we use the lines with $EW_s=10 - 200 \text{ m}\text{\AA}$ for abundance analysis, and most of them within $20 - 150 \text{ m}\text{\AA}$ except some of the s-process elements. The reliability of our EW measurements have been confirmed by the consistence in the comparison between our data and those of Smith et al. (1993) for 35 common lines of HD 216219 and HD 4395. This comparison is shown in Figure 2. The systematic difference between the two sets of data is small and could be given by a linear least square fit as:

$$EW_{\text{Smith93}} = 0.92(\pm 0.02)EW_{\text{this work}} + 2.19(\pm 1.30)m\text{\AA}, \quad (1)$$

with the standard deviation of 0.061.

3 STELLAR ATMOSPHERIC PARAMETERS

The stellar atmospheric model is composed of four basic parameters, i.e., effective temperature, surface gravity, metallicity and microturbulent velocity. In this section, we describe the determinations of these four model-atmosphere parameters.

3.1 Effective temperature

Effective temperatures T_{eff} were determined from $[\text{Fe}/\text{H}]$ and $B-V$ color indices by using the empirical calibration of Alonso et al. (1999 & 2001), which is suit-

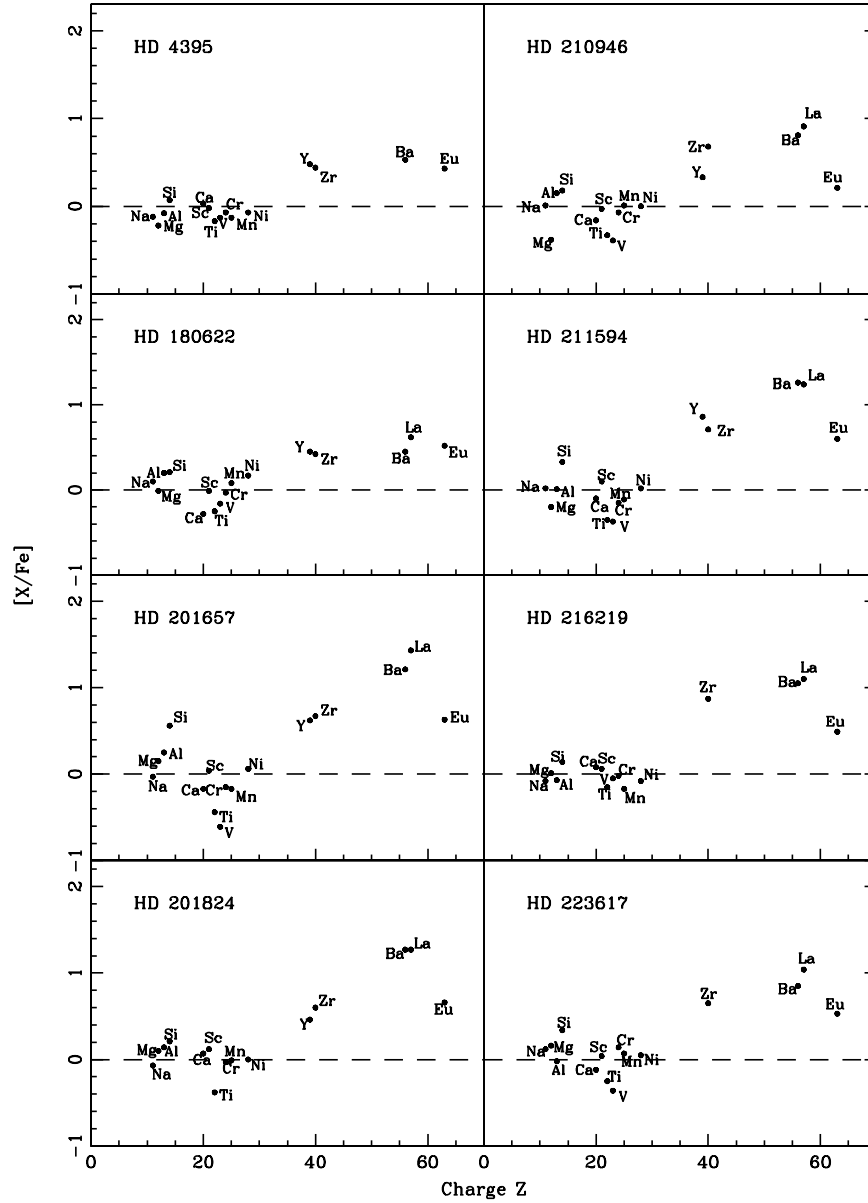


Fig. 3 The abundance patterns of sample stars.

able for giant stars. We use $B-V$ color here since the $B-V$ data are more complete than other color indices for the sample stars. Considering the uncertainties of photometric data, $[\text{Fe}/\text{H}]$, and the errors in the calibration relation, we estimate the uncertainty in T_{eff} is about 100 K for our sample stars.

Table 3 Atmospheric parameters of the sample stars: effective temperature (T_{eff}), surface gravity ($\log g$), mass (M/M_{\odot}) and their uncertainties, microturbulence velocity (ξ_t) and metallicity ([Fe/H]).

| HD | T_{eff} | $\log g$ | M/M_{\odot} | ξ_t | [Fe/H] |
|--------|------------------|----------|-------------------|---------|--------|
| 4395 | 5447 | 3.60 | 1.60(+0.13,−0.10) | 1.3 | −0.16 |
| 180622 | 4391 | 2.24 | 1.92(+1.07,−0.36) | 1.5 | 0.21 |
| 201657 | 4284 | 2.17 | 0.78(+0.08,−0.02) | 1.7 | −0.31 |
| 201824 | 4552 | 1.67 | 4.58(−,−3.32) | 1.5 | −0.40 |
| 210946 | 4577 | 2.42 | 1.40(+0.72,−0.28) | 1.6 | −0.22 |
| 211594 | 4490 | 2.44 | 0.90(+0.41,−0.09) | 1.6 | −0.23 |
| 216219 | 5553 | 3.64 | 1.48(+0.07,−0.08) | 1.4 | −0.34 |
| 223617 | 4501 | 2.27 | 1.78(+0.47,−0.33) | 1.5 | −0.10 |

3.2 Surface Gravity

Based on the *Hipparcos* parallaxes, precise value of the surface gravity of nearby stars can be obtained using the following relations:

$$\log \frac{g}{g_{\odot}} = \log \frac{\mathcal{M}}{\mathcal{M}_{\odot}} + 4 \log \frac{T_{\text{eff}}}{T_{\text{eff},\odot}} + 0.4 (M_{\text{bol}} - M_{\text{bol},\odot}) \quad (2)$$

and

$$M_{\text{bol}} = V + BC + 5 \log \pi + 5, \quad (3)$$

where \mathcal{M} is the stellar mass, M_{bol} the absolute bolometric magnitude, V the visual magnitude, BC the bolometric correction, and π the parallax. We adopt solar value $\log g_{\odot}=4.44$, $T_{\text{eff},\odot}=5770$ K, $M_{\text{bol},\odot}=4.77$ mag. The parallax π and its errors are taken from the *Hipparcos* Satellite observations (ESA 1997). Stellar mass was determined from the position of the star in $M_{\text{bol}}-\log T_{\text{eff}}$ diagram. We adopt the stellar evolutionary tracks of Yonsei-Yale (Yi et al. 2003), whose isochrones determined with high quality observational data cover the stage from pre-main-sequence birthline to the helium-core flash. The uncertainty of $\log g$ estimated by this method is about 0.2 dex generally for our sample stars.

3.3 Metal abundance

The initial metallicities of the sample stars in their model atmospheres were taken from literature if available. Otherwise, we adopt [Fe/H]=0 as the initial value and then the final model metallicity derived from the consistency with the other parameters in the abundance calculation. The estimated error in [Fe/H] is about 0.1 dex.

3.4 Microturbulence velocity

The value of microturbulence velocity ξ_t was determined from the abundance analysis by requiring a null correlation between [Fe/H] and the EWs. We applied this calculation with a large range of EWs (20 – 150 mÅ) for Fe I lines. With this selection, the uncertainty of the microturbulence velocity is about 0.2 km s^{−1}.

Table 3 presents the atmospheric parameters for the sample stars, where Column (1)-(6) list, consequently, the HD identifications, T_{eff} , $\log g$, mass, microturbulence velocity and [Fe/H]. The temperature coverage of the stars are from 4284 to 5553 K, the surface gravity coverage are from 1.67 to 3.64. The microturbulence velocity is from 1.3 to 1.7, and their [Fe/H] is from −0.40 to

Table 4 Element abundances of the sample stars.

| | HD 4395 | | | HD 180622 | | | HD 201657 | | | HD 201824 | | |
|--------|---------|-------------------|--------|-----------|-------------------|--------|-----------|-------------------|--------|-----------|-------------------|--------|
| [Fe/H] | -0.16 | | | 0.21 | | | -0.31 | | | -0.40 | | |
| Ion | N | log $\epsilon(X)$ | [X/Fe] | N | log $\epsilon(X)$ | [X/Fe] | N | log $\epsilon(X)$ | [X/Fe] | N | log $\epsilon(X)$ | [X/Fe] |
| Fe I | 51 | 7.34 | — | 35 | 7.71 | — | 45 | 7.18 | — | 28 | 7.10 | — |
| Fe II | 8 | 7.32 | — | 2 | 7.73 | — | 2 | 7.31 | — | 2 | 7.14 | — |
| Na I | 2 | 6.05 | -0.12 | 2 | 6.64 | 0.10 | 2 | 5.99 | -0.03 | 2 | 5.86 | -0.07 |
| Mg I | 2 | 7.20 | -0.22 | 1 | 7.78 | -0.01 | 1 | 7.42 | 0.15 | 2 | 7.28 | 0.10 |
| Al I | 4 | 6.23 | -0.08 | 3 | 6.88 | 0.20 | 3 | 6.41 | 0.25 | 3 | 6.21 | 0.14 |
| Si I | 13 | 7.46 | 0.07 | 6 | 7.97 | 0.21 | 4 | 7.80 | 0.56 | 6 | 7.36 | 0.21 |
| Ca I | 12 | 6.23 | 0.03 | 2 | 6.29 | -0.28 | 9 | 5.88 | -0.17 | 17 | 6.03 | 0.07 |
| Sc II | 2 | 2.99 | -0.02 | 3 | 3.37 | -0.01 | 3 | 2.90 | 0.04 | 3 | 2.89 | 0.12 |
| Ti I | 6 | 4.69 | -0.17 | 6 | 4.98 | -0.25 | 6 | 4.27 | -0.44 | 9 | 4.24 | -0.38 |
| V I | 1 | 3.71 | -0.13 | 3 | 4.05 | -0.16 | 1 | 3.08 | -0.61 | 0 | — | — |
| Cr I | 7 | 5.44 | -0.07 | 5 | 5.85 | -0.03 | 4 | 5.21 | -0.15 | 4 | 5.24 | -0.03 |
| Mn I | 2 | 5.10 | -0.13 | 2 | 5.68 | 0.08 | 2 | 4.91 | -0.17 | 2 | 4.98 | -0.01 |
| Ni I | 25 | 6.02 | -0.07 | 21 | 6.63 | 0.17 | 21 | 5.97 | 0.06 | 25 | 5.85 | 0.00 |
| Y I | 1 | 2.56 | 0.48 | 1 | 2.90 | 0.45 | 1 | 2.55 | 0.62 | 1 | 2.30 | 0.46 |
| Zr I | 3 | 2.88 | 0.44 | 4 | 3.23 | 0.42 | 3 | 2.84 | 0.67 | 2 | 2.80 | 0.60 |
| Ba II | 3 | 2.50 | 0.53 | 3 | 2.79 | 0.45 | 3 | 3.03 | 1.21 | 3 | 3.00 | 1.27 |
| La II | 0 | — | — | 1 | 2.00 | 0.62 | 1 | 2.29 | 1.43 | 1 | 2.04 | 1.27 |
| Eu II | 1 | 0.78 | 0.43 | 1 | 1.24 | 0.52 | 1 | 0.83 | 0.63 | 1 | 0.77 | 0.66 |

| | HD 210946 | | | HD 211594 | | | HD 216219 | | | HD 223617 | | |
|--------|-----------|-------------------|--------|-----------|-------------------|--------|-----------|-------------------|--------|-----------|-------------------|--------|
| [Fe/H] | -0.22 | | | -0.23 | | | -0.34 | | | -0.10 | | |
| Ion | N | log $\epsilon(X)$ | [X/Fe] | N | log $\epsilon(X)$ | [X/Fe] | N | log $\epsilon(X)$ | [X/Fe] | N | log $\epsilon(X)$ | [X/Fe] |
| Fe I | 51 | 7.28 | — | 49 | 7.27 | — | 51 | 7.15 | — | 34 | 7.39 | — |
| Fe II | 3 | 7.38 | — | 0 | — | — | 3 | 7.30 | — | 4 | 7.46 | — |
| Na I | 1 | 6.12 | 0.01 | 2 | 6.12 | 0.02 | 2 | 5.91 | -0.08 | 2 | 6.35 | 0.12 |
| Mg I | 2 | 6.98 | -0.38 | 1 | 7.15 | -0.2 | 3 | 7.25 | 0.01 | 2 | 7.64 | 0.16 |
| Al I | 2 | 6.40 | 0.15 | 2 | 6.25 | 0.01 | 3 | 6.06 | -0.07 | 1 | 6.35 | -0.02 |
| Si I | 4 | 7.51 | 0.18 | 8 | 7.65 | 0.33 | 13 | 7.35 | 0.14 | 8 | 7.79 | 0.34 |
| Ca I | 16 | 5.98 | -0.16 | 18 | 6.03 | -0.10 | 15 | 6.10 | 0.08 | 9 | 6.14 | -0.12 |
| Sc II | 3 | 2.92 | -0.03 | 5 | 3.04 | 0.10 | 4 | 2.89 | 0.06 | 3 | 3.11 | 0.04 |
| Ti I | 6 | 4.47 | -0.33 | 2 | 4.44 | -0.35 | 3 | 4.53 | -0.15 | 6 | 4.67 | -0.25 |
| V I | 3 | 3.39 | -0.39 | 1 | 3.40 | -0.37 | 2 | 3.61 | -0.05 | 2 | 3.54 | -0.36 |
| Cr I | 5 | 5.38 | -0.07 | 5 | 5.29 | -0.15 | 5 | 5.31 | -0.02 | 5 | 5.71 | 0.14 |
| Mn I | 2 | 5.18 | 0.01 | 2 | 5.05 | -0.11 | 2 | 4.88 | -0.17 | 2 | 5.36 | 0.07 |
| Ni I | 21 | 6.03 | 0.00 | 20 | 6.04 | 0.02 | 30 | 5.83 | -0.08 | 17 | 6.20 | 0.05 |
| Y I | 1 | 2.35 | 0.33 | 1 | 2.87 | 0.86 | 0 | — | — | 1 | 2.64 | 0.50 |
| Zr I | 3 | 3.06 | 0.68 | 2 | 3.08 | 0.71 | 3 | 3.13 | 0.87 | 3 | 3.15 | 0.65 |
| Ba II | 3 | 2.72 | 0.81 | 3 | 3.16 | 1.26 | 3 | 2.84 | 1.05 | 3 | 2.88 | 0.85 |
| La II | 1 | 1.86 | 0.91 | 1 | 2.18 | 1.24 | 1 | 1.93 | 1.10 | 1 | 2.11 | 1.04 |
| Eu II | 1 | 0.50 | 0.21 | 1 | 0.88 | 0.60 | 1 | 0.66 | 0.49 | 1 | 0.94 | 0.53 |

0.21. The uncertainties of the parameters are: $\sigma(T_{\text{eff}}) = 100$ K, $\sigma(\log g) = 0.2$, $\sigma([\text{Fe}/\text{H}]) = 0.1$, and $\sigma(\xi_t) = 0.2$ km s⁻¹.

The reliability of the derived atmospheric parameters $T_{\text{eff}}/\log g/\xi_t$ are confirmed by the further checks. Taking HD 216219 as a representative, Figure 4a give the Fe abundances from different Fe I lines as a function of their excitation potential, which fulfills the excitation equilibrium; Figure 4b shows that the Fe abundances from Fe I lines and Fe II lines are consistent within 0.2 dex, which illustrates the ionization equilibrium, and also shows that there is no trend between Fe abundances and EWs of the lines.

Comparing our results with those of Smith et al. (1993), the derived atmospheric parameters for HD 4395 are $T_{\text{eff}}=5447/5450$ K, $\log g=3.60/3.3$, $\xi_t=1.3/1.3$, $[\text{Fe}/\text{H}]=-0.16/-0.33$; for HD 216219 are $T_{\text{eff}}=5553/5600$ K, $\log g=3.64/3.2$, $\xi_t=1.4/1.6$, $[\text{Fe}/\text{H}]=-0.34/-0.32$. They are well consistent.

Table 5 The detailed uncertainties of the abundance analysis for one representative star HD 216219, and the total uncertainties on the abundances for all other sample stars.

| HD 216219 $T_{\text{eff}} = 5197$ $\log g = 3.39$ $[\text{Fe}/\text{H}] = -0.63$ $\xi_t = 1.4$ | | | | | | | |
|--|---------------|----------------------------------|-------------------------|--------------------------------------|------------------------|----------------|--------|
| | σ_{EW} | ΔT_{eff} +100K | $\Delta \log g$ +0.2 | $\Delta[\text{Fe}/\text{H}]$ +0.1 | $\Delta \xi_t$ +0.2 | σ_{tot} | |
| $\Delta[\text{Fe}/\text{H}]_I$ | 0.07 | 0.08 | -0.01 | 0.00 | -0.04 | 0.11 | |
| $\Delta[\text{Fe}/\text{H}]_{II}$ | 0.06 | -0.03 | 0.08 | 0.03 | -0.04 | 0.12 | |
| $\Delta[\text{Na}/\text{Fe}]$ | 0.04 | 0.06 | 0.00 | 0.00 | 0.00 | 0.07 | |
| $\Delta[\text{Mg}/\text{Fe}]$ | 0.07 | 0.07 | -0.06 | 0.01 | -0.03 | 0.12 | |
| $\Delta[\text{Al}/\text{Fe}]$ | 0.03 | 0.04 | -0.02 | -0.01 | -0.01 | 0.06 | |
| $\Delta[\text{Si}/\text{Fe}]$ | 0.05 | 0.03 | 0.00 | 0.00 | -0.02 | 0.06 | |
| $\Delta[\text{Ca}/\text{Fe}]$ | 0.08 | 0.08 | -0.04 | 0.00 | -0.06 | 0.13 | |
| $\Delta[\text{Sc}/\text{Fe}]$ | 0.09 | 0.01 | 0.06 | 0.02 | -0.07 | 0.13 | |
| $\Delta[\text{Ti}/\text{Fe}]$ | 0.04 | 0.10 | -0.01 | -0.01 | -0.02 | 0.11 | |
| $\Delta[\text{V}/\text{Fe}]$ | 0.04 | 0.11 | -0.01 | -0.01 | -0.02 | 0.12 | |
| $\Delta[\text{Cr}/\text{Fe}]$ | 0.04 | 0.07 | -0.01 | -0.01 | -0.02 | 0.08 | |
| $\Delta[\text{Mn}/\text{Fe}]$ | 0.07 | 0.09 | -0.02 | 0.00 | -0.05 | 0.13 | |
| $\Delta[\text{Ni}/\text{Fe}]$ | 0.06 | 0.08 | -0.01 | 0.00 | -0.04 | 0.11 | |
| $\Delta[\text{Zr}/\text{Fe}]$ | 0.04 | 0.13 | 0.00 | 0.00 | 0.00 | 0.14 | |
| $\Delta[\text{Ba}/\text{Fe}]$ | 0.06 | 0.04 | -0.02 | 0.04 | -0.05 | 0.10 | |
| $\Delta[\text{La}/\text{Fe}]$ | 0.04 | 0.03 | 0.08 | 0.04 | -0.03 | 0.11 | |
| $\Delta[\text{Eu}/\text{Fe}]$ | 0.03 | 0.00 | 0.08 | 0.02 | -0.02 | 0.09 | |
| σ_{tot} | 4395 | 180622 | 201657 | 201824 | 210946 | 211594 | 223617 |
| $\Delta[\text{Fe}/\text{H}]_I$ | 0.11 | 0.14 | 0.10 | 0.12 | 0.10 | 0.11 | 0.13 |
| $\Delta[\text{Fe}/\text{H}]_{II}$ | 0.13 | 0.24 | 0.22 | 0.19 | 0.20 | — | 0.20 |
| $\Delta[\text{Na}/\text{Fe}]$ | 0.08 | 0.16 | 0.14 | 0.10 | 0.13 | 0.13 | 0.14 |
| $\Delta[\text{Mg}/\text{Fe}]$ | 0.09 | 0.16 | 0.14 | 0.16 | 0.12 | 0.10 | 0.13 |
| $\Delta[\text{Al}/\text{Fe}]$ | 0.07 | 0.13 | 0.10 | 0.09 | 0.10 | 0.09 | 0.10 |
| $\Delta[\text{Si}/\text{Fe}]$ | 0.07 | 0.14 | 0.12 | 0.10 | 0.10 | 0.11 | 0.11 |
| $\Delta[\text{Ca}/\text{Fe}]$ | 0.15 | 0.18 | 0.20 | 0.21 | 0.18 | 0.19 | 0.20 |
| $\Delta[\text{Sc}/\text{Fe}]$ | 0.14 | 0.22 | 0.17 | 0.19 | 0.17 | 0.18 | 0.18 |
| $\Delta[\text{Ti}/\text{Fe}]$ | 0.12 | 0.24 | 0.21 | 0.20 | 0.19 | 0.22 | 0.21 |
| $\Delta[\text{V}/\text{Fe}]$ | 0.12 | 0.30 | 0.23 | — | 0.22 | 0.20 | 0.25 |
| $\Delta[\text{Cr}/\text{Fe}]$ | 0.10 | 0.21 | 0.15 | 0.15 | 0.14 | 0.14 | 0.19 |
| $\Delta[\text{Mn}/\text{Fe}]$ | 0.14 | 0.20 | 0.19 | 0.24 | 0.21 | 0.19 | 0.20 |
| $\Delta[\text{Ni}/\text{Fe}]$ | 0.11 | 0.17 | 0.14 | 0.19 | 0.13 | 0.15 | 0.15 |
| $\Delta[\text{Y}/\text{Fe}]$ | 0.12 | 0.26 | 0.24 | 0.22 | 0.17 | 0.23 | — |
| $\Delta[\text{Zr}/\text{Fe}]$ | 0.13 | 0.25 | 0.25 | 0.26 | 0.19 | 0.22 | 0.24 |
| $\Delta[\text{Ba}/\text{Fe}]$ | 0.16 | 0.17 | 0.09 | 0.09 | 0.13 | 0.13 | 0.11 |
| $\Delta[\text{La}/\text{Fe}]$ | — | 0.17 | 0.20 | 0.21 | 0.13 | 0.18 | 0.17 |
| $\Delta[\text{Eu}/\text{Fe}]$ | 0.11 | 0.15 | 0.10 | 0.14 | 0.11 | 0.12 | 0.11 |

4 STELLAR ATMOSPHERE MODEL AND SPECTRAL LINES

The stellar atmospheric model is implemented by ATLAS9 code (Kurucz 1993) to do the abundance analysis. This is LTE, plane-parallel, line-blanketed models. Abundances of chemical elements were determined by using the input atmospheric parameters given in Table 3 and the measured EWs of the absorption lines. All the lines adopted in determining element abundances are presented in Table 2, which shows the spectral lines and wavelengths, excitation potential χ , oscillator strengths $\log gf$, EWs and $\log \epsilon$ of each line. The selections of the lines have been described in Sect.2. The oscillator strengths $\log gf$ of spectral lines

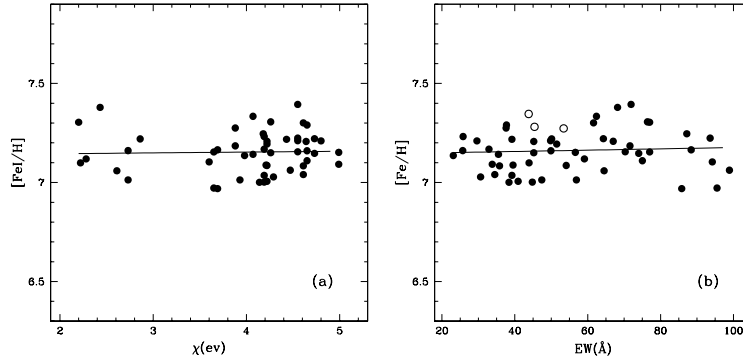


Fig.4 To check the reliability of the determined atmospheric parameters $T_{\text{eff}}/\log g/\xi_t$ of the stars by taking HD216219 as an example: (a). Fe abundances from Fe I lines as a function of excitation potential. There is no significant trend of $[\text{Fe}/\text{H}]$ with χ , indicating a correct temperature distribution in the model atmosphere. (b). The consistence of the Fe I and Fe,II abundances (the filled and open circles refer to the Fe I and Fe II abundances respectively), which mean that the determined $\log g$ are reliable; and an illustration of the determination of the microturbulence velocity since there is no significant trend between $[\text{Fe}/\text{H}]$ and EWs.

are taken from the NIST database (<http://physics.nist.gov>), Lambert & Warner (1968), Weise & Martin (1980), Biémont et al. (1981, 1982), Hannaford et al. (1982), Fuhr et al. (1988), Luck & Bond (1991), O’Brian et al. (1991), Bard & Kock (1994), Lambert et al. (1996), Nissen & Schuster (1997), Chen et al. (2000), Liang et al. (2003) and the references therein. Col. (5) of Table 2 gives these reference sources for the spectral lines.

5 CHEMICAL ABUNDANCES AND ANALYSIS

In this section, we present the determined abundances of the sample stars for about 20 elements based on the spectral observations and atmospheric model.

5.1 Abundance of barium stars

The derived element abundances of all the sample stars are given in Table 4, including $\log \epsilon$ and the corresponding $[X/\text{Fe}]$ values for all ions. The solar abundances are adopted from Grevesse & Sauval (1998).

Figure 3 directly presents the abundance results of our sample stars, including the chemical elements, Na, Mg, Al, Si, Ca, Sc, Ti, V, Cr, Mn, Ni, Y, Zr, Ba, La and Eu. It is obvious to show that the neutron capture process elements, Y, Zr, Ba, La, Eu, are overabundant than the solar abundances. Especially, Y and Zr exhibit as the first peak while Ba and La exhibit as the second peak, and the second peak is higher than the first one. Other elements from Na to Ni, such as α elements and iron elements, show similar abundances to the solar, which means that these Ba stars belong to disk stars. The behaviors of Sc and Mn are compatible to the results of Nissen et al. (2000) and Chen et al. (2000a), who demonstrated that decreasing $[\text{Sc}/\text{Fe}]$ with increasing metallicity in disk stars, whereas $[\text{Mn}/\text{Fe}]$ increases with increasing $[\text{Fe}/\text{H}]$.

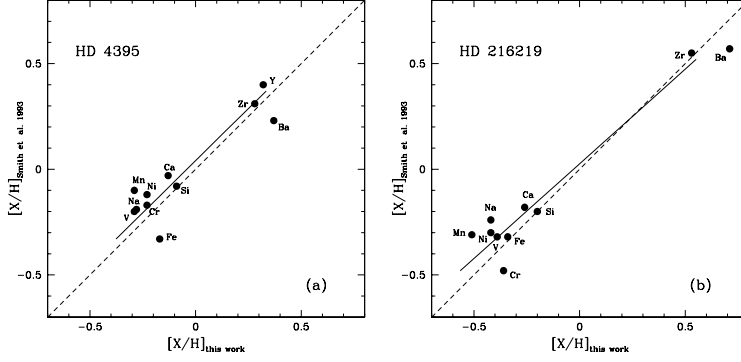


Fig. 5 The comparisons between our abundances determinations and those of Smith et al. (1993) for the two common stars: (a). for HD 4395; (b). for HD 216219. The solid lines are the least square fits for the data and the dashed lines are the one-to-one relations. Our results are consistent with theirs.

5.2 Uncertainties in the abundances

There are two kinds of uncertainties in the abundance determination: the systematic errors introduced by the atmospheric parameters, and the random errors in determining EWs, oscillator strengths, and damping constants. We ignore the uncertainties in atomic data since they could be small (Chen et al. 2000b) and consider the uncertainties in atmospheric parameter determinations and EW measurements. Assuming that the effects of the uncertainties of the parameters are independent, we can estimate the total uncertainty with Eq. (4):

$$\sigma_{total} = \sqrt{(\sigma_{EW})^2 + (\Delta T_{eff})^2 + (\Delta \log g)^2 + (\Delta [Fe/H])^2 + (\Delta \xi_t)^2}, \quad (4)$$

where σ_{EW} , ΔT_{eff} , $\Delta \log g$, $\Delta [Fe/H]$ and $\Delta \xi_t$ are the corresponding variations in the ion abundances due to the variations on equivalent widths, T_{eff} , $\log g$, metal abundance and microturbulent velocity, respectively.

For our spectra, the typical uncertainty of the EW is about 6.1%. Table 5 shows the effects on the derived abundances changed by 6.1% in EW, 100 K in effective temperature, 0.2 dex in surface gravity, 0.1 dex in metallicity, and 0.2 km s^{-1} in microturbulence velocity for one representative star, HD 216219. The total uncertainties on the output abundances have also be given in Table 5 for all other sample stars by considering the same errors as above in the individual atmospheric parameter.

5.3 Comparisons with Smith et al. (1993)

As for the two common stars with Smith et al. (1993), we compare our abundance determinations with theirs for HD 4395 and HD 216219. Figure 5 shows the consistences between our abundance estimations with theirs are within 0.2 dex, but most are in 0.1 dex.

6 COMPARING WITH WIND ACCRETION MODEL RESULTS

We try to use the wind accretion model to predict the theoretical heavy element abundances of Ba stars in binary systems, and then compare these theoretical predicts with the observed abundance patterns of our sample stars. Following Liang et al. (2000, 2003), the calculations of theoretical abundances are made in

Table 6 Orbital elements of the sample stars derived from literatures.

| HD | P (days) | e | Classes | Reference |
|--------|---------------|------|---------|-----------------------|
| 4395 | 6200 | 0.65 | — | Preston & Sneden 2001 |
| 180622 | 4049.2 | 0.06 | mild | Jorissen et al. 1998 |
| 201657 | 1710.4 | 0.17 | strong | Jorissen et al. 1998 |
| 201824 | 2837 | 0.34 | strong | Jorissen et al. 1998 |
| 210946 | 1529.5 | 0.13 | mild | Jorissen et al. 1998 |
| 211594 | 1018.9 | 0.06 | strong | Jorissen et al. 1998 |
| 216219 | 4098.0 | 0.10 | mild | Jorissen et al. 1998 |
| 223617 | 1293.7 | 0.06 | mild | Jorissen et al. 1998 |

two steps: the AGB nucleosynthesis based on the latest TP-AGB model and the branch path of the s -process nucleosynthesis, and the binary accretion based on the angular momentum conservation model of wind accretion.

The standard case of our wind accretion model is: $M_{1,0}=3.0M_{\odot}$, $M_{2,0}=1.3M_{\odot}$, $v_{ej}=15 \text{ km s}^{-1}$ ($M_{1,0}$ is the main sequence mass of the intrinsic AGB star, the present white dwarf, in the binary system; $M_{2,0}$ is the corresponding mass of the present Ba star; v_{ej} is the wind velocity). We assumed the standard accretion rate is 0.15 times of the Bondi-Hoyle's accretion rate (Liang et al. 2000; Boffin & Zacs 1994). The observed orbital elements of the sample stars are listed in Table 6, which are taken from Jorissen et al. (1998) and Preston & Sneden (2001). The observed orbital periods of our sample stars cover from 1018.9 to 6200 days and the eccentricities range from 0.06 to 0.65.

Figure 6 shows the comparisons between the theoretical abundances from the wind accretion model and the observed abundances of the sample stars, and the uncertainties of the observed abundances are marked as well. In the figure, the variable “ a ” represents the times of the corresponding standard neutron exposure in the ^{13}C profile in the AGB progenitor companion suggested by Gallino et al. (1998) and the higher a value reflects the higher neutron exposure occurred in interiors of the AGB progenitor. P refers to the orbital period of the sample star.

There is good agreement between our observed abundances and the theoretical ones for the sample stars. These mean that wind accretion can be the formation scenario of these Ba stars in binary systems. These are consistent with the suggestions of Jorissen et al. (1998), Zhang et al. (1999) and Liang et al. (2000), who mentioned that Ba stars with periods longer than 1500 or 1600 days could be formed through wind accretion. We should notice that the heavy element abundance patterns of two sample stars with $P > 1000$ days, HD 211594 and HD 223617, can also be explained by wind accretion. Figure 6 also shows that the strong Ba stars generally require the higher “ a ” values in the model than the mild Ba stars, i.e., the stronger neutron exposure occurred in the AGB progenitors in their s -process nucleosynthesis.

7 DISCUSSIONS AND CONCLUSIONS

The chemical compositions of six Ba stars and two CH subgiant stars were obtained on the basis of the high S/N ratio and high resolution spectra observed by using the 2.16m telescope at NAOC/Xinglong station. Their stellar atmospheric parameters were determined from the reliable methods, and show the ranges of $4284 < T_{\text{eff}} < 5553$, $1.67 < \log g < 3.64$, $-0.40 < [\text{Fe}/\text{H}] < 0.21$, and $1.3 < \xi_t < 1.7$. The model atmospheres were generated by using ATLAS9 code and the updated atomic data of the selected spectral lines for measuring EWs.

Then we obtain the abundances of chemical elements, Na, Mg, Al, Si, Ca, Sc, Ti, V, Cr, Mn, Ni, Y, Zr, Ba, La, Eu for our eight sample stars. The elements from

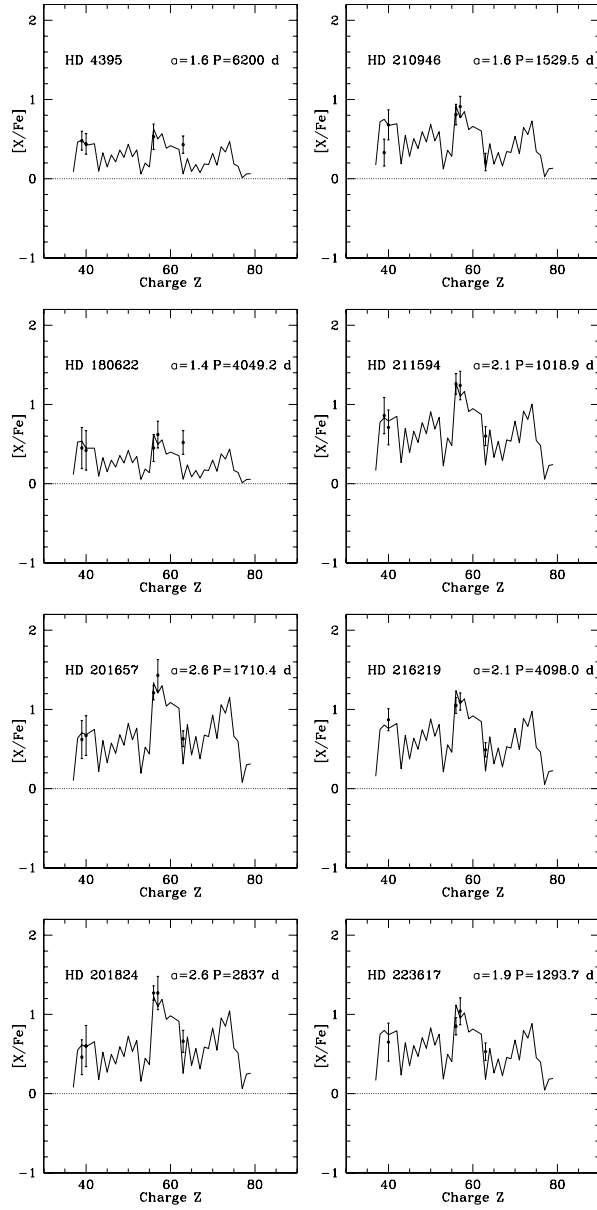


Fig. 6 The fitting of the theoretical to observed heavy-element abundances of sample stars with standard case of wind accretion. Label “ α ” represents the times of the corresponding standard neutron exposures in the ^{13}C profile in the AGB progenitor suggested by Gallino et al. (1998). P refers to the orbital period of the sample star.

Na to Ni, such as α and iron peak elements, show comparable abundances to the Sun, associated with the $[\text{Fe}/\text{H}]$ in a range of -0.40 to 0.21 , which mean these Ba stars belong to the Galactic disk. The neutron capture process elements Y, Zr, Ba, La, Eu show obvious overabundances than the solar abundances, for example, their $[\text{Ba}/\text{Fe}]$ values are from 0.45 to 1.27 . The abundance patterns of our sample stars are consistent with those obtained for other Ba stars in Začs (1994), Liang

et al. (2003), Smiljanic et al. (2007). Our study enlarge the sample of Ba stars with known chemical abundances. And we further check the formation scenario of these sample stars through theoretical wind accretion model.

We adopt the angular momentum conservation model of wind accretion to calculate the chemical abundances of Ba stars in the binary systems. The predicted results by the model can explain well the observed abundance patterns of the *s*-process elements. The abundance patterns of two sample stars, HD 211594 and HD 223617, can also be explained by the wind accretion model although their orbital periods are 1018.9 and 1293.7 days respectively, which are lower than the low limit of wind accretion formation of Ba stars suggested by Jorissen et al. (1998), 1500 days, and Zhang et al. (1999), Liang et al. (2000), 1600 days. This result could further decrease such low limit to be about 1000 days.

The masses of the sample stars are also determined and given in Table 3, as well as their errors. For most of them, their masses ($0.78\text{-}1.92M_{\odot}$) are close to the average masses of typical mild and strong Ba stars given in Jorissen et al. (1998) (their Table 9), who suggested that the average mass of typical mild Ba stars is 1.9 or $2.3M_{\odot}$ with the 0.60 or $0.67M_{\odot}$ companion white dwarfs, and the average mass of typical strong Ba stars is 1.5 or $1.9M_{\odot}$ with the 0.60 or $0.67M_{\odot}$ companion white dwarfs. However, the very high mass ($4.58M_{\odot}$) of HD 201824 should not be real and the reason could be the big error of its parallax, up to 3 times ($1.56/0.56$) uncertainty, which will cause the uncertainties of ~ 0.4 dex in $\log g$ and $3.2M_{\odot}$ in mass. This 0.4 dex uncertainty in $\log g$ is larger than the general case (0.2 dex) of the sample stars, but will not affect much the abundances. In Table 5 and Figure 6, we adopt the general uncertainties of $\log g$, 0.2 dex, to estimate the uncertainties on abundances for HD 201824.

The derived abundances of our sample stars confirm well their “strong” or “mild” Ba star properties. As shown in Table 4, Figure 3 and Figure 6, for the four mild Ba stars, namely, HD 180622, HD 210946, HD 216219 and HD 223617, their average abundances of *s*-process elements are $[\text{Ba}/\text{Fe}]=0.79$, $[\text{La}/\text{Fe}]=0.92$, $[\text{Y}/\text{Fe}]=0.43$, $[\text{Zr}/\text{Fe}]=0.66$, $[\text{Eu}/\text{Fe}]=0.44$; and for the three strong Ba stars, HD 201657, HD 201824 and HD 211594, their average abundances of *s*-process elements are $[\text{Ba}/\text{Fe}]=1.25$, $[\text{La}/\text{Fe}]=1.31$, $[\text{Y}/\text{Fe}]=0.65$, $[\text{Zr}/\text{Fe}]=0.66$, $[\text{Eu}/\text{Fe}]=0.63$. These show that the *s*-process element abundances of strong Ba stars are about 0.4 dex (or 0.2 dex) higher than those of the mild Ba stars. However, there are no obvious trend to show that the strong and mild Ba stars have different ranges in metallicity (also see Smiljanic et al. 2007). Also, there are no obvious indication to show that the orbital periods of mild Ba stars are longer than those of the strong Ba stars.

HD 4395 is a CH subgiant star. HD 216219 has also been classified as a CH subgiant (Smith et al. 1993 and the reference therein) or a mild Ba stars (Jorissen et al. 1998; Lü et al. 1991). CH subgiant was firstly discovered by Bond (1974). As Luck & Bond (1982) discussed, some of their CH subgiants might more properly be called subgiant barium stars or even main-sequence barium stars. We did not find obvious difference in the abundance patterns of our CH subgiant sample stars and the Ba sample stars except HD 4395 shows a bit relatively lower overabundances in its *s*-process elements. Moreover, the wind accretion models for binary system can explain well the observed overabundances of *s*-process elements in the CH subgiant stars as for other Ba stars. However, our results are not enough to check the suggested evolutionary relation between CH subgiants and classical Ba stars, which will need C/O and Li abundances (Smith et al. 1993; Lambert et al. 1993).

Acknowledgements We thank our referee for very valuable comments which help us a lot to improve this work. We would like to thank Prof. Gang Zhao, Yuqin Chen, Jianrong Shi, Yujuan Liu, Shu Liu, Kefeng Tan and the *Stellar Abundance and Galactic Evolution Group* at NAOC for sharing their programs for abundance analysis and the helpful discussions about data reduction and abundance analysis. This work was supported by the Natural Science Foundation of China (NSFC) Foundation under No.10403006, 10433010, 10673002, 10573022, 10333060, and 10521001; and the National Basic Research Program of China (973 Program) No.2007CB815404, 2007CB815406.

References

- Alonso S., Arribas S., Martínez-Roger C., 1999, A&AS, 140, 261
 Alonso S., Arribas S., Martínez-Roger C., 2001, A&A, 376, 1039
 Bard A., Kock M., 1994, A&A, 282, 1014
 Bidelman W. K., Keenan P. C., 1951, ApJ, 114, 473
 Biémont E., Grevesse N., Hannaford P., Lowe R. M., 1981, ApJ, 248, 867
 Biémont E., Karner C., Meyer G., Traeger F., Zu Putlitz G., 1982, A&A, 107, 166
 Boffin H. M. J., Jorissen A., 1988, A&A, 205, 155
 Boffin H. M. J., Začs L., 1994, A&A, 291, 811
 Bond H. E., 1974, ApJ, 194, 95
 Burbidge E. M., Burbidge G. R., Fowler W. A., Hoyle F., 1957, RvMP, 29, 547
 Carquillat J. M., Jorissen A., Udry S., Ginestet N., 1998, AAS, 131, 49
 Chen Y. Q., Nissen P. E., Zhao G., Schuster W. J., Zhang H. W., Benoni, T., 2000a, LIACo, 35, 219
 Chen Y. Q., Nissen P. E., Zhao G., Zhang H. W., Benoni T., 2000b, A&AS, 141, 491
 ESA 1997, the Hipparcos and Tycho Catalogues, ESA SP-1200
 Fuhr J. R., Martin G. A., Wiese W. L., 1988, JPCRD, 17, Suppl.4
 Gallino R., Arlandini C., Busso M. et al., 1998, ApJ, 497, 388
 Gómez A. E., Luri X., Grenier S. et al., 1997, A&A, 319, 881
 Grevesse N., Sauval A. J., 1998, Space Sci. Rev., 85, 161
 Griffin R. F., 1980, MNRAS, 193, 957
 Han Z. W., Eggleton P. P., Podsiadlowski P., Tout, C. A., 1995, MNRAS, 277, 1443
 Hannaford P., Lowe R. M., Grevesse N., Biémont E., Whaling W., 1982, ApJ, 261, 736
 Jorissen A., Mayor, M., 1988, A&A, 198, 187
 Jorissen A., Van Eck S., Mayor M., Udry, S., 1998, A&A, 332, 877
 Krishnaswamy K., Sneden C., 1985, PASP, 97, 407
 Kurucz R. L., 1993, CD-ROM, Vol. 13, Smithsonian Astrophysics Observatory, Cambridge
 Lambert D. L., Warner B., 1968, MNRAS, 139, 115
 Lambert D. L., Smith V. V., Heath J., 1993, PASP, 105, 568
 Lambert D. L., Heath J. H., Lemke M. et al., 1996, ApJS, 103, 183
 Liang Y. C., Zhao G., Zhang B., 2000, A&A, 363, 555
 Liang Y. C., Zhao G., Chen Y. Q., Qiu H. M., Zhang B., 2003, A&A, 397, 257
 Liu J. H., Zhang B., Liang Y. C., Peng, Q. H., 2000, A&A, 363, 660
 Luck R. E., Bond H. E., 1982, ApJ, 259, 792
 Luck R. E., Bond H. E., 1991, ApJS, 77, 515
 Lü Phillip K., 1991, AJ, 101, 2229

- McClure R. D., Fletcher J. M., Nemeč, J. M., 1980, *ApJ*, 238, L35
McClure R. D., 1983, *ApJ*, 268, 264
McClure R. D., Woodsworth A. W., 1990, *ApJ*, 352, 709
Mennessier M. O., Luri X., Figueras F. et al., 1997, *A&A*, 326, 722
Nissen P. E., Chen Y. Q., Schuster W. J., Zhao G., 2000, *A&A*, 353, 722
O'Brian T. R., Wickliffe M. E., Lawler J. E. et al., 1991, *JOSAB*, 8, 1185
Preston G. W., Sneden C., 2001, *AJ*, 122, 1545
Smith V. V., Coleman H., Lambert D., 1993, *MNRAS*, 417, 287
Smiljanic R., Porto de Mello G. F., da Silva L., 2007, *A&A*, 468, 679
Sneden C., 1983, *PASP*, 95, 745
Udry S., Jorissen A., Mayor M., Van Eck, S., 1998a, *A&AS*, 131, 25
Udry S., Mayor M., Van Eck S., Jorissen A., Prévot L., Grenier, S., Lindgren H., 1998b, *A&AS*, 131, 43
Weise W. L., Martin, G. A., 1980, *NSDRS-NBS*, 68
Yi S. K., Kim Y. C., Demarque P., 2003, *ApJS*, 144, 259
Začs L., 1994, *A&A*, 283, 937
Zhang B., Liu J. H., Liang Y. C., Peng Q. H., 1999, *ChA&A*, 23, 189
Zhao G., Qiu H. M., Chen Y. Q., Li Z. W., 2000, *ApJ*, 126, 461

Table 2 (continued)

| λ (Å) | Ion | χ | $\log gf$ | Ref. | HD 4395 | | HD 180622 | | HD 201657 | | HD 201824 | | HD 210946 | | HD 211594 | | HD 216219 | | HD 223617 | |
|---------------|------|--------|-----------|------|---------|-----------------|-----------|-----------------|-----------|-----------------|-----------|-----------------|-----------|-----------------|-----------|-----------------|-----------|-----------------|-----------|-----------------|
| | | | | | EW | $\log \epsilon$ | EW | $\log \epsilon$ | EW | $\log \epsilon$ | EW | $\log \epsilon$ | EW | $\log \epsilon$ | EW | $\log \epsilon$ | EW | $\log \epsilon$ | EW | $\log \epsilon$ |
| 5859.596 | Fe I | 4.55 | -0.66 | lz | — | — | — | — | — | — | — | — | — | — | — | — | 71.9 | 7.394 | — | — |
| 5862.368 | Fe I | 4.55 | -0.45 | lz | — | — | — | — | 94.1 | 6.912 | — | — | — | — | 87.6 | 6.871 | 70.3 | 7.155 | — | — |
| 5905.680 | Fe I | 4.65 | -0.73 | lz | — | — | — | — | 71.2 | 6.914 | — | — | — | — | 66.7 | 6.897 | 49.9 | 7.160 | 75.6 | 7.096 |
| 5927.797 | Fe I | 4.65 | -1.09 | lz | — | — | 81.3 | 7.617 | 50.0 | 6.906 | — | — | — | — | 45.6 | 6.884 | 37.7 | 7.290 | — | — |
| 5929.682 | Fe I | 4.55 | -1.41 | lz | — | — | — | — | 59.8 | 7.269 | 57.3 | 7.206 | 56.4 | 7.283 | 60.7 | 7.349 | — | — | 63.5 | 7.426 |
| 5930.191 | Fe I | 4.65 | -0.23 | lz | — | — | — | — | — | — | — | — | — | — | — | — | 75.0 | 7.110 | — | — |
| 5934.665 | Fe I | 3.93 | -1.17 | lz | 77.2 | 7.352 | — | — | — | — | — | — | — | — | — | — | 56.9 | 7.013 | — | — |
| 5952.726 | Fe I | 3.98 | -1.44 | nd | — | — | — | — | — | — | — | — | — | — | 81.0 | 7.033 | — | — | — | — |
| 6003.022 | Fe I | 3.88 | -1.12 | lz | 90.4 | 7.497 | — | — | — | — | — | — | — | — | — | — | 71.6 | 7.185 | — | — |
| 6024.068 | Fe I | 4.55 | -0.12 | nd | — | — | — | — | — | — | — | — | — | — | — | — | 93.6 | 7.224 | — | — |
| 6027.059 | Fe I | 4.07 | -1.09 | cn | 67.0 | 7.208 | — | — | — | — | — | — | 94.8 | 7.062 | 91.9 | 6.991 | — | — | 98.0 | 7.165 |
| 6034.033 | Fe I | 4.31 | -2.42 | nd | — | — | 45.2 | 7.847 | — | — | — | — | — | — | — | — | — | — | — | — |
| 6056.013 | Fe I | 4.73 | -0.46 | lz | 71.6 | 7.316 | — | — | 88.8 | 7.044 | 89.7 | 7.088 | 90.0 | 7.141 | 80.8 | 6.969 | 64.3 | 7.221 | 94.5 | 7.275 |
| 6079.016 | Fe I | 4.65 | -1.12 | lz | — | — | 86.8 | 7.746 | 68.6 | 7.251 | — | — | 73.3 | 7.404 | 66.5 | 7.278 | — | — | 77.2 | 7.507 |
| 6093.649 | Fe I | 4.61 | -1.50 | lz | 26.2 | 7.355 | 71.6 | 7.787 | 49.4 | 7.248 | 38.6 | 7.022 | 50.9 | 7.344 | 45.9 | 7.247 | — | — | 58.9 | 7.500 |
| 6094.370 | Fe I | 4.65 | -1.94 | nd | — | — | — | — | — | — | — | — | — | — | 32.1 | 7.472 | — | — | — | — |
| 6096.671 | Fe I | 3.98 | -1.93 | lz | 41.9 | 7.471 | 83.1 | 7.638 | 62.4 | 7.091 | — | — | 65.7 | 7.263 | 54.4 | 7.051 | 23.1 | 7.136 | 69.9 | 7.350 |
| 6105.150 | Fe I | 4.55 | -2.07 | nd | — | — | — | — | — | — | — | — | 32.2 | 7.492 | — | — | — | — | — | — |
| 6137.002 | Fe I | 2.20 | -2.87 | cn | — | — | — | — | — | — | — | — | — | — | — | — | 77.0 | 7.304 | — | — |
| 6151.623 | Fe I | 2.18 | -3.28 | cn | 56.6 | 7.213 | — | — | — | — | — | — | — | — | — | — | — | — | — | — |
| 6157.733 | Fe I | 4.07 | -1.26 | nd | — | — | — | — | — | — | — | — | — | — | — | — | 62.4 | 7.334 | — | — |
| 6159.370 | Fe I | 4.61 | -1.97 | nd | — | — | — | — | 37.2 | 7.494 | 28.7 | 7.288 | — | — | 42.0 | 7.643 | — | — | — | — |
| 6165.363 | Fe I | 4.14 | -1.47 | cn | 42.5 | 7.187 | 98.5 | 7.682 | 82.3 | 7.180 | — | — | 80.5 | 7.259 | 71.6 | 7.086 | — | — | 82.9 | 7.331 |
| 6173.341 | Fe I | 2.22 | -2.88 | cn | 79.3 | 7.301 | — | — | — | — | — | — | — | — | — | — | — | — | — | — |
| 6180.209 | Fe I | 2.73 | -2.58 | cn | 68.4 | 7.327 | — | — | — | — | — | — | — | — | — | — | 47.4 | 7.013 | — | — |
| 6187.995 | Fe I | 3.94 | -1.72 | cn | 55.8 | 7.482 | 97.8 | 7.657 | 84.8 | 7.208 | 75.1 | 7.066 | 70.1 | 7.074 | 83.5 | 7.294 | — | — | 86.8 | 7.401 |
| 6200.321 | Fe I | 2.61 | -2.44 | cn | 74.4 | 7.172 | — | — | — | — | — | — | — | — | — | — | 64.5 | 7.059 | — | — |

Table 2 (continued)

| λ (Å) | Ion | χ | $\log gf$ | Ref. | HD 4395 | | HD 180622 | | HD 201657 | | HD 201824 | | HD 210946 | | HD 211594 | | HD 216219 | | HD 223617 | |
|---------------|------|--------|-----------|------|---------|-----------------|-----------|-----------------|-----------|-----------------|-----------|-----------------|-----------|-----------------|-----------|-----------------|-----------|-----------------|-----------|-----------------|
| | | | | | EW | $\log \epsilon$ | EW | $\log \epsilon$ | EW | $\log \epsilon$ | EW | $\log \epsilon$ | EW | $\log \epsilon$ | EW | $\log \epsilon$ | EW | $\log \epsilon$ | EW | $\log \epsilon$ |
| 6213.437 | Fe I | 2.22 | -2.58 | nd | 89.2 | 7.197 | — | — | — | — | — | — | — | — | — | — | — | — | — | — |
| 6215.149 | Fe I | 4.19 | -1.13 | lz | 76.9 | 7.551 | — | — | — | — | 91.9 | 7.117 | — | — | — | — | 44.8 | 7.002 | — | — |
| 6229.232 | Fe I | 2.84 | -2.81 | cn | 42.7 | 7.168 | — | — | — | — | — | — | 86.5 | 7.065 | — | — | — | — | 99.2 | 7.313 |
| 6232.648 | Fe I | 3.65 | -1.22 | cn | 91.0 | 7.365 | — | — | — | — | — | — | — | — | — | — | 77.0 | 7.154 | — | — |
| 6240.653 | Fe I | 2.22 | -3.27 | cn | 70.9 | 7.514 | — | — | — | — | — | — | — | — | — | — | 43.9 | 7.099 | — | — |
| 6246.327 | Fe I | 3.60 | -0.88 | cn | — | — | — | — | — | — | — | — | — | — | — | — | 94.2 | 7.104 | — | — |
| 6270.231 | Fe I | 2.86 | -2.61 | cn | 63.1 | 7.377 | — | — | — | — | — | — | — | — | — | — | 50.1 | 7.220 | — | — |
| 6301.508 | Fe I | 3.65 | -0.72 | cn | — | — | — | — | — | — | — | — | — | — | — | — | 95.5 | 6.972 | — | — |
| 6330.852 | Fe I | 4.73 | -1.74 | nd | — | — | — | — | — | — | — | — | — | — | 49.1 | 7.683 | — | — | — | — |
| 6336.830 | Fe I | 3.69 | -0.86 | cn | — | — | — | — | — | — | — | — | — | — | — | — | 85.8 | 6.969 | — | — |
| 6344.155 | Fe I | 2.43 | -2.90 | cn | — | — | — | — | — | — | — | — | — | — | — | — | 68.2 | 7.379 | — | — |
| 6358.687 | Fe I | 0.86 | -4.17 | cn | 90.6 | 7.299 | — | — | — | — | — | — | — | — | — | — | — | — | — | — |
| 6380.750 | Fe I | 4.19 | -1.29 | cn | 59.8 | 7.375 | — | — | — | — | — | — | 97.5 | 7.431 | 85.2 | 7.195 | 39.2 | 7.036 | — | — |
| 6408.026 | Fe I | 3.69 | -1.01 | cn | — | — | — | — | — | — | — | — | — | — | — | — | 88.4 | 7.165 | — | — |
| 6419.956 | Fe I | 4.73 | -0.24 | nd | — | — | — | — | — | — | — | — | — | — | — | — | 74.0 | 7.147 | — | — |
| 6481.878 | Fe I | 2.28 | -2.97 | cn | 78.4 | 7.401 | — | — | — | — | — | — | — | — | — | — | 59.1 | 7.119 | — | — |
| 6551.676 | Fe I | 0.99 | -5.79 | nd | — | — | — | — | — | — | — | — | 58.2 | 7.187 | — | — | — | — | — | — |
| 6593.884 | Fe I | 2.43 | -2.42 | cn | 97.7 | 7.381 | — | — | — | — | — | — | — | — | — | — | — | — | — | — |
| 6597.561 | Fe I | 4.80 | -1.06 | lz | 40.4 | 7.379 | — | — | 57.0 | 7.171 | 58.7 | 7.155 | 60.3 | 7.276 | 51.2 | 7.118 | 29.6 | 7.210 | 66.1 | 7.401 |
| 6608.024 | Fe I | 2.28 | -4.04 | nd | 20.6 | 7.306 | 92.2 | 7.638 | — | — | — | — | — | — | — | — | — | — | — | — |
| 6609.118 | Fe I | 2.56 | -2.66 | cn | 71.3 | 7.233 | — | — | — | — | — | — | — | — | — | — | — | — | — | — |
| 6646.932 | Fe I | 2.61 | -3.99 | nd | 14.0 | 7.397 | — | — | — | — | — | — | 48.4 | 7.302 | 50.3 | 7.288 | — | — | — | — |
| 6703.576 | Fe I | 2.76 | -3.16 | lz | 42.5 | 7.400 | — | — | — | — | 74.5 | 6.942 | 95.8 | 7.433 | 92.6 | 7.340 | — | — | — | — |
| 6716.220 | Fe I | 4.58 | -1.93 | nd | 16.9 | 7.467 | — | — | — | — | — | — | — | — | — | — | — | — | — | — |
| 6725.353 | Fe I | 4.19 | -2.30 | nd | 15.0 | 7.378 | 55.9 | 7.741 | 42.2 | 7.367 | 26.8 | 7.039 | 37.0 | 7.362 | — | — | — | — | — | — |
| 6726.673 | Fe I | 4.61 | -1.00 | cn | 43.8 | 7.186 | 81.7 | 7.441 | 62.6 | 6.958 | — | — | 70.5 | 7.155 | 59.0 | 6.954 | 35.8 | 7.084 | 69.9 | 7.170 |
| 6733.151 | Fe I | 4.64 | -1.58 | lz | 18.4 | 7.222 | 64.8 | 7.745 | 52.1 | 7.395 | 32.7 | 6.991 | — | — | 52.5 | 7.455 | — | — | 52.7 | 7.473 |

Table 2 (continued)

| λ (Å) | Ion | χ | $\log gf$ | Ref. | HD 4395 | | HD 180622 | | HD 201657 | | HD 201824 | | HD 210946 | | HD 211594 | | HD 216219 | | HD 223617 | |
|---------------|------|--------|-----------|------|---------|-----------------|-----------|-----------------|-----------|-----------------|-----------|-----------------|-----------|-----------------|-----------|-----------------|-----------|-----------------|-----------|-----------------|
| | | | | | EW | $\log \epsilon$ | EW | $\log \epsilon$ | EW | $\log \epsilon$ | EW | $\log \epsilon$ | EW | $\log \epsilon$ | EW | $\log \epsilon$ | EW | $\log \epsilon$ | EW | $\log \epsilon$ |
| 6745.090 | Fe I | 4.58 | -2.17 | nd | — | — | 40.4 | 7.812 | — | — | 19.9 | 7.211 | 22.8 | 7.398 | — | — | — | — | — | — |
| 6746.932 | Fe I | 2.61 | -4.25 | nd | — | — | — | — | — | — | — | — | 23.0 | 7.079 | — | — | — | — | — | — |
| 6752.716 | Fe I | 4.64 | -1.20 | bk | 29.1 | 7.121 | — | — | — | — | — | — | — | — | 84.0 | 7.625 | — | — | — | — |
| 6786.856 | Fe I | 4.19 | -2.06 | nd | 26.6 | 7.459 | 71.6 | 7.779 | 47.6 | 7.221 | — | — | 55.3 | 7.438 | 46.7 | 7.281 | — | — | — | — |
| 6806.856 | Fe I | 2.73 | -3.21 | lz | 43.0 | 7.421 | — | — | — | — | 80.9 | 7.054 | 92.6 | 7.379 | 89.8 | 7.294 | 25.7 | 7.161 | 99.7 | 7.515 |
| 6810.267 | Fe I | 4.61 | -0.99 | cn | 51.5 | 7.311 | 91.6 | 7.605 | 76.5 | 7.177 | — | — | 77.0 | 7.249 | 67.1 | 7.077 | 34.5 | 7.040 | 79.2 | 7.320 |
| 6828.596 | Fe I | 4.64 | -0.92 | lz | 59.0 | 7.412 | — | — | 97.6 | 7.503 | 73.2 | 7.065 | 91.4 | 7.468 | 93.8 | 7.510 | 45.2 | 7.207 | — | — |
| 6839.835 | Fe I | 2.56 | -3.45 | lz | 42.9 | 7.477 | — | — | — | — | 76.6 | 6.997 | 97.6 | 7.483 | — | — | — | — | — | — |
| 6841.341 | Fe I | 4.61 | -0.75 | nd | — | — | — | — | — | — | — | — | — | — | — | 61.6 | 7.301 | — | — | |
| 6842.689 | Fe I | 4.64 | -1.32 | lz | — | — | 85.0 | 7.853 | 70.0 | 7.438 | 55.7 | 7.151 | 67.4 | 7.453 | 67.6 | 7.455 | — | — | 69.1 | 7.507 |
| 6843.655 | Fe I | 4.55 | -0.93 | lz | 62.3 | 7.390 | — | — | 97.5 | 7.394 | — | — | — | — | 88.0 | 7.305 | 49.8 | 7.211 | — | — |
| 6858.155 | Fe I | 4.61 | -0.93 | cn | 59.7 | 7.403 | 97.6 | 7.656 | 83.6 | 7.238 | — | — | 81.5 | 7.268 | 85.5 | 7.336 | — | — | 86.1 | 7.387 |
| 6999.885 | Fe I | 4.10 | -1.56 | nd | — | — | — | — | 91.9 | 7.331 | — | — | 90.7 | 7.418 | — | — | — | — | 96.1 | 7.549 |
| 7022.957 | Fe I | 4.19 | -1.25 | nd | — | — | — | — | 87.6 | 7.066 | 92.7 | 7.171 | — | — | 98.7 | 7.344 | — | — | — | — |
| 7071.866 | Fe I | 4.61 | -1.70 | lz | — | — | 68.8 | 7.891 | 51.7 | 7.463 | 42.2 | 7.246 | — | — | — | — | — | — | 55.9 | 7.605 |
| 7112.170 | Fe I | 2.99 | -2.99 | cn | — | — | — | — | — | — | — | — | 88.5 | 7.400 | 98.3 | 7.532 | — | — | — | — |
| 7132.985 | Fe I | 4.07 | -1.63 | cn | 47.5 | 7.308 | 93.8 | 7.573 | 75.3 | 7.077 | — | — | 69.6 | 7.079 | 77.6 | 7.199 | 35.5 | 7.142 | 77.6 | 7.234 |
| 7219.680 | Fe I | 4.07 | -1.35 | ow | — | — | — | — | — | — | 93.6 | 7.119 | — | — | — | — | — | — | — | — |
| 7284.842 | Fe I | 4.14 | -1.75 | nd | — | — | 80.1 | 7.528 | — | — | 70.8 | 7.193 | — | — | — | — | — | — | — | — |
| 7306.570 | Fe I | 4.18 | -1.74 | lz | — | — | 99.5 | 7.909 | 65.8 | 7.168 | — | — | 77.9 | 7.454 | 68.5 | 7.285 | — | — | 72.9 | 7.388 |
| 7401.691 | Fe I | 4.19 | -1.60 | cn | 46.4 | 7.366 | 91.9 | 7.638 | 75.3 | 7.189 | 64.9 | 6.994 | 76.1 | 7.289 | 73.2 | 7.229 | 32.9 | 7.168 | 92.7 | 7.604 |
| 7418.672 | Fe I | 4.14 | -1.38 | ow | — | — | — | — | 80.7 | 6.987 | — | — | 83.4 | 7.126 | 80.3 | 7.061 | 38.4 | 7.001 | 87.6 | 7.226 |
| 7443.026 | Fe I | 4.19 | -1.82 | nd | — | — | 85.5 | 7.742 | — | — | — | — | — | — | — | — | 25.8 | 7.232 | — | — |
| 7583.796 | Fe I | 3.02 | -1.88 | cn | 89.2 | 7.197 | — | — | — | — | — | — | — | — | — | — | — | — | — | — |
| 7710.367 | Fe I | 4.22 | -1.11 | cn | — | — | — | — | 99.0 | 7.107 | 93.1 | 7.023 | — | — | — | — | 54.1 | 7.086 | — | — |
| 7723.210 | Fe I | 2.28 | -3.62 | fm | 39.9 | 7.234 | — | — | — | — | — | — | 98.3 | 7.206 | — | — | — | — | — | — |
| 7746.605 | Fe I | 5.06 | -1.34 | nd | — | — | 58.1 | 7.874 | — | — | — | — | 34.0 | 7.355 | 42.8 | 7.519 | — | — | — | — |

Table 2 (continued)

| λ (Å) | Ion | χ | $\log gf$ | Ref. | HD 4395 | | HD 180622 | | HD 201657 | | HD 201824 | | HD 210946 | | HD 211594 | | HD 216219 | | HD 223617 | |
|---------------|-------|--------|-----------|------|---------|-----------------|-----------|-----------------|-----------|-----------------|-----------|-----------------|-----------|-----------------|-----------|-----------------|-----------|-----------------|-----------|-----------------|
| | | | | | EW | $\log \epsilon$ | EW | $\log \epsilon$ | EW | $\log \epsilon$ | EW | $\log \epsilon$ | EW | $\log \epsilon$ | EW | $\log \epsilon$ | EW | $\log \epsilon$ | EW | $\log \epsilon$ |
| 7751.116 | Fe I | 4.99 | -0.72 | cn | 40.4 | 7.175 | — | — | — | — | — | — | 79.7 | 7.440 | — | — | 33.8 | 7.092 | — | — |
| 7780.568 | Fe I | 4.47 | -0.09 | cn | — | — | — | — | — | — | — | — | — | — | — | — | 98.9 | 7.062 | — | — |
| 7941.096 | Fe I | 3.27 | -2.58 | nd | 51.6 | 7.445 | — | — | — | — | — | — | 72.8 | 7.036 | 73.6 | 7.005 | — | — | — | — |
| 5991.378 | Fe II | 3.15 | -3.56 | cn | 37.6 | 7.279 | 46.8 | 7.732 | — | — | — | — | — | — | — | — | 43.8 | 7.346 | — | — |
| 6084.110 | Fe II | 3.20 | -3.97 | nd | 20.3 | 7.318 | — | — | — | — | — | — | — | — | — | — | — | — | — | — |
| 6149.249 | Fe II | 3.89 | -2.72 | cn | 37.8 | 7.189 | — | — | — | — | — | — | — | — | — | — | 45.4 | 7.281 | 47.4 | 7.536 |
| 6247.562 | Fe II | 3.89 | -2.26 | lh | 68.5 | 7.371 | — | — | 51.7 | 7.319 | — | — | 64.5 | 7.351 | — | — | — | — | 62.1 | 7.412 |
| 6369.462 | Fe II | 2.89 | -4.36 | nd | 29.5 | 7.628 | — | — | — | — | — | — | — | — | — | — | — | — | — | — |
| 6416.928 | Fe II | 3.89 | -2.74 | cn | — | — | — | — | — | — | 50.6 | 7.109 | — | — | — | — | — | — | — | — |
| 6432.683 | Fe II | 2.89 | -3.58 | cn | 52.4 | 7.344 | 58.9 | 7.738 | 46.1 | 7.308 | — | — | 57.4 | 7.354 | — | — | 53.4 | 7.273 | 51.2 | 7.316 |
| 6456.391 | Fe II | 3.90 | -2.07 | cn | 76.1 | 7.335 | — | — | — | — | — | — | 77.1 | 7.435 | — | — | — | — | — | — |
| 7711.731 | Fe II | 3.90 | -2.47 | cn | 47.6 | 7.087 | — | — | — | — | 66.4 | 7.161 | — | — | — | — | — | — | 59.5 | 7.570 |
| 6154.230 | Na I | 2.10 | -1.57 | cn | 28.7 | 6.007 | 125.2 | 6.688 | 86.4 | 5.993 | 53.0 | 5.829 | — | — | 83.3 | 6.145 | 24.7 | 5.987 | 96.6 | 6.369 |
| 6160.753 | Na I | 2.10 | -1.23 | cn | 55.1 | 6.102 | 141.6 | 6.583 | 112.1 | 5.993 | 81.3 | 5.890 | 101.7 | 6.123 | 104.5 | 6.090 | 34.8 | 5.843 | 117.1 | 6.323 |
| 5528.418 | Mg I | 4.34 | -0.78 | nd | — | — | — | — | — | — | — | — | — | — | — | — | 193.0 | 7.286 | — | — |
| 5711.095 | Mg I | 4.34 | -1.82 | nd | 80.3 | 7.126 | 162.8 | 7.780 | 151.0 | 7.416 | 136.7 | 7.463 | 82.6 | 6.606 | — | — | 88.4 | 7.288 | 146.3 | 7.555 |
| 7657.606 | Mg I | 5.11 | -1.19 | nd | 91.3 | 7.265 | — | — | — | — | 104.6 | 7.103 | — | — | 111.5 | 7.148 | 80.8 | 7.176 | 153.1 | 7.722 |
| 6696.020 | Al I | 3.14 | -1.33 | lw | 43.3 | 6.211 | — | — | — | — | — | — | — | — | — | — | — | — | — | — |
| 6698.670 | Al I | 3.14 | -1.87 | cn | 19.7 | 6.275 | 105.9 | 6.987 | 71.4 | 6.374 | 43.0 | 6.207 | 50.8 | 6.321 | 64.4 | 6.452 | 13.3 | 6.134 | 56.0 | 6.352 |
| 7835.317 | Al I | 4.02 | -0.58 | cn | 42.5 | 6.258 | 129.3 | 7.032 | 110.5 | 6.653 | 67.6 | 6.304 | — | — | — | — | 23.3 | 5.944 | — | — |
| 7836.130 | Al I | 4.02 | -0.40 | cn | 48.7 | 6.169 | 111.8 | 6.625 | 88.4 | 6.201 | 67.9 | 6.128 | 96.5 | 6.488 | 68.5 | 6.055 | 40.9 | 6.092 | — | — |
| 5665.563 | Si I | 4.92 | -2.04 | cn | 37.0 | 7.382 | 103.6 | — | — | — | — | — | — | — | — | — | 32.8 | 7.330 | 78.9 | 7.918 |
| 5690.433 | Si I | 4.93 | -1.87 | cn | — | — | 79.3 | 7.882 | — | — | — | — | — | — | — | — | — | — | — | — |
| 5701.108 | Si I | 4.93 | -2.05 | cn | 51.6 | 7.655 | — | — | 67.1 | 7.749 | — | — | 57.0 | 7.524 | 43.9 | 7.329 | 31.7 | 7.328 | 66.7 | 7.729 |
| 5772.149 | Si I | 5.08 | -1.67 | cn | 47.9 | 7.349 | — | — | — | — | — | — | — | — | — | — | 46.0 | 7.338 | 88.1 | 7.882 |
| 5793.079 | Si I | 4.93 | -1.95 | cn | 53.7 | 7.582 | 88.1 | 8.112 | 76.9 | 7.810 | — | — | 62.1 | 7.505 | 71.7 | 7.701 | 43.7 | 7.438 | 71.4 | 7.706 |
| 5948.548 | Si I | 5.08 | -1.19 | cn | 84.7 | 7.447 | — | — | — | — | 84.6 | 7.127 | — | — | 120.5 | 7.866 | 74.7 | 7.304 | — | — |

Table 2 (continued)

| λ (Å) | Ion | χ | $\log gf$ | Ref. | HD 4395 | | HD 180622 | | HD 201657 | | HD 201824 | | HD 210946 | | HD 211594 | | HD 216219 | | HD 223617 | |
|---------------|------|--------|-----------|------|---------|-----------------|-----------|-----------------|-----------|-----------------|-----------|-----------------|-----------|-----------------|-----------|-----------------|-----------|-----------------|-----------|-----------------|
| | | | | | EW | $\log \epsilon$ | EW | $\log \epsilon$ | EW | $\log \epsilon$ | EW | $\log \epsilon$ | EW | $\log \epsilon$ | EW | $\log \epsilon$ | EW | $\log \epsilon$ | EW | $\log \epsilon$ |
| 6125.026 | Si I | 5.61 | -1.54 | lz | 42.5 | 7.642 | — | — | — | — | — | — | — | — | 77.7 | 8.177 | — | — | — | — |
| 6142.494 | Si I | 5.62 | -1.48 | ns | — | — | 58.0 | 7.940 | — | — | — | — | — | — | — | — | 31.8 | 7.415 | 50.8 | 7.686 |
| 6145.020 | Si I | 5.62 | -1.43 | ns | 41.2 | 7.519 | — | — | 55.3 | 7.771 | 41.3 | 7.253 | — | — | 29.7 | 7.229 | 32.1 | 7.370 | 53.5 | 7.685 |
| 7034.910 | Si I | 5.87 | -0.81 | cn | 51.7 | 7.279 | 83.7 | 8.001 | — | — | 53.7 | 7.135 | — | — | 60.1 | 7.463 | 51.9 | 7.287 | — | — |
| 7226.208 | Si I | 5.61 | -1.30 | nd | 35.1 | 7.226 | — | — | — | — | 49.5 | 7.235 | 61.4 | 7.617 | — | — | 32.4 | 7.189 | 68.9 | 7.801 |
| 7405.790 | Si I | 5.61 | -0.68 | cn | 84.2 | 7.360 | 118.4 | 8.070 | 110.9 | 7.855 | 97.6 | 7.404 | — | — | 119.4 | 7.884 | 82.5 | 7.334 | 115.6 | 7.889 |
| 7415.958 | Si I | 5.61 | -0.71 | cn | 94.9 | 7.549 | — | — | — | — | — | — | — | — | — | — | 93.4 | 7.524 | — | — |
| 7918.383 | Si I | 5.95 | -0.54 | cn | 79.9 | 7.433 | — | — | — | — | — | — | — | — | — | — | 65.8 | 7.245 | — | — |
| 7932.351 | Si I | 5.96 | -0.35 | cn | 106.1 | 7.576 | 98.0 | 7.823 | — | — | 134.4 | 7.982 | 83.7 | 7.411 | 93.4 | 7.574 | 94.9 | 7.435 | — | — |
| 5512.989 | Ca I | 2.93 | -0.53 | cn | — | — | — | — | 132.5 | 5.968 | 135.4 | 6.507 | 107.3 | 5.885 | 136.1 | 6.242 | 80.8 | 6.172 | — | — |
| 5581.979 | Ca I | 2.52 | -0.67 | cn | 111.3 | 6.364 | — | — | 192.2 | 6.336 | 153.5 | 6.440 | 147.9 | 6.179 | 184.3 | 6.481 | 98.7 | 6.222 | 159.5 | 6.358 |
| 5588.764 | Ca I | 2.52 | 0.06 | cn | — | — | — | — | 191.1 | 5.592 | 197.6 | 6.219 | 183.7 | 5.855 | 186.5 | 5.769 | — | — | 190.1 | 5.953 |
| 5590.126 | Ca I | 2.52 | -0.70 | cn | 102.6 | 6.267 | — | — | — | — | 118.7 | 5.864 | 128.0 | 5.908 | 133.2 | 5.890 | 93.1 | 6.164 | 149.8 | 6.255 |
| 5601.286 | Ca I | 2.52 | -0.52 | cn | 125.8 | 6.411 | — | — | 162.9 | 5.867 | 120.8 | 5.724 | — | — | 161.5 | 6.095 | 106.7 | 6.191 | — | — |
| 5867.572 | Ca I | 2.93 | -1.61 | cn | — | — | 81.9 | 6.367 | — | — | — | — | 45.4 | 5.942 | 43.3 | 5.830 | 18.5 | 6.101 | — | — |
| 6102.727 | Ca I | 1.88 | -0.79 | nd | 138.6 | 6.156 | — | — | — | — | 189.2 | 6.077 | 191.3 | 5.886 | — | — | — | — | — | — |
| 6122.226 | Ca I | 1.89 | -0.32 | nd | 185.2 | 6.107 | — | — | — | — | 199.5 | 5.727 | — | — | — | — | — | — | — | — |
| 6161.295 | Ca I | 2.52 | -1.19 | cn | 75.0 | 6.264 | — | — | — | — | 129.5 | 6.452 | 112.4 | 6.060 | 128.6 | 6.221 | 54.4 | 5.981 | — | — |
| 6163.754 | Ca I | 2.52 | -1.07 | nd | — | — | — | — | — | — | 136.0 | 6.429 | — | — | — | — | — | — | — | — |
| 6166.440 | Ca I | 2.52 | -1.19 | cn | 68.2 | 6.144 | 130.4 | 6.214 | 133.1 | 6.009 | 103.8 | 5.987 | 110.8 | 6.030 | 121.9 | 6.112 | 57.3 | 6.030 | 117.3 | 6.116 |
| 6169.044 | Ca I | 2.52 | -0.80 | lz | 97.9 | 6.251 | — | — | — | — | 125.2 | 5.980 | 145.3 | 6.168 | 125.2 | 5.773 | 82.0 | 6.048 | 153.7 | 6.293 |
| 6169.564 | Ca I | 2.52 | -0.51 | cn | — | — | — | — | — | — | 128.4 | 5.750 | 163.3 | 6.115 | 150.8 | 5.853 | 99.5 | 6.048 | 158.5 | 6.071 |
| 6439.083 | Ca I | 2.52 | 0.16 | cn | 168.9 | 6.201 | — | — | 185.7 | 5.328 | 166.5 | 5.625 | 193.5 | 5.763 | 188.4 | 5.604 | 148.9 | 5.998 | — | — |
| 6449.820 | Ca I | 2.52 | -0.50 | cn | 122.2 | 6.316 | — | — | — | — | — | — | — | — | 157.7 | 5.915 | — | — | — | — |
| 6455.605 | Ca I | 2.52 | -1.29 | cn | — | — | — | — | 110.9 | 5.736 | — | — | 93.3 | 5.821 | 100.7 | 5.847 | — | — | 105.4 | 5.981 |
| 6471.668 | Ca I | 2.52 | -0.69 | cn | 94.9 | 6.159 | — | — | — | — | 123.5 | 5.822 | 139.9 | 6.006 | — | — | 83.7 | 6.009 | — | — |
| 6493.788 | Ca I | 2.52 | -0.09 | cn | — | — | — | — | — | — | 168.1 | 5.952 | 178.6 | 5.954 | 185.6 | 5.942 | 116.9 | 5.981 | — | — |

Table 2 (continued)

| λ (Å) | Ion | χ | $\log gf$ | Ref. | HD 4395 | | HD 180622 | | HD 201657 | | HD 201824 | | HD 210946 | | HD 211594 | | HD 216219 | | HD 223617 | |
|---------------|-------|--------|-----------|------|---------|-----------------|-----------|-----------------|-----------|-----------------|-----------|-----------------|-----------|-----------------|-----------|-----------------|-----------|-----------------|-----------|-----------------|
| | | | | | EW | $\log \epsilon$ | EW | $\log \epsilon$ | EW | $\log \epsilon$ | EW | $\log \epsilon$ | EW | $\log \epsilon$ | EW | $\log \epsilon$ | EW | $\log \epsilon$ | EW | $\log \epsilon$ |
| 6499.654 | Ca I | 2.52 | -0.81 | cn | 88.6 | 6.156 | — | — | 141.4 | 5.750 | 106.0 | 5.620 | 127.5 | 5.921 | 129.3 | 5.856 | 71.0 | 5.893 | 139.2 | 6.096 |
| 6717.687 | Ca I | 2.71 | -0.52 | cn | — | — | — | — | 196.9 | 6.333 | 156.8 | 6.364 | — | — | 179.2 | 6.393 | 107.0 | 6.322 | — | — |
| 7148.150 | Ca I | 2.71 | -0.14 | cn | — | — | — | — | — | — | — | — | 191.7 | 6.180 | 190.5 | 6.058 | 137.2 | 6.292 | 189.5 | 6.179 |
| 5526.821 | Sc II | 1.77 | 0.13 | nd | — | — | 122.6 | 3.138 | 124.5 | 2.867 | 146.1 | 3.158 | 124.8 | 3.011 | 142.4 | 3.307 | 96.5 | 2.936 | 124.3 | 3.072 |
| 5657.880 | Sc II | 1.51 | -0.50 | nd | 81.5 | 3.056 | 121.3 | 3.384 | 102.2 | 2.734 | 104.2 | 2.617 | 96.0 | 2.766 | 102.4 | 2.887 | 85.1 | 3.069 | 110.2 | 3.080 |
| 5684.198 | Sc II | 1.51 | -0.20 | nd | — | — | — | — | — | — | — | — | — | — | 110.0 | 2.725 | 79.8 | 2.668 | — | — |
| 6245.620 | Sc II | 1.51 | -0.98 | lz | — | — | — | — | — | — | 97.2 | 2.894 | — | — | 98.0 | 3.233 | — | — | — | — |
| 6604.600 | Sc II | 1.36 | -1.16 | lz | 51.3 | 2.926 | 114.9 | 3.585 | 102.3 | 3.101 | — | — | 86.2 | 2.990 | 90.8 | 3.068 | 51.1 | 2.887 | — | — |
| 5866.461 | Ti I | 1.07 | -0.84 | cn | 42.2 | 4.519 | 178.3 | 5.360 | 141.3 | 4.315 | 86.0 | 3.949 | 117.1 | 4.444 | 110.6 | 4.196 | 36.0 | 4.522 | — | — |
| 5953.170 | Ti I | 1.89 | -0.21 | cn | 50.6 | 4.899 | 140.0 | 5.158 | 100.3 | 4.140 | 83.5 | 4.353 | — | — | — | — | 25.8 | 4.515 | 104.1 | 4.623 |
| 6126.224 | Ti I | 1.07 | -1.32 | cn | 29.3 | 4.731 | 129.7 | 4.875 | 131.7 | 4.556 | 108.9 | 4.760 | 93.7 | 4.494 | 114.3 | 4.689 | — | — | 112.8 | 4.736 |
| 6258.110 | Ti I | 1.44 | -0.43 | cn | 57.8 | 4.757 | — | — | — | — | 109.7 | 4.381 | — | — | — | — | 40.2 | 4.557 | 135.0 | 4.743 |
| 6261.106 | Ti I | 1.43 | -0.48 | cn | 65.1 | 4.925 | — | — | 137.8 | 4.313 | 109.2 | 4.406 | 121.3 | 4.577 | — | — | — | — | — | — |
| 6312.241 | Ti I | 1.46 | -1.55 | lz | — | — | 75.4 | 4.693 | 52.0 | 4.147 | 32.2 | 4.280 | 40.0 | 4.432 | — | — | — | — | 57.5 | 4.597 |
| 6599.110 | Ti I | 0.90 | -2.08 | lz | — | — | — | — | 73.4 | 4.146 | 39.6 | 4.178 | 62.5 | 4.529 | — | — | — | — | 84.9 | 4.736 |
| 6743.120 | Ti I | 0.90 | -1.63 | lz | 12.1 | 4.332 | 133.9 | 4.857 | — | — | 55.9 | 3.952 | 84.1 | 4.349 | — | — | — | — | 107.6 | 4.603 |
| 5727.057 | V I | 1.08 | -0.01 | cn | — | — | 164.1 | 4.431 | — | — | — | — | 128.3 | 3.907 | 194.5 | 4.807 | 41.1 | 3.806 | — | — |
| 6090.216 | V I | 1.08 | -0.14 | cn | 36.7 | 3.710 | 138.6 | 3.948 | 109.7 | 3.081 | — | — | 91.6 | 3.326 | 81.6 | 3.036 | 18.3 | 3.410 | 113.8 | 3.631 |
| 6216.358 | V I | 0.28 | -0.75 | lz | — | — | 162.5 | 3.772 | — | — | — | — | 103.2 | 2.940 | 70.3 | 2.349 | — | — | 137.5 | 3.440 |
| 5783.866 | Cr I | 3.32 | -0.20 | cn | 45.4 | 5.478 | 116.7 | 5.902 | 111.7 | 5.570 | — | — | 86.9 | 5.451 | 106.3 | 5.713 | 32.6 | 5.299 | 108.1 | 5.826 |
| 5787.926 | Cr I | 3.32 | -0.18 | cn | 38.5 | 5.333 | 109.6 | 5.749 | 86.3 | 5.118 | 75.2 | 5.263 | 70.7 | 5.158 | 62.1 | 4.939 | 31.7 | 5.266 | 87.8 | 5.430 |
| 6925.280 | Cr I | 3.45 | -0.33 | nd | 40.2 | 5.587 | — | — | 61.7 | 4.979 | 60.9 | 5.246 | 62.9 | 5.269 | 45.9 | 4.930 | 24.3 | 5.322 | — | — |
| 6978.383 | Cr I | 3.46 | 0.14 | cn | 63.1 | 5.536 | — | — | — | — | — | — | — | — | — | — | — | — | — | — |
| 6979.806 | Cr I | 3.46 | -0.41 | lz | 30.6 | 5.484 | 106.3 | 5.952 | — | — | 73.1 | 5.538 | 80.5 | 5.637 | 85.4 | 5.655 | 22.7 | 5.371 | 97.1 | 5.886 |
| 7355.891 | Cr I | 2.89 | -0.29 | cn | 63.0 | 5.351 | 155.6 | 5.806 | — | — | 89.9 | 4.927 | — | — | — | — | 54.4 | 5.272 | 152.4 | 5.860 |
| 7400.188 | Cr I | 2.90 | -0.17 | cn | 67.2 | 5.315 | 164.7 | 5.825 | 137.9 | 5.168 | — | — | 126.4 | 5.369 | 120.9 | 5.191 | — | — | 140.6 | 5.571 |
| 6013.497 | Mn I | 3.07 | -0.15 | lz | 94.8 | 5.413 | 177.0 | 5.800 | 140.0 | 5.004 | 124.5 | 5.102 | 138.4 | 5.270 | 136.7 | 5.164 | 67.2 | 4.989 | 147.9 | 5.449 |

Table 2 (continued)

| λ (Å) | Ion | χ | $\log gf$ | Ref. | HD 4395 | | HD 180622 | | HD 201657 | | HD 201824 | | HD 210946 | | HD 211594 | | HD 216219 | | HD 223617 | |
|---------------|------|--------|-----------|------|---------|-----------------|-----------|-----------------|-----------|-----------------|-----------|-----------------|-----------|-----------------|-----------|-----------------|-----------|-----------------|-----------|-----------------|
| | | | | | EW | $\log \epsilon$ | EW | $\log \epsilon$ | EW | $\log \epsilon$ | EW | $\log \epsilon$ | EW | $\log \epsilon$ | EW | $\log \epsilon$ | EW | $\log \epsilon$ | EW | $\log \epsilon$ |
| 6021.803 | Mn I | 3.07 | 0.02 | lz | 68.5 | 4.778 | 170.2 | 5.555 | 138.4 | 4.810 | 121.0 | 4.864 | 137.7 | 5.090 | 132.5 | 4.933 | 64.5 | 4.773 | 147.3 | 5.271 |
| 5578.729 | Ni I | 1.68 | -2.80 | cn | — | — | — | — | — | — | 135.5 | 6.412 | — | — | 146.8 | 6.608 | — | — | 124.7 | 6.324 |
| 5587.868 | Ni I | 1.93 | -2.14 | fm | — | — | — | — | — | — | 128.4 | 5.930 | 137.3 | 6.167 | — | — | 62.5 | 5.750 | — | — |
| 5593.746 | Ni I | 3.90 | -0.84 | cn | 51.9 | 6.202 | 93.2 | 6.575 | 77.1 | 6.079 | 66.4 | 5.835 | 67.7 | 5.988 | 82.9 | 6.254 | 38.0 | 5.990 | — | — |
| 5625.328 | Ni I | 4.09 | -0.70 | fm | — | — | — | — | — | — | — | — | — | — | 86.5 | 6.400 | 39.1 | 6.056 | — | — |
| 5694.991 | Ni I | 4.09 | -0.61 | cn | 48.4 | 6.091 | — | — | 85.1 | 6.222 | 64.9 | 5.802 | 73.7 | 6.085 | 71.5 | 6.046 | 40.6 | 5.991 | — | — |
| 5754.666 | Ni I | 1.93 | -2.33 | fm | — | — | — | — | — | — | 138.3 | 6.278 | — | — | 130.0 | 6.142 | 69.5 | 6.056 | — | — |
| 5805.226 | Ni I | 4.17 | -0.64 | cn | — | — | 72.2 | 6.297 | 49.7 | 5.742 | — | — | 63.9 | 6.033 | — | — | — | — | — | — |
| 6086.288 | Ni I | 4.26 | -0.53 | cn | 44.3 | 6.088 | — | — | 62.5 | 5.961 | 73.0 | 6.060 | 60.6 | 5.963 | — | — | 29.8 | 5.850 | 67.2 | 6.116 |
| 6108.125 | Ni I | 1.68 | -2.63 | lz | 72.1 | 6.033 | 149.6 | 6.512 | 147.3 | 6.103 | — | — | 132.2 | 6.138 | — | — | 53.9 | 5.776 | 134.2 | 6.222 |
| 6111.078 | Ni I | 4.09 | -0.81 | fm | 30.6 | 5.927 | 76.5 | 6.436 | — | — | — | — | 62.9 | 6.076 | — | — | — | — | 74.3 | 6.316 |
| 6128.984 | Ni I | 1.68 | -3.33 | fm | 36.7 | 6.074 | 117.8 | 6.636 | 89.0 | 5.812 | 80.1 | 5.718 | 80.2 | 5.903 | 71.9 | 5.725 | 16.8 | 5.699 | 92.7 | 6.129 |
| 6130.141 | Ni I | 4.26 | -0.96 | cn | 25.6 | 6.139 | 63.3 | 6.555 | — | — | 43.9 | 5.951 | 38.8 | 6.004 | — | — | 14.4 | 5.872 | 40.3 | 6.047 |
| 6176.816 | Ni I | 4.09 | -0.26 | cn | — | — | — | — | — | — | — | — | 97.0 | 6.117 | — | — | 52.9 | 5.842 | 99.6 | 6.228 |
| 6327.604 | Ni I | 1.68 | -3.11 | cn | 40.5 | 5.911 | 132.5 | 6.654 | 120.0 | 6.098 | 94.6 | 5.737 | 94.9 | 5.915 | 84.6 | 5.699 | 25.2 | 5.686 | 108.7 | 6.184 |
| 6482.809 | Ni I | 1.93 | -2.63 | fm | 46.0 | 5.785 | 132.6 | 6.477 | 110.8 | 5.785 | — | — | — | — | — | — | — | — | — | — |
| 6586.319 | Ni I | 1.95 | -2.73 | cn | 55.4 | 6.071 | 120.0 | 6.359 | 90.3 | 5.560 | — | — | 105.3 | 6.039 | — | — | 27.4 | 5.624 | 106.4 | 6.082 |
| 6635.150 | Ni I | 4.42 | -0.83 | lz | 25.7 | 6.143 | 86.2 | 7.014 | — | — | 52.0 | 6.140 | — | — | — | — | 20.9 | 6.067 | — | — |
| 6643.638 | Ni I | 1.68 | -2.30 | fm | 107.5 | 6.300 | — | — | 168.1 | 5.964 | 133.0 | 5.601 | 160.3 | 6.131 | — | — | 87.4 | 6.007 | 177.0 | 6.410 |
| 6767.784 | Ni I | 1.83 | -2.17 | cn | 82.3 | 5.859 | 171.6 | 6.421 | 141.4 | 5.638 | — | — | — | — | — | — | 71.4 | 5.732 | 148.8 | 6.061 |
| 6772.321 | Ni I | 3.66 | -0.95 | lz | 48.2 | 5.938 | — | — | 87.6 | 6.009 | 63.9 | 5.528 | 83.2 | 6.014 | 78.6 | 5.937 | 35.5 | 5.753 | 89.7 | 6.171 |
| 7001.600 | Ni I | 1.94 | -3.66 | nd | 13.4 | 6.031 | 85.6 | 6.611 | — | — | 38.7 | 5.619 | 48.0 | 5.981 | 43.5 | 5.872 | — | — | — | — |
| 7030.010 | Ni I | 3.54 | -1.73 | nd | 20.2 | 5.995 | — | — | — | — | 30.4 | 5.542 | 39.4 | 5.893 | — | — | 14.9 | 5.891 | — | — |
| 7110.905 | Ni I | 1.93 | -2.92 | nd | 46.5 | 6.036 | 147.6 | 6.889 | 142.2 | 6.480 | — | — | — | — | 125.7 | 6.428 | 20.6 | 5.589 | — | — |
| 7122.206 | Ni I | 3.54 | 0.04 | cn | — | — | — | — | — | — | 162.5 | 6.031 | — | — | — | — | 98.6 | 5.691 | 194.5 | 6.417 |
| 7385.244 | Ni I | 2.74 | -1.97 | cn | 57.7 | 6.128 | 145.6 | 6.934 | 108.7 | 6.095 | 74.0 | 5.509 | 83.5 | 5.840 | 99.2 | 6.078 | 28.1 | 5.646 | 97.5 | 6.100 |
| 7414.514 | Ni I | 1.99 | -2.57 | cn | — | — | — | — | — | — | 120.3 | 5.923 | — | — | — | — | 61.4 | 6.073 | — | — |

Table 2 (continued)

| λ (Å) | Ion | χ | $\log gf$ | Ref. | HD 4395 | | HD 180622 | | HD 201657 | | HD 201824 | | HD 210946 | | HD 211594 | | HD 216219 | | HD 223617 | |
|---------------|-------|--------|-----------|------|---------|-----------------|-----------|-----------------|-----------|-----------------|-----------|-----------------|-----------|-----------------|-----------|-----------------|-----------|-----------------|-----------|-----------------|
| | | | | | EW | $\log \epsilon$ | EW | $\log \epsilon$ | EW | $\log \epsilon$ | EW | $\log \epsilon$ | EW | $\log \epsilon$ | EW | $\log \epsilon$ | EW | $\log \epsilon$ | EW | $\log \epsilon$ |
| 7422.286 | Ni I | 3.63 | -0.33 | cn | 88.9 | 5.939 | 180.4 | 6.816 | 154.5 | 6.266 | 135.2 | 6.066 | — | — | 151.4 | 6.301 | 82.4 | 5.865 | — | — |
| 7525.118 | Ni I | 3.63 | -0.65 | cn | 78.8 | 6.092 | 152.3 | 6.823 | 131.4 | 6.284 | 120.8 | 6.143 | — | — | 128.6 | 6.323 | 59.0 | 5.796 | — | — |
| 7574.048 | Ni I | 3.83 | -0.61 | cn | 63.5 | 5.986 | 116.3 | 6.499 | 93.9 | 5.937 | 84.6 | 5.709 | 101.9 | 6.128 | 93.0 | 5.983 | 51.2 | 5.818 | 106.2 | 6.257 |
| 7714.310 | Ni I | 1.93 | -1.91 | cn | 110.0 | 6.085 | — | — | — | — | 178.1 | 6.094 | — | — | 195.7 | 6.251 | 87.6 | 5.779 | — | — |
| 7715.591 | Ni I | 3.70 | -0.95 | cn | 43.0 | 5.832 | 123.8 | 6.792 | 68.3 | 5.701 | 66.0 | 5.567 | 93.1 | 6.164 | 68.9 | 5.770 | 33.5 | 5.704 | 92.1 | 6.208 |
| 7727.616 | Ni I | 3.68 | -0.17 | cn | — | — | 154.5 | 6.421 | — | — | — | — | 130.3 | 5.930 | 113.4 | 5.664 | 77.9 | 5.663 | — | — |
| 7748.894 | Ni I | 3.70 | -0.33 | cn | 82.6 | 5.883 | 141.1 | 6.445 | 121.5 | 5.891 | 108.4 | 5.683 | 128.6 | 6.086 | 101.2 | 5.657 | 74.7 | 5.788 | 124.7 | 6.121 |
| 7788.933 | Ni I | 1.95 | -2.42 | fm | — | — | 196.8 | 7.008 | 155.9 | 6.114 | 125.4 | 5.762 | — | — | 137.1 | 6.038 | 75.3 | 6.089 | — | — |
| 7797.588 | Ni I | 3.90 | -0.30 | lz | 78.0 | 5.975 | — | — | 90.8 | 5.656 | 92.3 | 5.599 | — | — | 91.5 | 5.722 | 60.6 | 5.724 | — | — |
| 6435.000 | Y I | 0.07 | -0.82 | hl | 10.4 | 2.560 | 126.9 | 2.896 | 132.1 | 2.552 | 96.0 | 2.300 | 83.3 | 2.354 | 126.0 | 2.871 | — | — | 108.2 | 2.642 |
| 6127.460 | Zr I | 0.15 | -1.06 | bg | 6.5 | 2.833 | 119.6 | 3.231 | 110.8 | 2.677 | — | — | — | — | 87.1 | 2.769 | 7.5 | 3.042 | 80.0 | 3.181 |
| 6134.570 | Zr I | 0.00 | -1.28 | bg | 4.4 | 2.711 | 111.7 | 3.031 | 106.9 | 2.568 | 76.6 | 2.480 | 82.3 | 2.776 | — | — | 5.9 | 2.997 | 71.6 | 2.976 |
| 6140.460 | Zr I | 0.52 | -1.41 | bg | — | — | 76.8 | 3.444 | 88.4 | 3.307 | — | — | 58.3 | 3.435 | — | — | — | — | — | — |
| 6143.180 | Zr I | 0.07 | -1.10 | bg | 12.5 | 3.097 | 125.3 | 3.231 | 151.5 | 3.279 | 117.6 | 3.127 | 100.9 | 2.980 | 132.5 | 3.396 | 15.6 | 3.360 | 92.2 | 3.292 |
| 5853.688 | Ba II | 0.60 | -1.01 | wm | 112.5 | 2.559 | 171.7 | 2.888 | 257.0 | 3.110 | 268.5 | 3.215 | 182.6 | 2.790 | 252.5 | 3.214 | 160.0 | 3.039 | 197.1 | 3.010 |
| 6141.727 | Ba II | 0.70 | -0.08 | wm | 186.9 | 2.423 | 249.9 | 2.619 | 477.9 | 2.972 | 416.2 | 2.863 | 303.2 | 2.639 | 485.0 | 3.094 | 258.2 | 2.745 | 311.0 | 2.755 |
| 6496.908 | Ba II | 0.60 | -0.38 | wm | 178.7 | 2.517 | 270.8 | 2.854 | 431.1 | 3.013 | 378.4 | 2.921 | 288.9 | 2.725 | 445.7 | 3.164 | 222.3 | 2.735 | 302.8 | 2.871 |
| 6390.480 | La II | 0.32 | -1.45 | lb | — | — | 73.5 | 1.999 | 108.6 | 2.292 | 95.0 | 2.040 | 68.2 | 1.859 | 88.1 | 2.185 | 32.9 | 1.933 | 81.4 | 2.109 |
| 6645.110 | Eu II | 1.37 | 0.20 | bc | 19.1 | 0.776 | 59.6 | 1.236 | 50.3 | 0.829 | 58.8 | 0.774 | 27.2 | 0.500 | 45.6 | 0.880 | 16.1 | 0.656 | 48.2 | 0.938 |

^{bc} Biémont et al. 1982^{bg} Biémont et al. 1981^{bk} Bard & Kock 1994^{cn} Chen et al. 2000b^{fm} Fuhr et al. 1988^{hl} Hannaford et al. 1982^{lb} Luck & Bond 1991^{lh} Lambert et al. 1996^{lw} Lambert & Warner 1968^{lz} Liang et al. 2003nd NIST database (<http://physics.nist.gov>)^{ns} Nissen & Schuster 1997^{ow} O'Brian et al. 1991^{wm} Weise & Martin 1980